Linköping studies in science and technology. Dissertations, No 1066

# Tracking and threat assessment for automotive collision avoidance

Andreas Eidehall

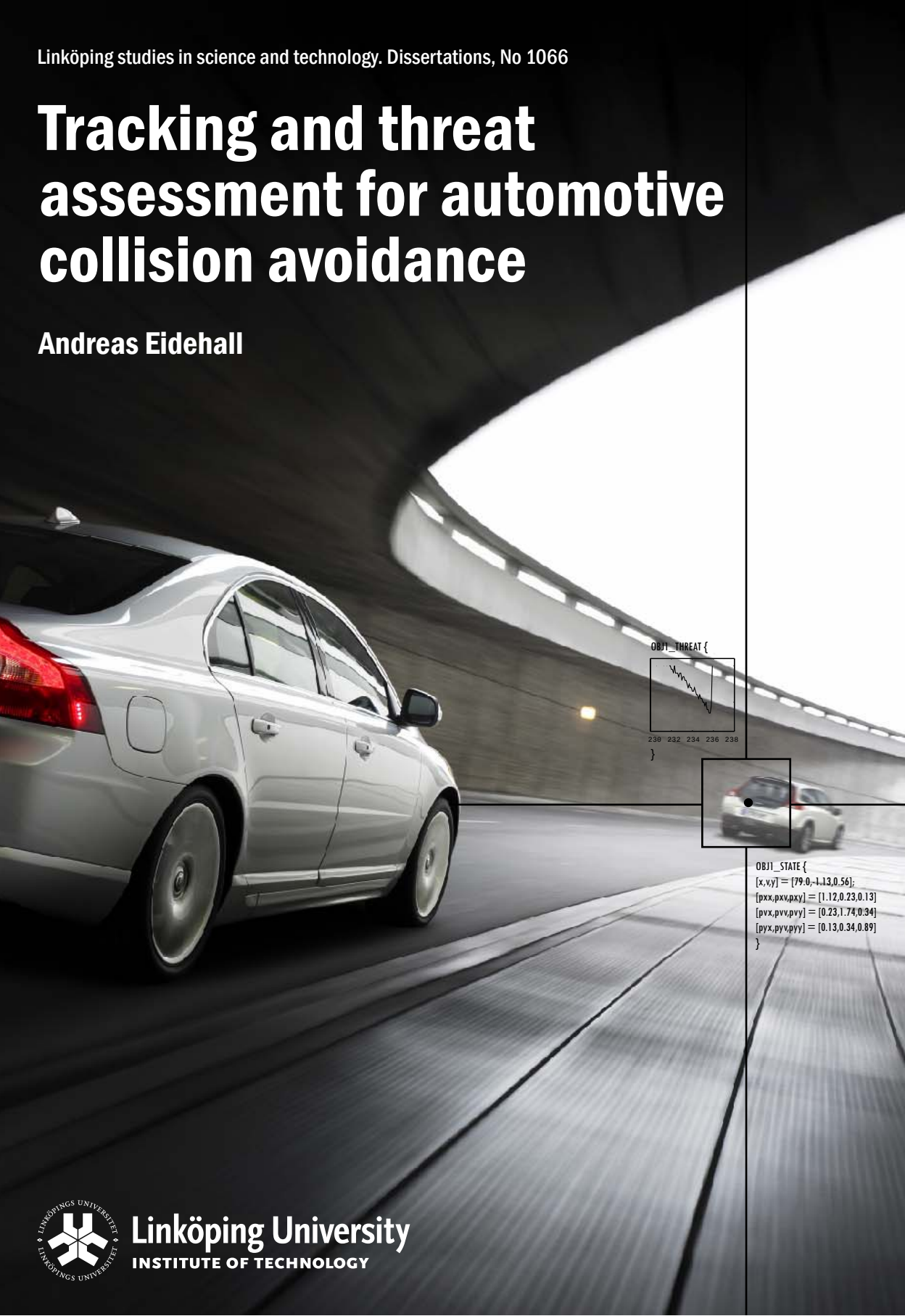


Linköping University
INSTITUTE OF TECHNOLOGY

Linköping Studies in Science and Technology. Dissertations.
No. 1066

# Tracking and threat assessment for automotive collision avoidance

**Andreas Eidehall**

Department of Electrical Engineering
Linköpings universitet, SE–581 83 Linköping, Sweden

Linköping 2007

**Tracking and threat assessment for automotive collision avoidance**



*eidehall@isy.liu.se*
*www.control.isy.liu.se*
*Division of Automatic Control*
*Department of Electrical Engineering*
*Linköpings universitet*
*SE–581 83 Linköping*
*Sweden*

ISBN 91-85643-10-6 ISSN 0345-7524

Printed by LiU-Tryck, Linköping, Sweden 2007

*To Anna*

# Abstract

This thesis is concerned with automotive active safety, and a central theme is a new safety function called Emergency Lane Assist (ELA). Automotive safety is often categorised into *passive* and *active* safety, where passive safety is concerned with reducing the effects of accidents and active safety aims at avoiding them. ELA detects lane departure manoeuvres that are likely to result in a collision and prevents them by applying a steering wheel torque. The ELA concept is based on traffic accident statistics, *i.e.*, it is designed to give maximum safety based on information about real life traffic accidents.

The ELA function puts tough requirements on the accuracy of the information from the sensors, in particular the road shape and the position of surrounding objects, and on robust threat assessment. Several signal processing methods have been developed and evaluated in order to improve the accuracy of the sensor information, and these improvements are also analysed in how they relate to the ELA requirements. Different threat assessment methods are also studied, and a common element in both the signal processing and the threat assessment is that they are based on driver behaviour models, *i.e.*, they utilise the fact that depending on the traffic situation, drivers are more likely to behave in certain ways than others.

Most of the methods are general and can be, and hopefully also will be, applied also in other safety systems, in particular when a complete picture of the vehicle surroundings is considered, including information about road and lane shape together with the position of vehicles and infrastructure.

All methods in the thesis have been evaluated on authentic sensor data from actual and relevant traffic environments.

# Acknowledgments

Working as a PhD student in industry is a little bit like tight-rope walking. Balance is required! On one hand, the problem chosen to study has to be relevant to the company, and stay relevant throughout the PhD project. On the other hand, it has to be academically interesting, the "squiggle level" (krumelurnivån) has to be sufficiently high as my previous manager Robert Hansson used to call it, and it has to be suitable for the tools that one's academic institution provides.

Many people have helped me stay in balance. My supervisors Fredrik Gustafsson at Linköping University and Jochen Pohl at Volvo Car Corporation have provided fantastic guidance and inspiration throughout the project and I hope I shall have the opportunity to keep working with both of you. I also want to thank Robert Hansson, my manager during the first half of the project, for recruiting me and for excellent motivation and guidance. I thank Jonas Ekmark, who became my manager during the second half of the project and who has provided constant support and guidance, and for maintaining the creative environment in our group at Volvo Cars. I also express my sincere gratitude towards Volvo Car Corporation and the PhD program committee for running the Volvo Cars PhD program. It is a fantastic opportunity for the students in the program and it supports the long-term development of the company. I would also like thank Lennart Ljung for allowing me to join the Automatic Control group in Linköping, the most ambitious and inspiring group of people imaginable.

Thomas Schön has been my co-author in two of the papers, and I have really enjoyed working with him. Thanks also to Jonas Jansson who has always found the time for many interesting discussions. Another co-author is Lars Petersson at NICTA in Canberra, Australia, with whom it was a privilege to work; thanks to him and Niklas Pettersson, also at NICTA, for looking after me when I was lost and lonely in Canberra. In addition I would like to thank Lena Westervall at Volvo Cars for her excellent help with developing and tuning the demonstrator.

The last two years have been funded by Intelligent Vehicle Safety Systems (IVSS), for which I am very grateful.

Balance between life and work is also important, and in order to keep this balance, my family and friends have been everything. Thanks to all for constantly supporting me. And last but certainly not least, thanks to Anna for putting up with all my travels and for being a wonderful person. She always helps me put my life in perspective by taking me kayaking, ice skating or mushrooming, although persuasion is sometimes required.

*Linköping, January 2007*

*Andreas Eidehall*

# Contents

# Part I

# Introduction

# 1

# Overview

In 2005, Folksam, a major Swedish insurance company, that also carry out research, released their report “Hur säker är bilen 2005” (How safe is the car 2005). Among many other things, they state that during slippery road conditions the contribution of an anti-skid system, often referred to as ESP or DSTC, to safety in a car is as high as that of the safety belt (Folksam, 2005). In such conditions, an anti-skid system cuts the risk of being killed or seriously injured by half. For researchers in automotive active safety this is an encouraging result, which shows that as passive safety systems reach a high level of maturity active safety systems have a huge potential.

This thesis is devoted to active safety research from a control and signal processing perspective. Active safety, as opposed to passive safety, aims at preventing accidents *before* they occur. A typical example is the anti-skid system referred to above, which tries to keep the driver in control when the vehicle is about loose grip, and thus hopefully avoid being involved in an accident. The thesis deals with three distinct but connected areas within the active safety field.

First, reducing the number of traffic accidents is extremely important. For instance, in the European Union nearly 40,000 people are killed in traffic accidents every year as a result of traffic accidents(European Road Federation, 2004). However, how to design new safety functions to reduce these numbers in the most efficient way is often unclear. The first part of the thesis tries to provide a structured approach to this problem. It compares different, possible, safety function designs and estimates which has the highest potential safety benefit.

Second, most current and future active safety functions will have certain parts in common. They involve some kind of sensor to measure physical properties and they involve some kind of signal processing in order to translate the measured properties to information about the traffic situation and the vehicle state. Furthermore, a decision mechanism to determine *when* to activate the response and a control unit to decide *what* to do in the case of a response are typically also required. While early active safety systems, *e.g.*, the

anti-skid system, mostly measure internal properties of the host vehicle, such as wheel speeds, steering wheel angle and yaw rate, currently-emerging and future safety systems will also include information about surrounding vehicles, the shape of the road and the position of the host vehicle in relation to the road. The main part of the thesis deals with signal processing in this context. Information from external sensors, *i.e.*, sensors measuring positions of surrounding objects and the shape of the road, is merged with information from internal sensors, measuring velocity, yaw rate etc. in order to estimate a complete picture of the surrounding traffic environment.

Third, active safety functions in general need a decision module, *i.e.*, the function needs to decide if and when to intervene or warn the driver. This is typically done by computing a threat level based on the available information, and then comparing this to a threshold. In the ESP case, the threat level computation is based on internal vehicle signals, but in many currently-emerging and future active safety systems, the threat level may be based on the position of surrounding vehicles relative to the host vehicle and relative to the lane. This topic is also addressed in the thesis.

## 1.1 Publications

This thesis is based on the following publications:

P1 Eidehall, A., Pohl, J., Gustafsson, F. and Ekmark, J. "A new approach to lane guidance systems". In *Proceedings of the IEEE Intelligent Transportation Systems 2005*, pages 108-112, Vienna, Austria. This is the first presentation of the ELA safety function.

P2 Eidehall, A. "Lane game". In *Traffic Technology International 2005 Annual Review*, pages 40-42. This is a popular science version of P1.

P3 Eidehall, A., Pohl, J., Gustafsson, F. and Ekmark, J. "Towards autonomous collision avoidance by steering". Accepted for publication in *IEEE Transactions on Intelligent Transportation Systems*, 2006. This is an extended version of P1 which also includes the development of the ELA concept based on accident statistics. It is included in the thesis as **Paper A**.

P4 Eidehall, A. and Gustafsson, F. "Combined road prediction and target tracking in collision avoidance". In *Proceedings of the IEEE Intelligent Vehicles Symposium 2004*, pages 619-624, Parma, Italy. This is the first implementation of the integrated filter for road shape and object tracking.

P5 Eidehall, A., Pohl, J. and Gustafsson, F. "Joint road geometry estimation and vehicle tracking". Provisionally accepted for publication in *Control Engineering Practice*, 2006. This is an extended version of P4 which is a more mature implementation and also includes a more thorough analysis of the performance. It is included in the thesis as **Paper B**.

P6 Schön, T. B., Eidehall, A. and Gustafsson, F. "Lane Departure Detection for Improved Road Geometry Estimation". In *Proceedings of the IEEE Intelligent Vehicles Symposium 2006*, pages 546-551, Tokyo, Japan. This paper shows how a Kalman filter model can be adapted online according to changes in the behaviour of the tracked vehicles. It is included in the thesis as **Paper C**.

P7 Eidehall, A. and Petersson, L. "Threat assessment of general road scenes using Monte Carlo sampling". In *Proceedings of the IEEE Intelligent Transportation Systems 2006*, pages 1173-1178, Toronto, Canada. This is a threat assessment algorithm for long term predictions based on stochastic driver models.

P8 Eidehall, A. and Petersson, L. "Statistical threat assessment of general road scenes using Monte Carlo sampling". *Submitted to IEEE Transactions on Intelligent Transportation Systems*, 2006. This is an extended version of P7 which also includes evaluation on authentic sensor data. It is included in the thesis as **Paper D**.

P9 Eidehall, A., Schön, T. B. and Gustafsson F. "The Marginalised Particle Filter for Automotive Tracking Applications". In *Proceedings of the IEEE Intelligent Vehicles Symposium 2005*, pages 369-374, Las Vegas, USA. This shows how the marginalised particle filter can be used in the combined road shape/object tracking filter. It is included in the thesis as **Paper E**.

P10 Eidehall, A. and Gustafsson, F. "Obtaining reference road geometry parameters from recorded sensor data". In *Proceedings of the IEEE Intelligent Vehicles Symposium 2006*, pages 256-260, Tokyo, Japan. This paper presents a method to obtain ground truth data that can be used for filter tuning. It is included in the thesis as **Paper F**.

## 1.2 The scientific contribution of the thesis

The main contributions of the thesis are:

- The development of the new safety function Emergency Lane Assist (ELA), including an assessment method for the potential benefit of new safety functions. The ELA safety function has also been evaluated in simulations, in artificial scenarios on a test track and with authentic traffic data. This function is discussed mainly in Paper A.

- Derivation and evaluation of different geometric models in an integrated filter for combined road shape estimation and target tracking. The derivation is presented in Paper B but integrated road and object tracking in general is also discussed in Papers E and C.

- A demonstration of how change detection can be used to detect lane changes of

leading vehicles. This is then used to improve the accuracy of the lane shape estimate in the integrated filter. This is presented in Paper C

- A demonstration of how a marginalised particle filter can be used instead of the extended Kalman filter in the integrated filter, which is based on a nonlinear model. This is presented in Paper E.
- A method to obtain true road geometry parameters from recorded sensor data. This can be used as a reference for filter tuning and does not require extra sensors or other hardware. This is presented in Paper F.
- A statistical threat assessment method based on vehicle dynamics and a stochastic driver behaviour model. Using this, more accurate and longer predictions can be made. It also considers interactions between objects in the road scene. This is presented in paper D.
- A dynamic vehicle model that can be used in curved, road-aligned coordinates, *i.e.*, a coordinate system that is shaped according to the road shape. Using this model, threat assessment can be done in the road-aligned coordinates directly. Previously, road-aligned coordinates has only been used for tracking applications. This is also presented in paper D.

# 2

# Trends in automotive active safety

## 2.1 Active safety functions

This section gives a brief overview and some of the milestones of the development of active safety functions that have become available on the market during the last few decades. The overview starts with the ABS system which was introduced in 1978, which can be claimed to be the first electronic active safety system, *i.e.*, its goal is to help the driver *avoid* accidents, and then moves on towards more modern systems. A problem is that it is often unclear when a safety system was actually introduced on the market. For instance, it is often announced that a certain system will be introduced on a certain model, but then the introduction is then delayed. Furthermore, systems are often launched on different markers at different times. Here, the goal has been to find the first year that a system was introduced, regardless of which market.

**ABS (Anti-lock Braking System, 1978)** ABS prevents the wheels from locking and will maintain the steering ability of the vehicle during hard braking. During bad road conditions, ABS will also reduce the stopping distance. The system measures the velocity of all four wheels, and if one of the sensors reports an abnormal deceleration (higher than a physically reasonable value) it concludes that the wheel is about to lock, and the pressure in the braking system is reduced. The German automotive supplier Bosch actually has a patent from 1936 for a "mechanism to prevent locking of the wheels of a motor vehicle". The first ABS prototype was tested in 1970, but reliability of the electronics was too low and it was not before 1978 that the first system was put into production, manufactured by Bosch. Since 1978, ABS technology has been developed further, Figure 2.1 shows that the physical size of the system has been reduced significantly.

**Traction control (1985)** The functioning of the traction control system is very similar to that of the ABS. The system prevents the wheels from slipping during acceleration

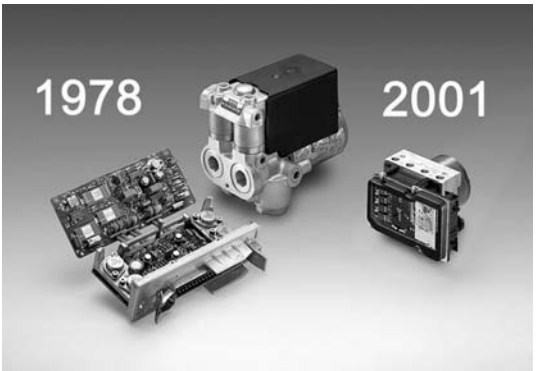


***Figure 2.1:*** *1978 and 2001 ABS unit. The 2001 system is much more compact. Photo: Bosch*

by using the same velocity sensors as the ABS. If a vehicle starts to slip, the engine power is reduced in order to maintain lateral control of the vehicle. The first traction control system was launched in 1985 and was also a Bosch system.

**Stability control (1995)** Again, Bosch was first with their stability control system ESP (Electronic Stability Program) in 1995. While slightly different configurations exist, a stability control system basically measures the yaw rate of the vehicle, i.e., the rotation in the ground plane, and compares it with the desired trajectory. If the deviation is greater than a certain threshold, the system will activate the brakes on one side of the vehicle to correct this.

**Adaptive Cruise Control (1998)** While sources differ on this, Jones (2001) claims that in May 1998 Toyota became the first to introduce an Adaptive Cruise Control (ACC). ACC uses a forward looking sensor, usually radar or laser, to monitor the distance to leading vehicles. If the cruise control is active and time gap to the leading vehicle falls below a certain threshold, the vehicle's ACC system will automatically brake in order to maintain distance. ACC is often not considered a safety system in isolation: it usually comes bundled with a forward collision warning. In Europe, government restrictions typically limit the permitted braking rate to 3.0 or 3.5 m/s$^2$. If the vehicle detects that a higher deceleration is required to avoid colliding with the leading vehicle, an audible warning is given to the driver.

**Forward collision mitigation (2003)** Forward collision mitigation refers to systems that will try to reduce the impact speed by applying the brakes when a collision with the leading vehicle appears to be unavoidable. While many car manufacturers have announced short-term availability of such systems, there are only a few manufacturers that currently sell them. Honda has sold a Collision Mitigation System (CMS) since 2003. Most systems have a similar functionality when it comes to the intervention strategy. They use increasing warning levels as the threat approaches. Hondas system, for example, uses the following technique:

**Primary warning** When there is a risk of collision with the vehicle ahead or if the distance between the vehicles has become too close, an alarm sounds, and the message "BRAKE" appears on the multi-information display in the instrument panel, prompting the driver to take preventative action.

**Secondary warning** If the distance between the two vehicles continues to diminish, CMS applies light braking, and the seat belts are retracted gently two or three times, providing the driver with a tactile warning. At this point, if the driver applies the brakes, the system interprets this action as emergency braking, and activates the brake assist function to reduce impact speed.

**Collision damage reduction** If the system determines that a collision is unavoidable, the seat belt pretensioners are activated with enough force to compensate for seat belt slack or baggy clothing. The CMS also activates the brakes forcefully, at approximately 6 m/s$^2$, to further reduce the speed of impact.

The system was presented by Kodaka and Gayko (2004). It has not been revealed how many systems are actually sold, but it was mentioned that customer acceptance of the system has been quite low. For example, it seems that the false alarm rate, especially for aggressive drivers, has been high.

***Figure 2.2:*** *The Volvo Blind Spot Information System (BLIS). Photo: Volvo Car Corporation.*

**Lane Guidance System (2003)** Lane guidance system refers to systems that try to help the driver stay in the lane. Systems typically use an audible warning or a steering-wheel torque to alert the driver if the vehicle is approaching the lane markings. The steering-wheel torque used by some of the proposed systems will automatically steer the vehicle back into the centre of the lane, thus working almost like an autopilot. In Japan, Honda has been selling their Honda Intelligent Driver Support

(HIDS), which includes the Lane Keeping Assist System (LKAS), since 2003. The system combines an audible warning and steering-wheel torque. However, Honda's idea is that the driver should be kept in the loop at all times. Therefore, the system only supplies 80% of the required torque, the remaining 20% has to be provided by the driver. Their system has been approved by the Japanese Ministry of Land, Infrastructure and Transport and is permitted on expressways in Japan. Ishida and Gayko (2004) provides further details.

A rather recent idea is to try to mimic the sounds and vibrations that are generated by rumble strips, *i.e.*, the grooved lane markings that are sometimes used on motorways to indicate lane departure. A lane guidance system like this has recently been put into production by Citroën (Citroën, 2005). This system differs from the Lane guidance system discussed earlier which uses a camera mounted in the windscreen. The system from Citroën uses dedicated infrared sensors mounted in front of the front wheels, looking straight down. This construction makes the system very robust, but at the same time it cannot measure the distance to the line, nor can it distinguish between lane markers and, for example zebra crossings.

**Blind-spot warning (2005)** The general idea behind a blind-spot warning system is to lower the risk of lane change accidents by warning the driver about vehicles in the blind spot. There are different techniques for achieving this but usually ocular vision or radar is used. Blind-spot warning systems have been announced several times in the past by different car manufacturers, but it was not until 2005 that Volvo released their Blind Spot Information System (BLIS) and became the first to actually put the system on the market. Figure 2.2 shows a BLIS camera.

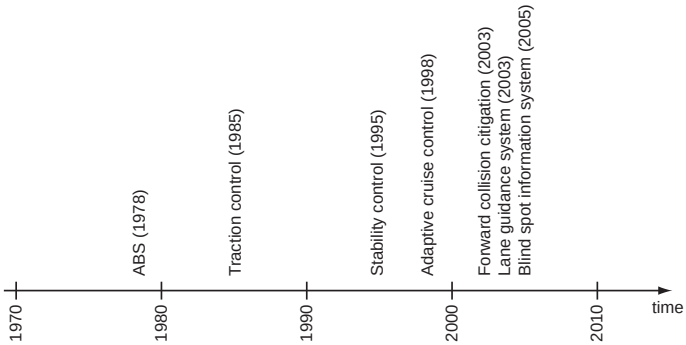


***Figure 2.3:*** *Milestones in the development of active safety systems during the last few decades.*

The market introduction years for these active safety systems are also illustrated in Figure 2.3.

## 2.2 Autonomous vehicles

This section gives an overview of a parallel research field during about the same time period, which is concerned with autonomous driving and robot cars based on computer vision. Most vision-based safety functions that are almost ready to market, and most future vision-based functions, are based on the research in this field. It also gives a hint of what can be expected in consumer products in the close future. This information is mainly provided by Dickmanns (2002), Schmidhuber (2005), DARPA (2006) and Thrun et al. (2006).

The first milestone in this field was the demonstration in 1987 of an autonomous vehicle called *VaMoRs* by Dickmanns and Zapp (1987) and Universität der Bundeswehr München (UBM). VaMoRs was capable of autonomous longitudinal and lateral control and drove autonomously a distance of over 20 km on the German Autobahn. VaMoRs was a 5-ton DB 508D Mercedes van, which used a vision sensor only and relied on lane markers with well-defined edges. It was able to process images at 13 Hz and could handle speeds up to 100 km/h (limited by engine power). One of the results of this was a change of focus in the European *Prometheus* research project (1987 - 1994) on autonomous cars. Prometheus was a major research project (over €800 million), focusing on reducing road accidents and improving traffic efficiency (Williams, 1992, Braess and Reichart, 1995a,b), funded by EUREKA (2006), and which included most European car manufacturers. The original idea, to control a vehicle laterally using buried wires was dropped in favour of using computer vision as the primary sensor.

At about the time Prometheus was active in Europe, Takeo Kanade and Charles Thorpe, among others, also carried out research on autonomous driving at Carnegie Mellon University (CMU). In their NavLab test vehicle, which apart from the vision system also included a laser scanner, they demonstrated the SCARF vision system, for instance for lane and road following (Crisman and Thorpe, 1993). While the European efforts were based on control theory, much of the American early work had a background in computer science and machine learning (Thorpe, 1990). Kanade and Thorpe's research led to the famous demonstration in 1995 called 'No hands across America', when their vehicle NavLab 5 drove 98% of a total distance of 5000 km from Washington DC on the East coast to Los Angeles on the West coast. However, the computer only provided lateral control; a human operator had to control the vehicle longitudinally.

Later the same year, UBM's vehicle, *VaMP*, of UBM drove automatically on the German Autobahn, autonomously controlled both laterally and longitudinally, including overtaking manoeuvres. It drove 95% of a total distance of 1600 km from Munich in Germany to Odense in Denmark, at speeds up to 180 km/h.

More recently, an important contribution to the autonomous driving research field has come from DARPA (Defense Advanced Research Projects Agency), in its Grand Challenge contests (DARPA, 2006). The first contest was held on March 13, 2004 and required autonomous vehicles to navigate a 230 km course through the Mojave desert in southwest United States, in no more than 10 hours. The prize was $1 million. 107 teams registered and 15 teams qualified to the final event. However, no team was able to complete the entire track; in fact, the record was only about 12 km. On October 8, 2005, the Grand Challenge took place again, this time with an increased prize of $2 million. 195 teams registered for the competition and 23 raced in the final. Of these, five teams


***Figure 2.4:*** *The winner of the 2005 DARPA Grand Challenge was Stanley from Stanford University. Photo: DARPA*

made it over the finish line and the winner was "Stanley" from Stanford University (Thrun et al., 2006). It completed the track in 6 hours and 53 minutes and the team was awarded the $2 million, see Figure 2.4. Second and third places went to CMU with "Sandstorm" and "H1lander" which finished 11 and 21 minutes later, respectively. The sensors on Stanley are mounted on a roof rack and it featured five laser scanners for 3D road surface scanning, a colour camera for road detection and two 24GHz radar sensors for long range detection of obstacles. The radars had a range of up to 200 metres with a 20 degrees field of view.

DARPA has also announced the 2007 challenge, this time called the 'Urban Challenge' which is to be held in an urban environment (Figure 2.5). Apart from navigating streets, there will also be interaction with other vehicles and dummy pedestrians; thus traffic rules such as yield situations and traffic lights need to be considered. This time the first prize is again $2 million, but in addition, $500,000 and $250,000 will be awarded to the second and third placed teams to complete the race. The official announcement states that "To succeed, vehicles must autonomously obey traffic laws while merging into moving traffic, navigating traffic circles, negotiating busy intersections and avoiding obstacles". In addition, DARPA has decided to give development funding of up to $1 million based on applications from the teams.

## 2.3 Discussion

It is clear that active safety technology in vehicles is becoming more and more advanced, and is utilising more and more information from the vehicle surroundings. But at the same time there is a huge gap between research in the academic world and what is being deployed in the automotive industry. The work that lies in adapting academic results to industrial requirements in terms of cost and robustness should not be underestimated. This

***Figure 2.5:*** *While the previous 'Grand Challenges' from DARPA took place in the desert, the 2007 'Urban Challenge' will be held in an urban environment. Photo: Wikipedia*

is illustrated by Figure 2.6, while the academia is working on more and more advanced technology, the industry is occupied with increasing robustness and decreasing size and cost, here referred to as technical maturity. Today, the lane-guidance systems that started development in the late 1980's are being taken to the market. It is mainly reductions in size, cost and power consumption and an increase of micro-processor computing power of micro processors that has enabled this. So the question is, will there always be a 20 year gap between the technical frontier in intelligent vehicles and products that are available to consumers? Will the gap decrease or increase? Today, prototype vehicles are navigating desert roads autonomously. Will normal cars have this capability in 2025?

There is also another question that is currently highly debated. In the long-term future of intelligent vehicles, will the driver remain in detailed control of the vehicle or not? In one vision, vehicles are fully autonomous. A driver enters the vehicle and states his or her destination, and is taken there by the vehicle. All passengers can work or read a newspaper on the way. A computer will automatically plan the route and control the vehicle. This side is mainly represented by academia. In the other vision, the driver is in control of the vehicle as usual but is given advice on hazards, upcoming traffic jams, slippery road conditions, etc. The basis for this vision is that people enjoy driving and it leaves more room for driver experience and for vehicle manufacturers to profile their products. This side is naturally mainly represented by the industry. Of course, the future path of vehicle development could be somewhere in between. The detailed lateral and longitudinal control could be handled by the vehicle, while important decisions, such as route selection, overtaking, or perhaps even negotiating intersections, are handled by the

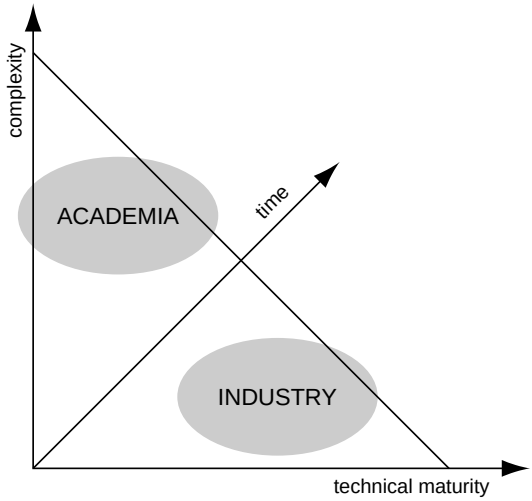


***Figure 2.6:*** *Deployment of technology for autonomous vehicles in academia and in industry. The reason that industry is "behind" in terms of complexity is that it has tough requirements for hardware costs, robustness, size and power consumption, referred to here as technical maturity.*

drivers. In the end, the decision on which of these development trends that will prevail will be determined by the car consumers.

# 3

# Overview of the papers

## 3.1 The benefit of active safety functions

As was discussed in the overview, traffic accidents are a huge global problem, both personally for the individuals affected and financially for the society. In order to understand the mechanisms behind traffic accidents, accident causes have to be studied. Figure 3.1 shows an example of a sequence of events leading to an accident. The example shows a drowsy driver who strays into the opposite lane and crashes into an oncoming vehicle. In order to understand how to design countermeasures, accident statistics is needed. However, the problem with most currently available statistics is that it is focusing on *passive* safety, *i.e.*, the last step in the chain of events in Figure 3.1. This means that it contains a lot of information about deformations, impact energies and accident offsets, but very little information about what actually *caused* the accidents. An active safety system can enter at any of the earlier steps in the sequence. One step in this direction is taken by National Highway Traffic Safety Association (NHTSA, 2001) in their General Estimate System (GES), which focuses on the last step before the accident, see Figure 3.2. The categories are “Head on”, “Rear end”, “Hit fixed object” etc. However, no clue is given to what caused the dangerous situation. In an attempt to get more detailed information about the earlier events in Figure 3.1, Paper A defines new accident categories that mainly focus on the first and second event in the accident sequence. For instance, the main categories are “Collision with object in same lane”, “Lane change accidents” etc. Preferably, these accidents are then divided into subcategories as the example in Figure 3.3 shows. In order to find the frequencies for these categories, a new traffic accident database called “European Accident Causation Survey” was consulted, which, as the name indicates, focuses on accident causes.

These frequencies has then been used to analyse new, potential safety functions. A list of such functions has been developed in a creative process and is presented in Paper A. Based on the statistics, the expected benefit of these functions can be computed, which

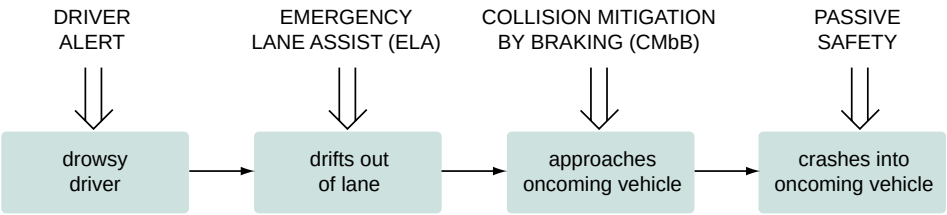


***Figure 3.1:*** *An example of a sequence of events leading to an accident. Here, a drowsy driver strays into the opposite lane and crashes into an oncoming vehicle. The accident can be avoided or mitigated by deploying countermeasures at different stages. The figure shows the names of countermeasures developed by Volvo for this specific accident sequence. Driver Alert warns drivers who are about to fall asleep, Emergency Lane Assist, a central topic of this thesis, prevents dangerous lane departure manoeuvres and Collision Mitigation by Braking automatically brakes the vehicle just before the accident. In the event that the accident occurs anyway, the occupants are protected by traditional passive safety,* e.g.*, energy-absorbing crumple zones and seat belts.*

can aid in choosing the one which has the highest safety potential.

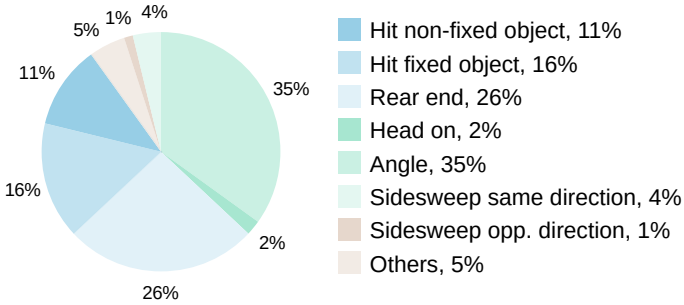


***Figure 3.2:*** *The General Estimate System (GES) traffic accident categories from 2001.*

Somehow, the cost or the complexity of a potential safety function also needs to be computed. For instance, if all cars were driven autonomously, there would (hopefully) be no accidents. However, the cost of developing and installing autopilots in all vehicles is probably quite high. Thus, we need to take smaller and cheaper steps in the right direction. In Paper A, a method for computing the total cost of the installed system per vehicle is presented. It is based on the sum of the hardware costs, *e.g.*, radar or laser scanner, and the development costs of the function.

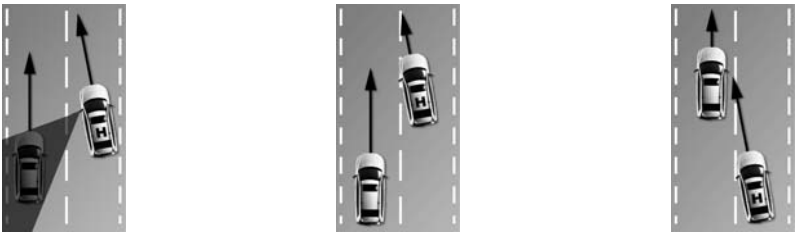

Blind-spot related accident | Collision with a faster moving vehicle | Collision with a slower moving vehicle

***Figure 3.3:*** *This is an example of how lane change related accidents can be divided into subcategories. H indicate the host vehicle,* i.e.*, the vehicle to be equipped with the safety function.*

## 3.2 Emergency Lane Assist

The result of the evaluation method is a new active safety function called Emergency Lane Assist (ELA). ELA is similar to traditional lane guidance systems in that it tries to prevent lane departure by applying a steering wheel torque in the opposite direction. Such systems typically use a camera mounted in the windscreen to monitor lane markings. Then, as the vehicle is about to cross the lane markings, a steering-wheel torque is applied or the driver is alerted by an audible signal. The difference is that ELA only prevents *dangerous* lane departure manoeuvres. This is achieved by also monitoring traffic in adjacent lanes. If there is no traffic in adjacent lanes, the lane markings can be crossed without intervention. But if a lane departure manoeuvre is commenced in such a way that a collision is likely, for instance with an oncoming vehicle or a faster moving vehicle approaching from behind, then a steering-wheel intervention will be initiated. The function also includes some logic for determining if the departure manoeuvre is intentional or not. Figure 3.4 shows a few examples of ELA behaviour. ELA addresses several important accident categories, of which the most dangerous is accident with an oncoming vehicle. But there are also many accidents on motorways, in particular in Germany, where vehicles change lanes in order to overtake, and are hit from behind by a vehicle in the “faster lane”. ELA is presented in detail in Paper A that is entitled “Towards autonomous collision avoidance by steering”. This refers to the fact that it is actually a practicable step towards automatic steering intervention for collision avoidance.

## 3.3 Tracking

In order to realise the ELA function, rather accurate information about the host vehicle surroundings is needed. First, in order to determine when a lane change is commenced, and to be able to steer back into the original lane, the position and orientation of the host

No ELA intervention since there is no threat in the adjacent lane. ELA intervention. ELA intervention.

***Figure 3.4:*** *Examples of the behaviour of the ELA function.*

vehicle in relation to the lane is needed. Second, the position of surrounding objects is also needed in order to determine wether a commenced lane change is likely to result in a collision or not. Third, the lateral position of other objects in relation to the lane is also needed. The purpose of this is to determine which objects are actually occupying the lane that the host vehicle is about to enter. Consider an example where we assume that the intervention takes two seconds to carry out, *i.e.*, it takes two seconds to get the host vehicle back safely into the original lane. If the host vehicle is travelling at 90 km/h and there is an oncoming vehicle travelling at the same speed, then the two vehicles approach each other at 50 m/s. If we need to initiate the intervention two seconds before the collision, then the decision must be made when the distance to the oncoming vehicle is 100 m. Thus, vehicles need to be assigned to the correct lane when 100 metres away, which is dependent on knowing both the position of the object and the shape of the road. Figure 3.5 illustrates how the leading vehicle lane assignment is dependent on the current estimate of road radius.

It was noticed early on that the position estimate of tracked vehicles, which is based on radar measurements, and also the positioning of the host vehicle in relation to the lane, which is based on a camera and image processing, was sufficiently accurate. However, the positioning of tracked vehicles in relation to the lane has been a great challenge, primarily due to the difficult task of road shape estimation. The conclusion was that this needed improvement.

The first step is to develop some sort of quality measure in order to be able to evaluate potential improvement methods. Such a quality measure is typically based on comparing estimated values, in this case, of the parameters describing the road shape with reference or “true” values, or with another estimate where the error is significantly lower. For instance, the reference data could come from a better sensor; it could be extracted from a detailed map; or it could be obtained from the local road authorities. Another solution is presented in Paper F, which consists of an algorithm for computing a reference value of the road shape parameters based on recorded sensor data. Since an enormous amount

***Figure 3.5:*** *Lane assignment of leading vehicles is dependent on road shape estimation. Which lane the leading vehicle is assigned to depends on the current road radius estimate.*

of such data is usually already available, this is a faster and cheaper method than the alternatives mentioned earlier. It uses recorded sensor data in order to recreate the actual shape of the road that was driven, and by being able to access the entire data set, *i.e.*, also future sensor measurements, a rather accurate value of the parameters describing the road shape can be obtained. This reference data can then be used in various ways. For instance, the mean error of different estimation methods can be computed and compared. Statistical properties, *e.g.*, standard deviation, can also be obtained.

When quantifying the requirements for estimation error, it can be found, for instance, that in order to assign a leading vehicle 100 metres away to the correct lane, an error in the road *curvature* estimate of $5 \cdot 10^{-4}$ (1/m) or less is needed, where the curvature is defined as one divided by the road radius. Using the proposed method for obtaining ground truth data, this requirement can easily be verified. Figure 3.6 shows how the errors in the vision system curvature estimate can be distributed. In this case, the error is above the requirement for about 7.5 percent of the time. Note that this is an unusually good result. The vision system is very sensitive to changed visibility conditions, and is affected by weather, hills and slopes which reduce the visibility, and also by the conditions of the lane markings. In the case of very worn lane markings, the performance can be significantly reduced.

Paper B discusses how the accuracy of this parameter can be increased. The first natural step is to include more information. In the vehicle we have access to yaw rate and velocity, for instance, and the camera also provides lateral position in the lane. This is a much more accurate signal than the lane geometry information. However, in order to use this information a model is needed to relates the new information to the lane shape parameters.

The lane shape is described by two states: $c_0$ is the local lane curvature around the host vehicle, *i.e.*, one divided by the road radius, and $c_1$ which is the clothoid parameter, defined as the distance derivative (the change rate) of $c_0$. Paper B also includes a parameter $W$ denoting lane width, but it is not essential here and has been excluded. The host

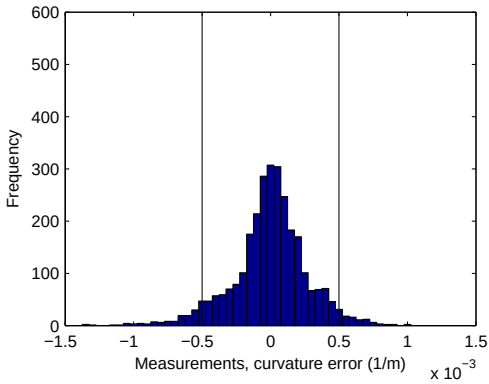


***Figure 3.6:*** *Error distribution in the vision system. The error level $5 \cdot 10^{-4}$ is a requirement for making correct lane assignments at long distances. Here, the error is higher than the requirement 7.5 percent of the time.*

state in relation to the lane is described by $y_{\text{off}}$ and $\Psi_{\text{rel}}$, where $y_{\text{off}}$ is the lateral position measured from the centre of the lane, and $\Psi_{\text{rel}}$ is the heading angle in relation to the lane markings. For a summary of these parameters, see Figure 3.7. A model relating these parameters can then be written:

$$\dot{y}_{off} = v\Psi_{\text{rel}} \tag{3.1a}$$

$$\dot{\Psi}_{\text{rel}} = \dot{\Psi}_{\text{abs}} - vc_0 \tag{3.1b}$$

$$\dot{c}_0 = vc_1 \tag{3.1c}$$

$$\dot{c}_1 = 0 \tag{3.1d}$$

where $v$ is the velocity and $\dot{\Psi}_{\text{abs}}$ is the measured yaw rate of the host vehicle. This model is derived and discussed more in detail in the paper. The states $y_{\text{off}}$, $\Psi_{\text{rel}}$ and $c_0$ are directly measurable. It is interesting to note that using this model, the state $c_0$ is observable from $y_{\text{off}}$ and $\Psi_{\text{rel}}$ only. This suggests that to include these measurements should improve the accuracy of $c_0$. The improvement can be seen in Fig, 3.8, where the same data sequence as in Figure 3.6 is processed with a Kalman filter based on the new model. The time that the error is higher than the requirement is reduced to 4.5 percent.

Is it possible to include even more information to achieve further improvement? One idea that was raised by Dellaert and Thorpe (1997) and Zomotor and Franke (1997), for example, is to include the motion of surrounding vehicles to support the estimate. The idea is rather brilliant and relates to the way that humans drive. The assumption is that other vehicles are very likely to keep following their current lane, and since their position can be measured accurately using the radar, this assumption can be used to support the road shape estimate. This is very similar to how drivers behave during reduced visibility, *e.g.*, fog or darkness, where the tail lights of leading vehicles can be seen more clearly than the lane markings at long distances. If a leading vehicle starts to move left it is natural to assume that the it is entering a curve to the left. Note that it is important not to

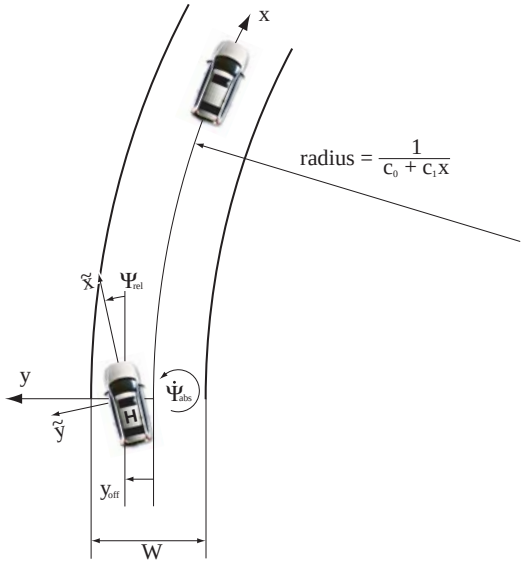


***Figure 3.7:*** *$y_{\text{off}}$ and $\Psi_{\text{rel}}$ are the host vehicle states while $c_0$ and $c_1$ describe the shape of the road.*

rely too much on this assumption. The best solution is to say that it is *highly probable* that the car is entering a curve, but also remain open to the alternative that the car is changing lanes or exiting the road. In order to achieve this model (3.1), above, needs to be related to the motion of surrounding vehicles. Paper B discusses different methods of doing this. The common feature of these methods is that they use a curved, road-aligned coordinate system and that the motion of tracked vehicles is modelled in these coordinates. The road-aligned coordinates are denoted $(x, y)$ and are also shown in Figure 3.7. The model describing the lateral motion of tracked vehicles then simply becomes

$$\dot{y} = 0, \tag{3.2}$$

where $y$ is the lateral position of the tracked vehicle in the lane, which simply says that vehicles will keep following the road, *i.e.*, not move laterally. This is then related to the road shape states $c_0$ and $c_1$ via a measurement equation. The simplest one used in Paper B is

$$\tilde{y} = y - y_{\text{off}} - \Psi_{\text{rel}} x + c_0 x^2/2 + c_1 x^3/6. \tag{3.3}$$

This is a Taylor expansion of an exact geometric model that includes trigonometric formulas; the distance to the vehicle is $x$ and $\tilde{y}$ is the lateral position in relation to the *host* vehicle (see Figure 3.7) in which the sensors are positioned.

Here, if $x$ is used as a state in the filter, then the model becomes nonlinear and the standard Kalman filter cannot be used. The other, more complex methods/models discussed in Paper B are also nonlinear. The most common choice in such cases is the *extended*

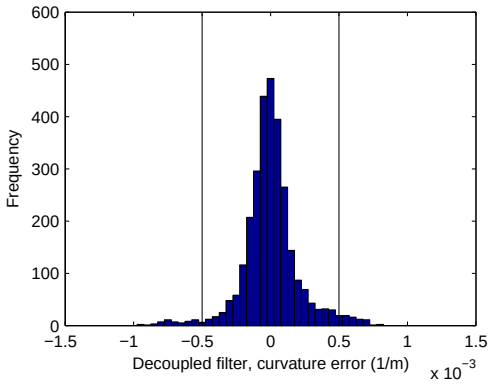


***Figure 3.8:*** *Error distribution after initial filtering. The error level* $5 \cdot 10^{-4}$ *is a requirement for making correct lane assignments at long distances. The time that the error is higher than the requirement is reduced to 4.5 percent.*

Kalman filter (EKF), and this is what has been used mainly in this work. Other alternatives include the *particle filter* (PF) and the *unscented Kalman filter* (UKF). Paper E investigates how a marginalised particle filter (MPF), which is a special version of the Particle Filter in which a linear substructure of the problem is utilised to get a more efficient implementation, can be applied to this problem. The outcome is that slightly better results than the EKF can be obtained, but at much higher computational cost. The conclusion from Paper E is that the MPF is probably not worth the extra computational cost today, but it might be needed in the future in order to include other types of information that are "more nonlinear". For instance, information from a map database. A thorough investigation of the MPF is given by Schön (2006). The unscented Kalman filter is suitable for this application but its performance has not been investigated so far. Since the improvement of the MPF over the EKF was not that high, the UKF can not be expected to give much improvement either.

The result of using EKF can be seen in Fig, 3.9. The time that the error is higher than the requirement is reduced to 1.5 percent. One of the main prerequisites of this method is, of course, that there is a leading vehicle. As soon as there are no vehicles around, the performance drops to the level indicated in Figure 3.8.

## 3.4 Change detection

The last step is dependent on the assumption that vehicles keep following their lane. The degree to which we want to rely on this assumption can be determined in the design of the Kalman filter. Since vehicles actually do change lanes and exit the road, the choice has to be a compromise. On one hand, if we rely too much on it, every lane change and road exit will be misinterpreted as a curve entry. On the other hand, if we rely too little on it, the benefit of including surrounding vehicles into the filter will be gone. When implementing

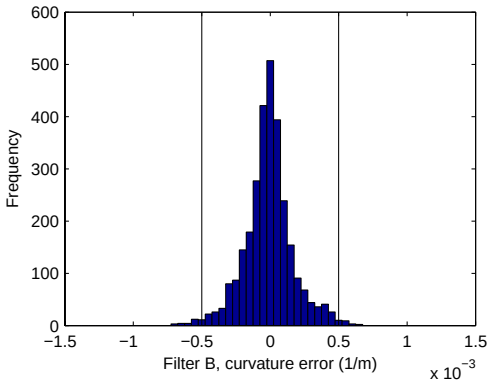


***Figure 3.9:*** *Error distribution when including information from the motion of surrounding vehicles. The error level* $5 \cdot 10^{-4}$ *is a requirement for making correct lane assignments at long distances. The time that the error is higher than the requirement is now reduced to 1.5 percent.*

the filter, (3.2) is discretised and then stochastic, white process noise with variance $Q_{\text{lat}}$ is added. A low $Q_{\text{lat}}$ then corresponds to relying on (3.2) very strongly, *i.e.*, there is a strong connection between the motion of surrounding vehicles and road model, while a high value of $Q_{\text{lat}}$ relaxes the connection.

Paper C investigates whether $Q_{\text{lat}}$ can be changed automatically as the traffic situation changes. More specifically, if a lane departure or road exit of a leading vehicle could be detected, $Q_{\text{lat}}$ could be raised temporarily. In that case, there would be no need to compromise and $Q_{\text{lat}}$ could be kept very low when the assumption that surrounding vehicles follow their lane is valid. The goal is then that the filter performance will be improved further.

There are different approaches to achieve this. Paper C analyses a method called the CUSUM test (from CUmulative SUM). The CUSUM test is designed to detect changes in the filter residuals that are connected to lateral movement. The test is designed in order to alarm when a lane change or departure is taking place and then raise $Q_{\text{lat}}$ temporarily. An example is shown in Figure 3.10. Being able to keep $Q_{\text{lat}}$ low gives advantages during curve entry and exit. The key is then to detect when vehicles deviate from the “typical” behaviour, otherwise the performance of the filter will deteriorate. This is what happens just after time 4270 s in Figure 3.10. A leading vehicle lane change to the right makes the filter believe that it is entering a curve to the right. In Paper C it is demonstrated how this can be detected and used in order, temporarily, to raise $Q_{\text{lat}}$ during such events.

It is clear that this method gives better performance during curve entry and exit, but how the average, long term performance is affected is not yet fully investigated. In order to make a detector robust, there has to be a delay before an alarm can be triggered, and in this case, it means that the performance will be slightly degraded during these delays. Whether this is acceptable compared to the benefit that the detector can give in curves probably depends on the application.

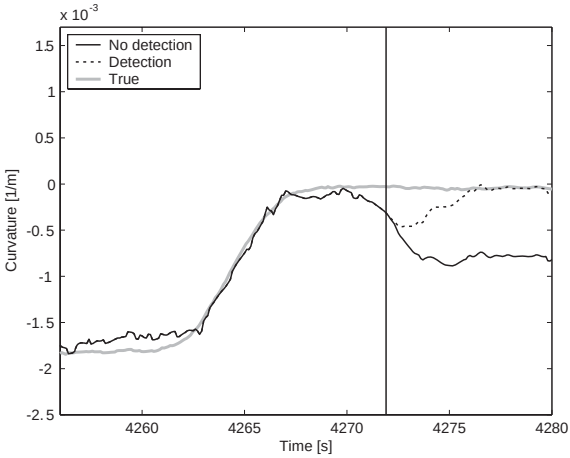


***Figure 3.10:*** *Being able to keep $Q_{lat}$ low gives advantages during curve entries and exits. This works as long as leading vehicles do not deviate from the lane, which occurs just after time 4270 s. The vertical line shows when the CUSUM algorithm detects this and adapts the model.*

## 3.5 Threat assessment

Active safety functions, such as Emergency Lane Assist (ELA), needs a decision unit that decides if and when to warn the driver or intervene. As discussed in the overview, such a decision is typically based on computing a threat level and if the threat is higher than a predefined threshold, a warning or an intervention is activated. In ELA and other emerging active safety functions, this threat is typically based on the surrounding traffic situation, rather than internal vehicle signals.

In order to evaluate the ELA concept, Paper A introduces a rather simple decision module. As was discussed in Section 3.2, the function aims at preventing dangerous lane departures. Three things needs to be checked before an intervention can be triggered. First, we need to check that a lane departure manoeuvre is in progress. This can be done by studying the lateral motion of the host vehicle in relation to the lane.

Second, potential conflicts with other vehicles if the lane change is completed need to be found. This is done by predicting the positions of other vehicles to the time when the host vehicle is expected to enter the adjacent lane. This prediction is the most difficult step, since the prediction time is very long: typically around two to three seconds but sometimes more. The road-aligned coordinates $(x, y)$ in Figure 3.7 that were discussed above simplify these predictions significantly. Predicting vehicles movement in a straight line within the road coordinates means that they will also follow the road in curves. But despite this fact, a lot of things can happen in two or three seconds. Other drivers may decide to change lane, brake in order to avoid an obstacle, etc. Other methods of prediction are addressed later in this section.

Third, when it has been established that a lane change has been commenced and is

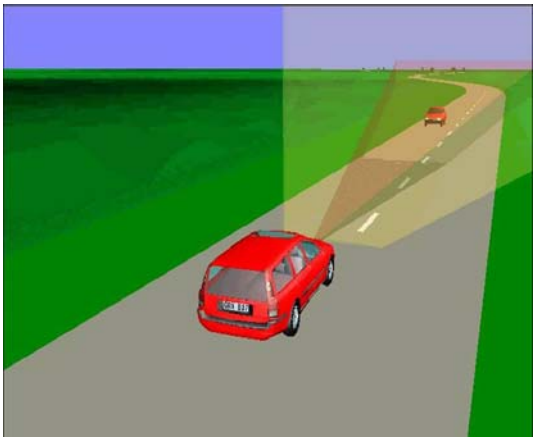

***Figure 3.11:*** *Video clip of the simulation environment.*

likely to result in a collision, we also need to check that the host vehicle's original lane, that we are about to steer back into, is conflict free. If there is also a threat in this lane, then the steering intervention will not avoid the collision. Instead, it is preferable to leave situations like this to autonomous braking systems: *e.g.*, a Collision Mitigation System (Jansson, 2005). Furthermore, since the aim of the function is to avoid unintentional lane departures, for example by distracted drivers it is also appropriate to try to detect *intentional* manoeuvres. For instance, this could be done by interpreting a very resolute steering manoeuvre as if the drive is in control of the situation, and for some reason still chooses to enter the dangerous situation. In such cases, an intervention of ELA is undesirable, since the driver might for example be trying to avoid another threat that the system is unaware of.

The intervention is carried out by activating a lateral controller connected to the steering system of the host vehicle. The controller tries to achieve $y_{\text{off}} = \Psi_{\text{rel}} = 0$, *i.e.*, driving straight ahead in the centre of the original lane. A simulated ELA intervention is shown in Figure 3.11 and Figure 3.12. The simulation is carried out in a traffic simulation tool developed by Volvo Car Corporation, which is based on detailed models of vehicle dynamics and sensor behaviour. In the scenario, a lane departure manoeuvre is commenced just as an oncoming vehicle approaches. The result of the ELA intervention can be seen in Figure 3.12. As the intervention is initiated, a steering-wheel torque controller is engaged to steer the vehicle back towards the centre of the original lane.

In Paper A, an ELA situation is emulated on a test track, where an inflatable mock-up is used to represent a threatening oncoming vehicle. Note that no actual steering intervention takes place, instead the ELA threat assessment algorithm is run off-line without the steering wheel controller engaged. This is a technique that has been used extensively throughout the research project. By only collecting data with the sensors, without carrying out actual interventions, threat assessment algorithms can be evaluated and, more importantly, tuned off-line. For this purpose, an intervention would "ruin" the data set. Of course, in order to design the actual intervention, closed loop development has to be

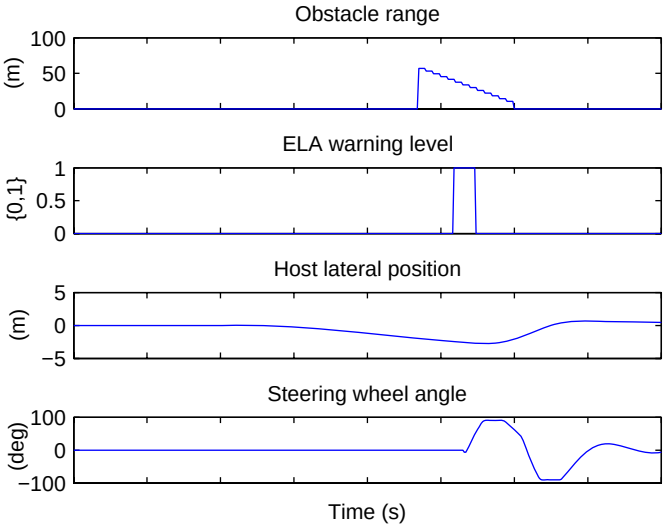


***Figure 3.12:*** *In this simulation, the host vehicle drifts into the lane of an oncoming vehicle. The ELA algorithm detects a threat and successfully steers the vehicle back into the original lane.*

used. But since lateral controllers with satisfactory performance already exist at Volvo Car Corporation, this has only been a minor part of the research project.

The system has been tested in a demonstrator, see Figure 3.13, and people who used the system generally reacted very positively reactions. Many of the drivers felt that the intervention was very gentle and not at all dramatic. Even drivers who were afraid before the test drive that the intervention would be very dramatic agreed on this. Since the system brings the car back into the safe lane and leaves it in a safe position, it generally gives the driver a positive feeling of security. Many who tested who tested the system also believed in the usefulness of ELA as a safety system and can relate to personal experiences where the system might had prevented accidents. At the same time, there are always people who are skeptical to interfering with such a safety critical component as the steering system.

As mentioned before, one of the weaknesses in the simple threat assessment algorithm presented in Paper A is the length of time required for the prediction: two seconds or more. The main problem is the uncertainty in future driver input. In two or three seconds, drivers have the opportunity to change course, change speed, avoid threats, etc., a fact that is difficult to include in threat assessment algorithms. What makes it difficult is the fact that drivers do stay in their lane most often, and keep following their current path, which is why deterministic predictions, as the one discussed earlier, are often very accurate. However, it is on the few occasions when drivers deviate from these expected paths that threatening situations often occur.

Again, one solution lies in studying how actual drivers react to such situations. For instance, a physical driver easily judges how other vehicles will behave based on the


***Figure 3.13:*** *Demonstration of a typical ELA intervention.*

traffic environment. A oncoming might be forced to swerve by an obstacle at the side of the road, a bicycle might be forced to brake in order to avoid a reversing car etc. Situations like this can be foreseen by an actual driver by studying the interaction between objects in the road scene.

Paper D introduces a statistical method that tries to mimic this behaviour by predicting many future possible paths simultaneously, paths which also take into account interaction between other vehicles. A threat assessment algorithm is then based on these predictions. The base is a statistical driver behaviour model, which tries to emulate typical driving behaviour. It leaves room for drivers to deviate from their current trajectory as much as vehicle dynamics and road friction allows but will at the same time capture the fact that certain manoeuvres are more likely than others. The driver model is based on three aspects of typical driver behaviour. First, drivers have a goal in their driving, *i.e.*, they want to get from A to B as quickly as possible, but at the same time not exceeding safe speeds. This can be modelled simply by giving any manoeuvre that deviates from the intended path and velocity a low probability. Also, drivers prefer a comfortable ride. This is why any manoeuvre including rapid acceleration, laterally or longitudinally, is also given low probability. Third, drivers have a natural collision-avoidance tendency, which is why the algorithm mainly focuses on collision-free manoeuvres. Again, the road-aligned coordinate system simplifies these models considerably, which is explained further later.

The threat assessment algorithm then uses these predictions to estimate a general threat based on the current road scene. The main idea is that the host vehicle should not only stay clear of the most likely path but instead of an entire set of future paths. The size of this set is chosen so that its probability mass equals a predefined level. The threat is then computed as the shortest time to collision for any of these paths. An example can be seen in Figure 3.14, which shows a simulation where it is predicted that an oncoming vehicle will have to swerve in order to avoid an obstacle and thus becomes a threat to the host vehicle. Note that this is a *general* threat assessment algorithm, *i.e.*, it judges the threat in a road scene without a specific accident type or safety function in mind.

The algorithm has also been evaluated on simulated data and on authentic, recorded

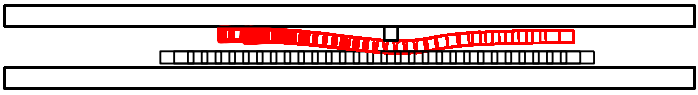

***Figure 3.14:*** *In this scenario, the host vehicle (black) is moving from left to right in a straight line, and an oncoming vehicle (red) is moving from right to left. The system predicts the probability that the oncoming vehicle will have to swerve left in order to avoid the obstacle, and thus become a threat to the host vehicle.*

sensor data, which is also demonstrated in Paper D. The authentic data set consists of 4.5 hours of recorded sensor data from German motorways. The tracking system is the same as described in Section 3.3. Although the threat assessment algorithm is still immature, the results are promising. During the 4.5 hours, 68 alarms were triggered. When viewing video recordings from these situations, 67 of the alarms were actually judged to correspond to situations involving some sort of threat, thus leaving only a single false alarm. The correct alarms fall into three main categories:

1. The host vehicle is approaching a leading vehicle at high velocity.
2. The host vehicle is driving close to a leading vehicle, at about the same speed.
3. The host vehicle is drifting out of its lane in the direction of a vehicle in the adjacent lane.

It is interesting to note that these warnings all correspond to existing safety functions, or functions that are under development. The first category corresponds exactly to the Collision Mitigation by Braking safety function (Jansson, 2005), the second category to a distance warning system that warns when the distance to the leading vehicle becomes too short (Kamiya et al., 1996), and the third category corresponds to the Emergency Lane Assist (ELA) presented in Paper A of this thesis.

The fact that typical ELA scenarios were identified as threatening provides additional support for the ELA function and also suggests that the new threat assessment algorithm is suitable to use in the ELA decision unit.

Furthermore, since no specific safety function is considered when the threat is evaluated, it could be used in a general decision unit in a future vehicle equipped with many safety functions. Instead of having several function doing threat assessment independently, one central threat assessor could be used to trigger different warning and intervention depending on the type of threat.

## 3.6 Road-aligned coordinates

Since the Road-Aligned Coordinates (RAC) appear as a central theme in almost all the papers in this thesis, this section is devoted entirely to this topic. First, it was demonstrated how RAC could be used to improve tracking performance of the road geometry estimates. This was done by modelling the motion of surrounding vehicles in relation to the RAC

instead of global, cartesian coordinates. First of all, the motion model can be greatly simplified. The assumption that cars will stay in their lane can be simply expressed as $\dot{y} = 0$ where $y$ denotes lateral position in the road coordinates. In a Cartesian or polar coordinate system, a higher order system would have to be used and would still only describe a more primitive shape, see Figure 3.15.

This also relates to predicting future positions of other vehicles. With the $\dot{y} = 0$ motion model, vehicles are predicted to follow straight lines, which in RAC means that they will follow the road. Prediction with a higher order model can be difficult since many people tend to wander slightly when driving. This means that a prediction, say 50 or 100 metres ahead will often be outside the road. This is illustrated to the right in Figure 3.15.

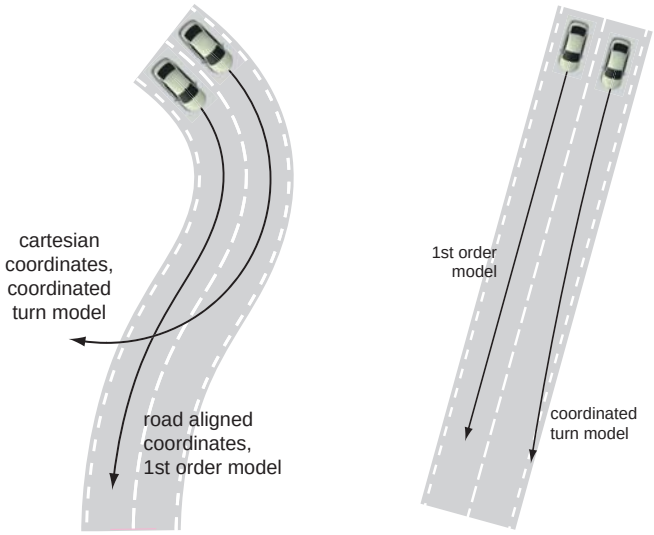


***Figure 3.15:*** *Left: Comparison between a road-aligned coordinate system with a low order motion model and a Cartesian coordinate system with a higher order motion model. In order to illustrate this difference, the curvature and clothoid parameters of this road have been exaggerated. Right: Prediction with a higher order motion model can be difficult since most people tend to wander slightly when driving.*

Also, since all positions are already given in the road coordinates, it is easier to design automotive applications. For instance, Adaptive Cruise Control (ACC) controls the speed of the host vehicle based on the distance to and speed of the leading vehicle. Using RAC, leading vehicles can be found simply as vehicles with $y$-coordinate close to zero. They will be in the same lane as the host vehicle, also in curves. Similarly, the ELA function is also dependent on the lane position of surrounding vehicles. Specifically, vehicles that are occupying the adjacent lanes need to be found. With RAC, this can be done by simply defining an interval in the $y$-coordinate.

In the statistical threat assessment algorithm in Paper D, RAC also gives several advantages. First, in the driver-behaviour model discussed above, it was noted that vehicles are very likely to keep following the road, *i.e.*, manoeuvres that behave in this way should

be given a high probability. For a specific manoeuvre, this is implemented by measuring the average distance to the intended path and then computing the probability based on that. In RAC, this simply means computing the lateral distance to a straight line, which is easier than measuring the distance to a circle or a clothoid segment. Second, the road edges, shown for example in Figure 3.14, can always be modelled as straight lines. This means that all objects in the algorithm can be modelled as polygons. In a Cartesian coordinate system, a new object class with circular shapes would have to introduced, or the road borders have to be approximated with straight segments.

One of the things that need to be considered before implementing decision algorithms based on curved coordinates is the change in the dynamics. There are certain limitations in the way that a vehicle can manoeuvre, caused, for example, by tire-to-road friction or limited engine power, which puts boundaries on the forces that can be exerted on the vehicle. These are then translated to accelerations via Newton's law. However, Newton's law cannot be applied directly in a non-Cartesian coordinate system, which is why Paper D derives modified dynamic equations. It turns out that these modifications can be implemented as a simple offset to the ordinary dynamic relationships. Using these modifications, all threat measures that are normally used in fixed Cartesian coordinates can be translated directly into the RAC.

# Bibliography


Braess, V. H.-H. and Reichart, G. (1995a). Prometheus: Vision des 'intelligenten automobils' auf 'intelligenter strasse'? versuch einer kritischen würdigung - teil 1. *ATZ Automobilitechn. Zeitschrift 97*.

Braess, V. H.-H. and Reichart, G. (1995b). Prometheus: Vision des 'intelligenten automobils' auf 'intelligenter strasse'? versuch einer kritischen würdigung - teil 2. *ATZ Automobilitechn. Zeitschrift 97*.

Citroën (2005). An innovation award for the LDWS. Press release, `www.citroen.com/CWW/en-US/NEWS/NEWSRELEASES/ArchivesNewsReleases/200506/23032005\_PRIXAFIL.htm`.

Crisman, J. and Thorpe, C. (1993). Scarf: A color vision system that tracks roads and intersections. *IEEE Transactions on Robotics and Automation*, 9(1):49 – 58.

DARPA (2006). DARPA Grand Challenge. web page, `www.darpa.mil/grandchallenge`.

Dellaert, F. and Thorpe, C. (1997). Robust car tracking using Kalman filtering and Bayesian templates. In *Proceedings of the SPIE conference on Intelligent Transportation Systems*, volume 3207.

Dickmanns, E. D. (2002). The development of machine vision for road vehicles in the last decade. In *Proceedings of the IEEE Intelligent Vehicles Symposium*, pages 268–281, Versailles, France.

Dickmanns, E. D. and Zapp, A. (1987). Autonomous high speed road vehicle guidance by computer vision. In *Selected Papers from the 10th Triennial World Congress of the International Federation of Automatic Control*, pages 221–226, Munich, Germany. Pergamon.

EUREKA (2006). Eureka | A Europe-wide network for market-oriented industrial R&D and innovation. web page, `www.eureka.be`.

European Road Federation (2004). European road statistics 2004. web page, `http://www.erf.be/section/statistics`.

Folksam (2005). Hur säker är bilen 2005. web page, `www.folksam.se/resurser/pdf/sakrabilar2005.pdf`.

Ishida, S. and Gayko, J. E. (2004). Development, evaluation and introduction of a lane keeping assistance system. In *Proceedings of the IEEE Intelligent Vehicles Symposium*, pages 943–344, Parma, Italy.

Jansson, J. (2005). *Collision Avoidance Theory with Application to Automotive Collision Mitigation.* PhD thesis, Linköping University, Linköping University, 581 83 Linköping, Sweden.

Jones, W. D. (2001). Keeping cars from crashing. *IEEE Spectrum*, pages 40–45.

Kamiya, H., Fujita, Y., Tsuruga, T., Nakamura, Y., Matsuda, S., and Enomoto, K. (1996). Intelligent technologies of honda asv. In *Proceedings of the IEEE Intelligent Vehicles Symposium 1996*, pages 236–241, Tokyo, Japan.

Kodaka, K. and Gayko, J. E. (2004). Intelligent systems for active and passive safety - collision mitigation brake system. In *Proceedings of the ATA 12th international symposium*, Parma, Italy.

NHTSA (2001). Traffic safety facts. web page, `www-nrd.nhtsa.dot.gov/pdf/nrd-30/NCSA/TSFAnn/TSF2001.pdf`.

Schmidhuber, J. (2005). Robot cars - autonomous vehicles - history of self-driving cars. web page, `www.idsia.ch/~juergen/robotcars.html`.

Schön, T. (2006). *Estimation of Nonlinear Dynamic Systems - Theory and Applications.* PhD thesis, Linköping, Sweden.

Thorpe, C. E. (1990). *Vision and Navigation: the Carnegie Mellon Navlab.* Kluwer Academic Publishers.

Thrun, S., Montemerlo, M., Dahlkamp, H., Stavens, D., Aron, A., Diebel, J., Fong, P., Gale, J., Halpenny, M., Hoffmann, G., Lau, K., Oakley, C., Palatucci, M., Pratt, V., Stang, P., Strohband, S., Dupont, C., Jendrossek, L.-E., Koelen, C., Markey, C., Rummel, C., van Niekerk, J., Jensen, E., Alessandrini, P., Bradski, G., Davies, B., Ettinger, S., Kaehler, A., Nefian, A., and Mahoney, P. (2006). Winning the darpa grand challenge. *Journal of field Robotics.* accepted for publication.

Williams, M. (1992). The prometheus programme. In *IEE Colloquium Towards Safer Road Transport - Engineering Solutions.*

Zomotor, Z. and Franke, U. (1997). Sensor fusion for improved vision based lane recognition and object tracking with range-finders. In *Proceedings of the IEEE Conference on Intelligent Transportation Systems.*

# Part II

# Publications

# Paper A

# Towards autonomous collision avoidance by steering

**Authors:** Andreas Eidehall, Jochen Pohl, Fredrik Gustafsson and Jonas Ekmark

Extended version of “A new approach to lane guidance systems”. In *Proceedings of the IEEE Intelligent Transportation Systems 2005*, pages 108-112.

Accepted for publication in *IEEE Transactions on Intelligent Transportation Systems*, 2006.

Preliminary version published as Technical Report LiTH-ISY-R-2754, Department of Electrical Engineering, Linköping University, Linköping, Sweden.

# Towards autonomous collision avoidance by steering

Andreas Eidehall[⋆§], Jochen Pohl[§], Fredrik Gustafsson[⋆] and Jonas Ekmark[§]

[⋆]Department of Electrical Engineering
Linköping University
SE–581 83 Linköping, Sweden

[§]Vehicle Dynamics and Active Safety
Volvo Car Corporation
SE–405 31 Göteborg, Sweden

**Abstract**

This paper presents a new automotive safety function called Emergency Lane Assist (ELA). ELA combines conventional lane guidance systems with a threat assessment module that tries to activate the lane guidance interventions according to the actual risk level of lane departure. The goal is to only prevent *dangerous* lane departure manoeuvres.

The ELA safety function is based on a statistical method which evaluates a list of safety concepts and tries to maximise the impact on accident statistics while minimising development and hardware component costs.

ELA runs in a demonstrator and it successfully intervenes during lane changes that are likely to result in a collision and is also able to take control of the vehicle and return it to a safe position in the original lane. It has also been tested on 2 000 km of roads in traffic without giving any false interventions.

# 1 Introduction

Active safety technology is currently becoming a major area of research in the automotive industry. One of the big issues is of course which technology or safety area to concentrate on. There are countless possibilities, but the best choice would, of course, be the one which gives most in return when it comes to improved safety. A method for evaluating active safety concepts has been developed in an attempt to systematically respond to this issue. Each safety concept or function is given a grade which is high when the estimated impact on accident statistics is high and the estimated cost per equipped vehicle is low. The result from the study is a new safety function concept "Emergency Lane Assist" (ELA), which is a new type of lane guidance system.

Lane guidance refers to technology that tries to prevent lane departure, typically by monitoring the lane markings using a vision system. The work on lane guidance and lane tracking already began in the late 1980's with work by Dickmanns and Zapp (1987), and also Thorpe (1990). These activities focused mainly on autonomous driving, rather than driver assistance and active safety. Early driver assistance systems was introduced by, for instance Chen et al. (1995) and LeBlanc et al. (1996) which discuss audio warning systems, and Isomoto et al. (1995) who presented a lane keeping system that used a steering wheel torque in order to keep the vehicle in the lane. More recent lane keeping systems have been presented by Lee and Kwon (2001) or Pohl and Ekmark (2003). Another rather recent idea to try to mimic the sounds and vibrations that are generated by rumble strips, *i.e.*, the grooved lane markings that are sometimes used on motorways. Pilutti and Ulsoy (2003) have investigated this, but a similar system has also recently been put into production by Citroën (Citroën, 2005). González-Mendoza et al. (2004) have presented an interesting overview of different decision methods and a comparison of lane departure warning concepts.

However, there are two concerns common to these systems. The first is of false alarm during intentional lane change. It is often claimed that this can be solved by disabling the interventions when the indicator is used, but studies have shown that in general, people do not use indicators for every lane change. In addition, it is very common behaviour to slightly cross the lane markings on the inside of bends; usually referred to as "curve cutting".

The second problem is misuse. A system that applies a steering wheel torque in order to keep the vehicle in the lane can almost be used as an autopilot system. For instance, the driver could rely on the system completely for short periods of time while carrying out distractive tasks like changing CDs or writing text messages, which are clearly very dangerous situations. Honda has proposed a solution where they only apply 80% of the required torque to keep the vehicle in the lane (Ishida and Gayko, 2004). This is in order to keep the driver at attention at all times. The problem is that if the driver is actually not at attention, *i.e.*, is distracted or misjudges the situation, the system will not prevent the lane departure. Honda's studies certainly shows that people find the vehicle more stable and easier to steer, but this makes the system more of a convenience system than a safety system. Of course, such systems might also contribute to safety by reducing the driver's workload (Naab and Reichart, 1994). Another possible solution is to combine the lane guidance system with some sort of driver monitoring device (Petersson et al., 2004). Clearly, if the system could be activated only when the driver is distracted or drowsy, this

would reduce the number of false alarms. As driver monitoring systems improve, this may become an interesting combination for further evaluation. Of course, such a combination would raise further questions, consider for example the issue of responsibility when the driver falls asleep but the system autonomously keeps the vehicle in the lane.

This article proposes a new safety function, called Emergency Lane Assist (ELA), which provides a method to reduce false alarms and problems of misuse associated with conventional lane guidance systems. This is achieved by only intervening during lane departure manoeuvres that are actually *dangerous*. The system includes a threat assessment module that monitors vehicles in adjacent lanes, and as soon as a lane change has begun which is likely to result in a collision, a steering intervention system is activated in order to return the vehicle to a safe state in the original lane.

The article begins with the evaluation method for active safety functions in Section 2. The ELA function itself is presented in Section 3 while Sections 4 and 5 presents the tracking system and the decision algorithm. The evaluation and results are discussed in Section 6. Appendix A presents definitions of the critical accident types used in the evaluation method and in Appendix B the evaluated safety functions are discussed.

# 2 Active safety technology evaluation

The first step in the analysis is to create a list of potential active safety systems. These potential systems are then evaluated based on utility and complexity. Utility is estimated using road accident statistics and complexity is based on the total cost-per-unit; the total development cost and hardware cost.

## 2.1 Statistics

Rather than projecting accident statistics directly on our potential active safety systems, statistics are first grouped into relevant categories and subcategories. For instance, all lane change accidents are identified as one main category, and then grouped into different subcategories depending on the relative speed and the relative position of the vehicles. Other main categories are “unintentional lane departure”, “intersection accidents” etc. Detailed definitions can be found in Appendix A.

Since statistics will be used for the evaluation of active safety systems, early events in an accident sequence are always the most interesting, *i.e.*, a car unintentionally leaving its lane and causing an accident is put in the group of “unintentional lane departure” regardless of what it hit and the category of damage on the vehicle. Any potential active safety system can then be evaluated by adding frequencies of the accident categories it would affect. This method is more flexible compared to evaluating specific active safety systems directly from statistics, since new systems can easily be added and evaluated.

The list of active safety systems that is evaluated is presented in Appendix B. Some of these concepts have been presented before and some of them are new and have been developed during creative discussions.

## 2.2 Estimating system utility

In the first stage a European traffic accident database called European Accident Causation Survey (EACS, 1996) is used which contains just under 2 000 accidents. The database is biased towards severe accident since half of the accidents are fatal accidents.

First, assume $n$ different accident categories are defined, and that these have the statistical frequencies $\mathbf{a} = (a_1, a_2, \ldots, a_n)$. Then the utility of a system $j$ can be estimated by first forming a vector $\mathbf{x}_j = (x_{1j}, x_{2j}, \ldots, x_{nj})$ where $0 \leq x_{ij} \leq 1$ describes the assumed or estimated effect the active safety system $j$ has on accident category $i$. (For example, $x_{ij} = 0.25$ would imply that system $j$ has a $25\%$ reduction of the number of accidents in category $i$.) The total system utility can then be defined as

$$u_j = \sum_{i=1}^{n} a_i x_{ij}. \tag{1}$$

The accident frequencies from EACS are presented in Figure 1. The definitions of the accident categories can be found in Appendix A. These accident categories are created to reflect important issues in potential active safety systems, but not with a particular active safety function in mind. Note that so far, only the data in category 8x has been divided into its subcategories. The reason for this is that for the other categories, the data was not sufficiently detailed. Table 1 shows the full utility matrix with the safety effects ($x_{ij}$) and

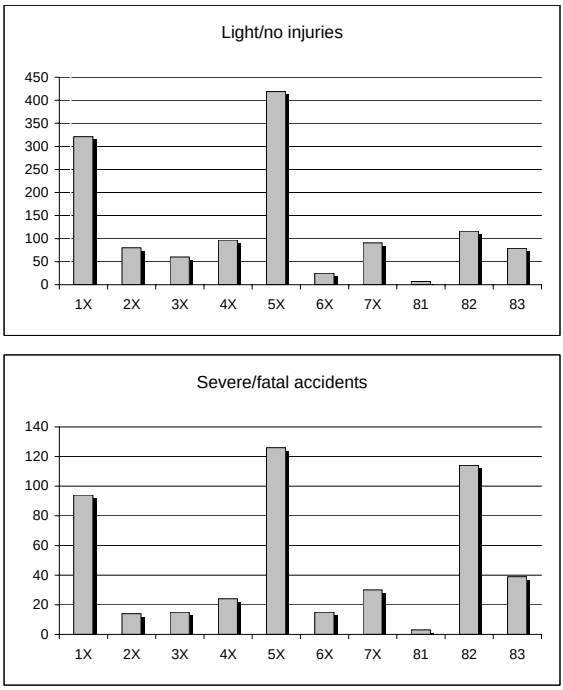


***Figure 1:*** *Diagram of data from the EACS database.*

corresponding active safety systems. Empty positions represent the value zero.

| | Accident type 1x | Accident type 2x | Accident type 3x | Accident type 4x | Accident type 5x | Accident type 6x | Accident type 7x | Accident type 81 | Accident type 82 | Accident type 83 | Light/no personal injuries | Fatal/severe accidents |
|---|---|---|---|---|---|---|---|---|---|---|---|---|
| LKA - Lane Keeping Aid | 20% | | | | | | | | | | 64.2 | 18.8 |
| LCA - Lane Change Aid | | | 10% | | | | | | | | 6 | 1.5 |
| CMbB | 5% | 30% | 5% | | | 5% | | | | | 44.3 | 10.4 |
| CMbB2 (CMbB + RFD) | 5% | 33% | 5% | | | 5% | | | | | 46.7 | 10.82 |
| CMbB3 (CMbB2 + RFD + Driver monitoring) | 5% | 40% | 5% | | | 5% | | | | | 52.3 | 11.8 |
| CW - Curvature Warning | | | | 15% | | | | | | | 14.55 | 3.6 |
| LAS1 - Lane Assist System (LKA + LCA) | 20% | | 10% | | | | | | | | 70.2 | 20.3 |
| LAS2 (LAS1 + traffic outside blind spot) | 20% | | 25% | | | | | | | | 79.2 | 22.55 |
| ELA (LAS2 + traffic in opposite direction) | 30% | | 25% | | | | | | | | 111.3 | 31.95 |
| GWW - Give Way Warning | | | | | 5% | | | | | | 20.95 | 6.3 |
| WS - Wildlife Scanner | | | | | | | | 10% | | | 0.7 | 0.3 |
| PBS - Pedestrian & Bicycle scanner | | | | | | | | | 25% | 25% | 48.75 | 38.25 |
| OGS - Overtaking Guidance System | | | | | | 10% | | | | | 2.5 | 1.5 |
| True CAbS - Collision Avoidance by Steering | 30% | 40% | 25% | | | 10% | | | | | 145.8 | 39.05 |
| True CAbS2 (True CAbS + RFD + Driver mon.) | 30% | 50% | 25% | | | 10% | | | | | 153.8 | 40.45 |
| Frequencies: | 321 | 80 | 60 | 97 | 419 | 25 | 91 | 7 | 116 | 79 | Light/no personal injuries | |
| | 94 | 14 | 15 | 24 | 126 | 15 | 30 | 3 | 114 | 39 | Fatal/severe accidents | |

***Table 1:*** *Utility matrix with the assumed impact on the different accident categories and the resulting utility value of each system.*

## 2.3 Estimating system complexity

The complexity/cost of a system is based on the cost of its hardware components and a template development cost. The development cost is divided into three different areas:

- Engineering
- Test objects
- Tooling and production equipment

The sum of these costs is then divided by an estimated volume multiplied by the expected penetration of the system throughout the product line. These figures are all estimated based on the vast experience of the engineers at the department of *Vehicle Dynamics & Active Safety* at Volvo Car Corporation. For system $j$, these are labelled $c_j^E$, $c_j^T$ and $c_j^P$ respectively. Now, if the total volume is $V$ and $p_j$ denotes the number of these vehicles, system $j$ is installed in ($p_j \in [0, 1]$ is usually referred to as *penetration* or *take rate*), then the development cost $c_j^D$ per unit can be calculated as

$$c_j^D = \frac{c_j^E + c_j^T + c_j^T}{p_j V}. \tag{2}$$

The system hardware cost can be estimated in a similar way to system utility. This time, a set of $m$ hardware components with a cost vector $\mathbf{b} = (b_1, b_2, \ldots, b_m)$ are used. Next,

for system $j$, the vector $\mathbf{y}_j = (y_{1j}, y_{2j}, \ldots, y_{mj})$ is constructed, where $y_{kj} = 1$ if system $j$ involves hardware component $k$, if not $y_{kj} = 0$. The component cost $c_j^C$ of system $j$ can then be calculated as

$$c_j^C = \sum_{i=1}^{n} b_i y_{ij}. \tag{3}$$

The hardware components and their costs are presented in Table 2.

| Component | Assumed cost per unit (MU) |
|---|---:|
| Laser | 900 |
| Front view camera | 600 |
| Side mirror camera | 900 |
| Infrared camera | 2100 |
| RTI (GPS navigation system) | 750 |
| Steering wheel sensor | 0 |
| Gyro | 0 |
| Road friction detector | 6 |
| Driver monitoring system | 450 |
| Brake actuator | 0 |
| Steering actuator | 0 |

***Table 2:*** *Cost of the hardware components in monetary units (MU). A cost of zero means that the component already is available in the vehicle,* i.e.*, the cost is carried by other systems.*

The total cost per unit is then obtained as the sum of (2) and (3):

$$c_j = c_j^D + c_j^C. \tag{4}$$

Component and development costs are summarised in Table 3. Again, empty positions represent the value zero.

## 2.4 Results

In Table 4, for each system, the ratio $u_j/c_j$, utility/cost is computed, based on the information in Table 1 and Table 3. This is a way of comparing systems of different complexity and fields of application. The goal function $u_j/c_j$ seems plausible, although other functions, such as $u_j^2/c_j$ could also be studied.

In Table 4 the target function is calculated in two columns, first light/no injuries and second severe/fatal accidents. In addition, to indicate potential candidates, the values higher than half of the highest value of that column are highlighted with arrows. Inspecting the decision matrix (Table 4) shows that the following choices have a high goal function value:

- Lane Keeping Aid (LKA)

| | Hardware components | | | | | | | | | | | | |
|---|---|---|---|---|---|---|---|---|---|---|---|---|---|
| | Laser | Wide Laser | Front view camera | Side mirror camera | Infrared camera | RTI - GPS | Road friction detector | Driver monitoring | Braking actuator | Steering actuator | Component cost/unit (MU) | Development cost/unit (MU) | Total cust/unit (MU) |
| LKA - Lane Keeping Aid | | | 1 | | | | | 1 | | 1 | 1050 | 198 | 1248 |
| LCA - Lane Change Aid | | | | 1 | | | | | | | 900 | 198 | 1098 |
| CMbB | 1 | | 1 | | | | | | 1 | | 1500 | 36 | 1536 |
| CMbB2 (CMbB + RFD) | 1 | | 1 | | | | 1 | | 1 | | 1506 | 39 | 1545 |
| CMbB3 (CMbB2 + RFD + Driver monitoring) | 1 | | 1 | | | | 1 | 1 | 1 | | 1956 | 261 | 2217 |
| CW - Curvature Warning | | | | | | 1 | 1 | | | | 756 | 108 | 864 |
| LAS1 - Lane Assist System (LKA + LCA) | | | 1 | 1 | | | | | | | 1500 | 426 | 1926 |
| LAS2 (LAS1 + traffic outside blind spot) | | 1 | 1 | 1 | | | | | | | 2850 | 630 | 3480 |
| ELA (LAS2 + traffic in opposite direction) | | 1 | 1 | 1 | | | | | | 1 | 2850 | 690 | 3540 |
| GWW - Give Way Warning | | | 1 | | | 1 | 1 | | 1 | | 1356 | 372 | 1728 |
| WS - Wildlife Scanner | | | 1 | | 1 | | 1 | | 1 | | 2706 | 360 | 3066 |
| PBS - Pedestrian & Bicycle scanner | | 1 | 1 | | | | | | 1 | | 1950 | 32.4 | 1982 |
| OGS - Overtaking Guidance System | 1 | | 1 | 1 | | 1 | | | | | 3150 | 408 | 3558 |
| True CAbS - Collision Avoidance by Steering | | 1 | 1 | 1 | | | | | 1 | 1 | 2850 | 1050 | 3900 |
| True CAbS2 (True CAbS + RFD + Driver mon.) | | 1 | 1 | 1 | | | 1 | 1 | 1 | 1 | 3306 | 1212 | 4518 |
| Cost per unit (MU) | 900 | 1350 | 600 | 900 | 2100 | 750 | 6 | 450 | 0 | 0 | | | |

***Table 3:*** *Cost matrix. The costs are expressed in Monetary Units (MU).*

- Collision Mitigation by Braking (CMbB)
- Lane Assist System (LAS)
- Emergency Lane Assist (ELA)
- Pedestrian & Bicycle scanner
- Collision Avoidance by Steering (CAbS)

Note that early versions of Lane Keeping Aid and CMbB systems are already on the market. The Lane Assist System is simply a combination of Lane Keeping Aid and Lane Change Aid (sometimes also referred to as Blind Spot Warning) which is soon also to be launched on the market. Emergency Lane Assist is a new system which has a high estimated impact on accident statistics. To the best of the author's knowledge, this type of system is not currently being researched. Pedestrian & Bicycle scanner also receives a high grade, in particular when it comes to severe or fatal accidents.

The system CAbS is based on ELA and CMbB. Given the fact that CMbB is already being developed, developing ELA seems to be a good direction for our future work. ELA is a valuable system on its own, but also a first step towards more advanced safety functions since it requires a more complete picture of the vehicle surroundings, *i.e.*, both lane shape and orientation *and* position of surrounding vehicles.

| | Total cost/unit | Utility (light/no injuries) | **Ratio (100*utility/cost)** | Utility (severe/fatal accidents) | **Ratio (100*utility/cost)** |
|---|---|---|---|---|---|
| LKA - Lane Keeping Aid | 1248 | 64.2 | **5.1** < | 18.8 | **1.5** < |
| LCA - Lane Change Aid | 1098 | 6.0 | **0.5** | 1.5 | **0.1** |
| CMbB | 1536 | 44.3 | **2.9** < | 10.4 | **0.7** |
| CMbB2 (CMbB + RFD) | 1545 | 46.7 | **3.0** < | 10.8 | **0.7** |
| CMbB3 (CMbB2 + RFD + Driver monitoring) | 2217 | 52.3 | **2.4** | 11.8 | **0.5** |
| CW - Curvature Warning | 864 | 14.6 | **1.7** | 3.6 | **0.4** |
| LAS1 - Lane Assist System (LKA + LCA) | 1926 | 70.2 | **3.6** < | 20.3 | **1.1** < |
| LAS2 (LAS1 + traffic outside blind spot) | 3480 | 79.2 | **2.3** | 22.6 | **0.6** |
| ELA (LAS2 + traffic in opposite direction) | 3540 | 111.3 | **3.1** < | 32.0 | **0.9** |
| GWW - Give Way Warning | 1728 | 21.0 | **1.2** | 6.3 | **0.4** |
| WS - Wildlife Scanner | 3066 | 0.7 | **0.0** | 0.3 | **0.0** |
| PBS - Pedestrian & Bicycle scanner | 1982 | 48.8 | **2.5** | 38.3 | **1.9** < |
| OGS - Overtaking Guidance System | 3558 | 2.5 | **0.1** | 1.5 | **0.0** |
| True CAbS - Collision Avoidance by Steering | 3900 | 145.8 | **3.7** < | 39.1 | **1.0** < |
| True CAbS2 (True CAbS + RFD + Driver mon.) | 4518 | 153.8 | **3.4** < | 40.5 | **0.9** |

***Table 4:*** *Decision matrix: Values higher than half of the maximum value have been highlighted using arrows.*

# 3 Emergency Lane Assist

The Emergency Lane Assist (ELA) system is a new type of lane guidance system in which the goal is to prevent *dangerous* lane departure manoeuvres. The system monitors adjacent lanes and as long as there are no other vehicles approaching, lane markings can be crossed without ELA intervention, but as soon as a commenced lane change manoeuvre is assessed as being dangerous with respect to, for example an oncoming vehicle, a torque is applied to the steering wheel in order to prevent lane departure. The level of risk of a lane change manoeuvre is evaluated based on the position and motion of vehicles in the adjacent lanes, but road edges, guard rails or even solid lane markings could also be used to trigger intervention. This approach makes ELA a pure safety system rather than a comfort/convenience system. Figure 2 shows critical ELA situations.

A prerequisite is that ELA must never prevent an avoidance manoeuvre, *i.e.*, if the driver is trying to avoid an obstacle in the current lane, ELA must never produce a steering wheel torque leading the vehicle towards this threat. Avoidance manoeuvres could be detected, for instance by looking for threats in the lane of the host vehicle, but also by using some sort of driver interpretation module which analyses the strength and speed of the steering wheel manoeuvre.

# 4 Tracking system

Active safety technology, such as the Emergency Lane Assist system will require detailed knowledge about vehicle surroundings. In this case, vehicle surroundings refers to lane

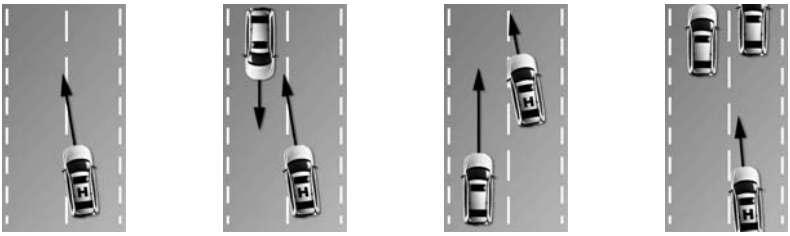

No ELA intervention since there is no threat in the adjacent lane. | ELA intervention. | ELA intervention. | No ELA intervention since there is a threat also in the own lane.

***Figure 2:*** *Critical ELA situations. The letter "H" indicate the ELA host vehicle.*

geometry and other vehicles. Typically, lane information is obtained from a vision system and vehicles are detected using vision and radar.

The importance of integrating data from object tracking and road geometry tracking is a fairly new research field (Dellaert and Thorpe, 1997, Zomotor and Franke, 1997, NHTSA, 2000, Polychronopoulos et al., 2004). The main idea is to try to improve the road geometry estimate by studying the motion of target vehicles and vice versa. For instance, if a couple of tracked vehicles suddenly all move to the right, one of two things may have happened. The first is that they all started a lane change manoeuvre and the road remains straight. The second possibility is that we enter a curve and the vehicles still follow the centre of their lanes. These possibilities can be treated in a Bayesian framework, *e.g.*, the Kalman filter, using the information from the lane tracker, to build a new estimator.

The sensors, consisting of a vision system and a radar, measures $L$ and $R$, the distances to the left and right lane markers, $\Psi_{\text{rel}}$, the angle of host vehicle in relation to the lane, and $c_0$, the road curvature. For each observed vehicle, the relative position $(\tilde{x}, \tilde{y})$ in the host vehicle coordinate frame is also provided, see Figure 3. The radar also delivers range rate using doppler phase shift. The goal is then, using an extended Kalman filter, to estimate the states $W$ - lane width, $y_{\text{off}}$ - host vehicle lateral position, $\Psi_{\text{rel}}$, $c_0$ and $c_1$, where $c_1$ is the so called clothoid parameter, *i.e.*, the change rate of $c_0$. For other vehicles, the relative position $(x, y)$ in the road-aligned coordinate system, and the relative longitudinal velocity $v$ is estimated. In order to do this, a new object measurement equation based on the road geometry needs to be formulated.

## 4.1 Motion model

In the road coordinates $(x, y)$, the motion model for the target vehicles can be greatly simplified. For instance, it allows us to use the equation $\dot{y} = 0$, which simply means that

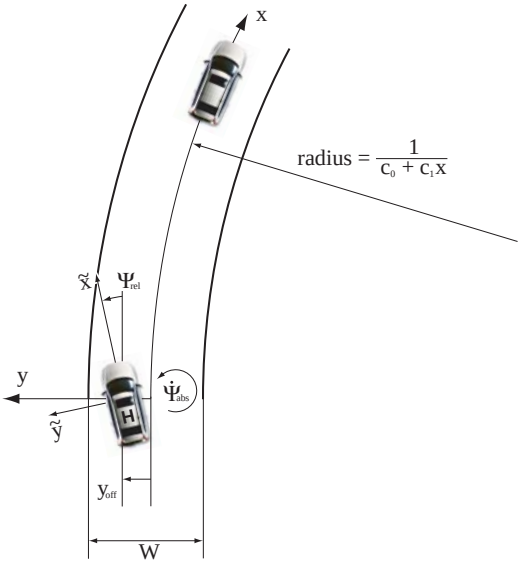


***Figure 3:*** *The coordinate systems used in formulating the dynamic motion model. Here, $(x, y)$ denotes the position in a curved coordinate system which moves with the host vehicle, but is aligned with the road. Furthermore, $(\tilde{x}, \tilde{y})$ denotes the position in a Cartesian coordinate system which is attached to the moving host vehicle.*

the target vehicles will follow their own lanes. The longitudinal model is simply $\ddot{x} = 0$. Hence, the following motion model is obtained:

$$\dot{x}^i = v^i, \tag{5a}$$

$$\dot{v}^i = 0, \tag{5b}$$

$$\dot{y}^i = 0, \tag{5c}$$

where $i$ is used to index all tracked vehicles. $v^i$ is the longitudinal velocity *i.e.*, the time derivative of $x^i$. For the road geometry parameters first it is clarified that $\Psi_{\text{rel}}$ is the angle between the host vehicle and the lane, whereas $\Psi_{\text{abs}}$ is the angle to some fixed reference point. A relationship between the two can be obtained by differentiating $\Psi_{\text{rel}}$ with respect to time:

$$\begin{aligned} &\Psi_{\text{rel}} = \Psi_{\text{abs}} + \gamma \quad \Rightarrow \\ &\dot{\Psi}_{\text{rel}} = \dot{\Psi}_{\text{abs}} + \dot{\gamma} = \dot{\Psi}_{\text{abs}} + \frac{v}{r} = \dot{\Psi}_{\text{abs}} + c_0 v, \end{aligned} \tag{6}$$

where $r$ is the road radius and $c_0$ is the road curvature at the host vehicle position, which means that $r = 1/(c_0 + c_1 x)|_{x=0} = 1/c_0$. We also write $v$ for the velocity of the host vehicle and $\gamma$ denotes the angle between the lane and some fixed reference. $\dot{\Psi}_{\text{abs}}$ can typically be measured using a yaw rate sensor. In addition,

$$\dot{y}_{\text{off}} = \sin(\Psi_{\text{rel}})v \approx \Psi_{\text{rel}} v. \tag{7}$$

To summarise, the motion of host vehicle is modelled as s

$$\dot{y}_{\mathit{off}} = v\Psi_{\text{rel}}, \tag{8a}$$
$$\dot{\Psi}_{\text{rel}} = vc_0 + \dot{\Psi}_{\text{abs}}. \tag{8b}$$

A dynamic model for the shape of the road is also used. The two parameters $c_0$ and $c_1$ can be shown to be connected via $\dot{c}_0 = vc_1$. For the width of the lane, the model $\dot{W} = 0$ is be used. To summarise,

$$\dot{W} = 0, \tag{9a}$$
$$\dot{c}_0 = vc_1, \tag{9b}$$
$$\dot{c}_1 = 0. \tag{9c}$$

The discrete-time dynamics is then given by the standard sampling formula, assuming piece-wise constant input signals and sampling time $T_s$ (Rugh, 1996). Furthermore, adding stochastic process noise, the discrete-time motion equations for the target vehicles (5) become

$$x^i_{t+1} = x^i_t + T_s v^i_t + w^i_{1,t}, \tag{10a}$$
$$v^i_{t+1} = v^i_t + w^i_{2,t}, \tag{10b}$$
$$y^i_{t+1} = y^i_t + w^i_{3,t}. \tag{10c}$$

The host vehicle dynamics (8) become

$$\begin{aligned} y_{\mathit{off},t+1} &= y_{\mathit{off},t} + vT_s\Psi_{\text{rel},t} + v^2T_s^2c_{0,t}/2, \\ &\quad + v^3T_s^3c_{1,t}/6 + vT^2\dot{\Psi}_{\text{abs},t}/2 + w_{5,t}, \end{aligned} \tag{11a}$$
$$\begin{aligned} \Psi_{\text{rel},t+1} &= \Psi_{\text{rel},t} + vT_sc_{0,t} + v^2T_s^2c_{1,t}/2, \\ &\quad + T_s\dot{\Psi}_{\text{abs},t} + w_{6,t}, \end{aligned} \tag{11b}$$

and for the road model (9) we get

$$W_{t+1} = W_t + w_{4,t}, \tag{12a}$$
$$c_{0,t+1} = c_{0,t} + vT_sc_{1,t} + w_{7,t}, \tag{12b}$$
$$c_{1,t+1} = c_{1,t} + w_{8,t}. \tag{12c}$$

The variables $\{w_{i,t}\}_{i=1\ldots8}$ are white, zero-mean Gaussian process noise, with covariance matrices $Q_{host}$ and $Q_{obj}$ for the host and object states, respectively.

## 4.2 Measurement model

The measurements for the host vehicle are $\Psi^m_{\text{rel}}$, $c^m_0$, see Figure 3. $L^m$ and $R^m$ are the distances to the left and right lane markings. Superscript $m$ denotes measured quantities. For the other vehicles we measure the position, $\tilde{x}^m$ and $\tilde{y}^m$, which is expressed in the

Cartesian coordinate system attached to the vehicle. These relate to the states as

$$L_t^m = W_t/2 - y_{\text{off},t} + e_{1,t}, \tag{13a}$$

$$R_t^m = -W_t/2 - y_{\text{off},t} + e_{2,t}, \tag{13b}$$

$$\Psi_{\text{rel},t}^m = \Psi_{\text{rel},t} + e_{3,t}, \tag{13c}$$

$$c_{0,t}^m = c_{0,t} + e_{4,t}, \tag{13d}$$

$$\begin{bmatrix} \tilde{x}_t^{i,m} \\ \tilde{y}_t^{i,m} \end{bmatrix} = T(x_t^i, y_t^i) + \begin{bmatrix} e_{5,t} \\ e_{6,t} \end{bmatrix}^i, \tag{13e}$$

where the variables $\{e_{i,t}\}_{i=1\ldots6}$ denote white, zero-mean Gaussian measurement noise with covariance matrices $R_{host}$ and $R_{obj}$ for the host/road and object states, respectively. $T$ is the geometric transformation from the $(x, y)$ coordinates to the $(\tilde{x}, \tilde{y})$ coordinates and $i$ is used to index the tracked objects. The transformation $T$ is given by Eidehall and Gustafsson (2004) as

$$T(x, y) = R(\Psi_{\text{rel}}) \begin{bmatrix} (1 + c_0 y)\sin(c_0 x) \\ (1 + c_0 y)\cos(c_0 x) - 1 - c_0 y_{\text{off}} \end{bmatrix} \frac{1}{c_0}, \tag{14}$$

where $R(\Psi_{\text{rel}})$ is the rotation matrix

$$R(\Psi_{\text{rel}}) = \begin{bmatrix} \cos(\Psi_{\text{rel}}) & \sin(\Psi_{\text{rel}}) \\ -\sin(\Psi_{\text{rel}}) & \cos(\Psi_{\text{rel}}) \end{bmatrix}. \tag{15}$$

A Kalman filter can then be based on this model in order to estimate the desired parameters to be used in the decision algorithm. Note that the measurement equation (13e) is nonlinear and thus the extended Kalman filter has to be used, where (13e) is linearised online.

# 5 Decision algorithm

As was indicated in Section 3, the goal of the decision algorithm is to detect when a commenced lane change manoeuvre will result in a dangerous situation. This can be done in the following steps:

1. Check whether a lane change is in progress. This can be done by testing for the host vehicle $y_{\text{off}} > T_y, \Psi_{\text{rel}} > T_\Psi$ for a lane change to the left and $y_{\text{off}} < -T_y, \Psi_{\text{rel}} < -T_\Psi$ for a lane change to the right. Here, $T_y$ and $T_\Psi$ are thresholds, typically determined by empirical studies. In other words, it is required that the host vehicle is close to one of the lane markings and at the same time moves toward it.

2. Check which objects are in the "next" lane. If $N$ is the total number of tracked vehicles, these can be found as $I = \{i \in [1, N] : y^i \in L\}$ where $L = [W/2, 3W/2]$ if the host vehicle changes lanes to the left or $L = [-3W/2, -W/2]$ if the host vehicle changes lanes to the right. If the set $I$ is empty, then there is no threat and the algorithm can be terminated.

3. The times to crossing lane markings A and B in Figure 4 are calculated, these are referred to as $T_{\mathrm{A}}$ and $T_{\mathrm{B}}$, respectively. These can be computed in different ways, as is demonstrated by van Winsum et al. (2000) or Mammar et al. (2006). Here, a simple formula is chosen:

$$T_{\mathrm{A}} = \frac{W/2 - |y_{\text{off}}|}{|\sin \Psi_{\text{rel}}| v}, \tag{16}$$

$$T_{\mathrm{B}} = \frac{3W/2 - |y_{\text{off}}|}{|\sin \Psi_{\text{rel}}| v}, \tag{17}$$

where $W/2 - |y_{\text{off}}|$ is the distance to lane marking A, $3W/2 - |y_{\text{off}}|$ is the distance to lane marking B and $|\sin \Psi_{\text{rel}}| v$ is the lateral velocity.

4. A region is defined in the longitudinal dimension (region C in Figure 4), where the length is the sum of the host vehicle length, the threat vehicle length and an extra safety buffer zone. Formally, $C = [-L - B/2, L + B/2]$ where $L$ is a typical vehicle length and $B$ is the length of the safety buffer.

5. The position of all objects in $I$ between time $T_{\mathrm{A}}$ and $T_{\mathrm{B}}$ are predicted. At the times $T_{\mathrm{A}}$ and $T_{\mathrm{B}}$, the positions of object $i$ are referred to as $x^i_{\mathrm{A}}$ and $x^i_{\mathrm{B}}$, see Figure 4. They are based on a constant velocity assumption and are computed as

$$x^i_{\mathrm{A}} = x^i + v^i T_{\mathrm{A}}, \tag{18}$$

$$x^i_{\mathrm{B}} = x^i + v^i T_{\mathrm{B}}. \tag{19}$$

The set $R_i$ is then defined as the interval between these points, *i.e.*, $R_i = [x^i_{\mathrm{A}}, x^i_{\mathrm{B}}]$.

6. If for any $i \in I$, $R_i$ and $C$ overlap, *i.e.*, the intersection $R_i \bigcap C$ is nonempty, then there is a conflict with object $i$. This means that if the lane change is completed, there will be a collision. Note that no distinction needs to be made between vehicles coming from different directions.

7. The final step is to check for objects in the host vehicle lane. First form the set $J = \{j \in [1, N] : y^j \in [-W/2, W/2]\}$, *i.e.*, all objects in the host vehicle lane are chosen. Then, for all $j \in J$, compute a threat level $T_j = f_{\text{THREAT}}(x^j, v^j)$, where $x^j$ and $v^j$ are the relative distance to and the relative velocity of the tracked vehicle. Take for example,

$$f_{\text{THREAT}}(x, v) = \frac{v^2}{2xG}, \tag{20}$$

where $G$ is the gravitational acceleration. This is sometimes referred to as the Brake Threat Number (BTN) and relates the deceleration required to avoid an obstacle with the maximum available deceleration, assuming a friction coefficient of one. This is then compared to a threshold $T_{\text{BTN}}$ which in the present application is based on empirical studies, and is usually somewhere between 0.1 and 0.3. If

$$\max_{j \in J} T_j < T_{\text{BTN}} \tag{21}$$

the host lane is regarded as conflict-free, and the ELA intervention can safely be initiated.

Furthermore, if the sensors have the capability of detecting solid lane markings, road barriers or even road edges, this could also be incorporated into the algorithm. If a lane change manoeuvre commences in the direction of a solid lane marking, ELA could also be activated and give rise to a steering wheel torque, to try to prevent lane departure, even though there are no threatening objects in the adjacent lane.

One appealing property of the road-aligned coordinate system is that these kinds of decision algorithms can be specified without having to take into account the curvature of the road. If the road coordinate system was not used we would have to, for each obstacle observed, judge its lane position based on its polar $(\phi, r)$-coordinates. It also makes the accuracy of predicted positions $x_{\mathrm{A}}$ and $x_{\mathrm{B}}$ higher, since the assumption is that they will follow their lane, not their current tangent.

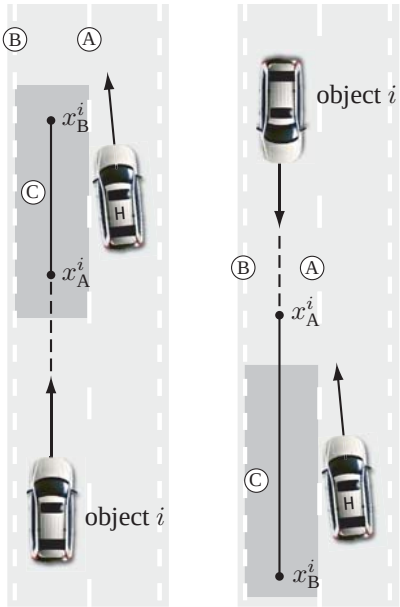


***Figure 4:*** *$T_{\mathrm{A}}$ and $T_{\mathrm{B}}$ are the times to cross lane A and lane B respectively and $x_{\mathrm{A}}^i$ and $x_{\mathrm{B}}^i$ are the positions of target vehicle $i$ at these times. A lane change manoeuvre is considered dangerous if the system predicts another vehicle entering region C during the time interval $[T_{\mathrm{A}}, T_{\mathrm{B}}]$. The same strategy can be applied to vehicles in both directions.*

To carry out the intervention a lateral controller is activated. Lateral control for vehicles is a well-studied problem (Hessburg and Tomizuka, 1991, Chaib et al., 2004, Ishida and Gayko, 2004, Beji and Bestaoui, 2005, Naranjo et al., 2005) and for the ELA application an existing lateral controller from Volvo Car Corporation was used. The controller is based on work done by Pohl and Ekmark (2003) but is modified so that the time to


***Figure 5:*** *Demonstration of a typical ELA intervention.*

collision affects the strength of the steering wheel torque. A short time to collision will yield a strong steering wheel torque and vice versa.

# 6 Evaluation

Evaluation and verification of active safety systems is a great challenge for the automotive industry. With early active safety technology such as ABS (Anti-lock Brake System) and ESP (Electronic Stability Program) there are only a limited number of road surfaces and vehicle manoeuvres to test, but with currently emerging forward collision warning and mitigation systems, and with future safety functions such as ELA, there is an explosion of different possible real world scenarios that can occur. For example, all possible positions, velocities and behaviours of surrounding vehicles will cause different behaviours in the system. Typically, the way that such systems are tested is not by analysing performance in all possible situations, although this could be done using a simulation (Jansson, 2005). Instead, a combination of testing in real traffic and for a number of specific critical scenarios is carried out. First, a couple of concepts for testing the performance of warning/alarm systems in general are defined:

**True positive** This refers to situations where the system correctly triggers an alarm, *i.e.*, intervenes in a lane departure that would probably have resulted in a collision.

**False positive** In these cases, the system triggers an alarm for a situation where it should not have done so, *i.e.*, false alarms. For instance, an intervention for a safe lane change, or an intervention not at all related to a lane change.

**True negative** In this case, the system correctly does not trigger an alarm, *i.e.*, does not intervene during normal driving and safe lane changes.

**False negative** In these situations the system fails to trigger an alarm for a situation where it should have done so, *i.e.*, missed alarms, for instance during a lane change that is likely to result in a collision with a vehicle in the adjacent lane.

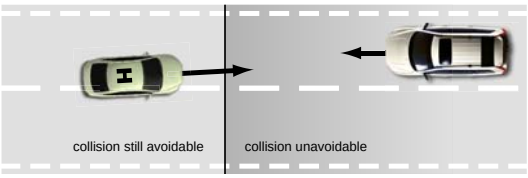


***Figure 6:*** *The "unavoidable zone" refers to positions where no steering or braking manoeuvre can avoid the collision, a vehicle which has entered this zone has no way of escaping the collision. Thus, a collision avoidance system will have to intervene before this zone is entered. The same region can also be defined in the time domain which, in some cases, can be more intuitive.*

In order to evaluate positive performance, *i.e.*, the probability of an alarm in a situation where an alarm is desired, accident situations will need to be artificially reconstructed, which is typically done on a test track. Negative performance, *i.e.*, the probability of a false alarm, is usually verified by running the system on public roads for long distances to ensure that no false alarms or interventions occurs.

For an automotive active safety system, especially for collision avoidance systems, it is also important to understand that there are two types of "false" actions. First, since the system, by definition, should avoid the collision, the intervention must take place *before* the collision becomes unavoidable, see Figure 6. Consequently, the driver still has a chance to avoid the collision by steering or braking. Thus, there will thus be situations where the system intervenes even though the situation would not have resulted in a collision since the driver intended to perform a late avoidance manoeuvre. Therefore, the system acts correctly according to its definition, but the driver still perceives this as an error. Similarly, there might be situations where a driver expects a warning or intervention but the system will not have triggered an alarm yet.

The second type of error is where the system does *not* act according to its definition, typically due to sensing or tracking errors.

This is important to keep in mind when trying to eliminate false alarms. The first type of errors is addressed by working with the decision algorithm and the second type of error is addressed by tuning the tracking system and setting requirements on the sensors.

## 6.1 Demonstrator vehicle

For evaluation, a Volvo V70 equipped with a forward looking radar and a vision system was used. The radar is the type normally used for adaptive cruise control applications, and the camera is an of-the-shelf system with lane tracking and vision based object detection. The system has so far not been tested with rear looking sensors.

## 6.2 Positive performance

In order to evaluate positive performance, a closed test track with artificially created critical accident situations was used. For this particular test, a straight track of length 300

metres with two lanes of width 3.2 metres each was used. An inflatable dummy vehicle was placed in one of the lanes in order to trigger the intervention. It is the same type of test object that is used in, for instance, the testing of Collision Mitigation by Braking systems (Jansson, 2005). The dummy is designed to resemble a real car to the sensors, but at the same time it must not damage the host vehicle in a collision. Tests have been carried out using both stationary and movable dummy vehicles, but so far not with multiple objects simultaneously. Figure 7 shows a typical intervention sequence were a selection of signals in the system are plotted. Just after 3 seconds, the dummy is detected and just before 4 seconds the ELA intervention system is triggered. In this test sequence, the actual intervention was not active, instead the host vehicle was allowed to collide with the dummy. This is in order to allow for off line tuning of the threat assessor, since an intervention would affect the data sequence. The vehicle has also been run with the interventions activate, and the controller is able to steer the vehicle back to the centre of the original, safe lane and achieve a heading angle close to zero.

Note that just after 5 seconds, the lane change is completed, which, by definition is when all four wheels of the host vehicle have crossed the lane markings. From this time, lateral positions are measured in relation to the new lane, this is the reason for the jump in the lateral positions at the top plot of Figure 7. At the same instant, the ELA warning level drops to zero. This is due to the fact that the obstacle is now in our lane, not in the adjacent lane. In the figure it can be seen that the lateral position of the obstacle jumps from around -3 metres to around 0 metres. An ELA intervention now would imply that the system steers the vehicle towards to centre of the new lane, which is an undesired behaviour. Instead, this situation is left to forward collision warning and mitigation systems.

To clarify, an intervention that has been commenced will always be completed until the host vehicle is safely positioned in the centre of the original lane, even if the ELA warning level drops to zero. The fact that the warning level is zero only means that the system will not trigger a new intervention.

## 6.3 Negative performance

In order to verify that no false interventions are given, two different types of tests are carried out. In the first, several “near miss” tests with the inflatable dummy are done, where either the lane change towards the threat is done very late in order to just miss the object or the test driver of the host vehicle would manually steer around the obstacle just before the collision. The second test consist of a large database of recorded sensor data that has been used to verify the functionality of the system.

In the first test, where false interventions are triggered intentionally, a couple of interventions has been detected, even though there were no collisions. A typical case is when the host vehicle starts to make an unsafe lane change, similar to when positive performance is tested, but then steers to avoid collision at a very late stage. This is in fact a general problem for any collision *avoidance* system. By definition, in order to avoid the collision, the system needs to act *before* it becomes unavoidable. This means that there will always be situations where the system intervenes even though the driver is in control of the situation and was planning a late avoidance manoeuvre.

In the second test a large amount of data is used, which is recorded during typical driving situations. The entire database consists of 40 000 km of data, so far the system

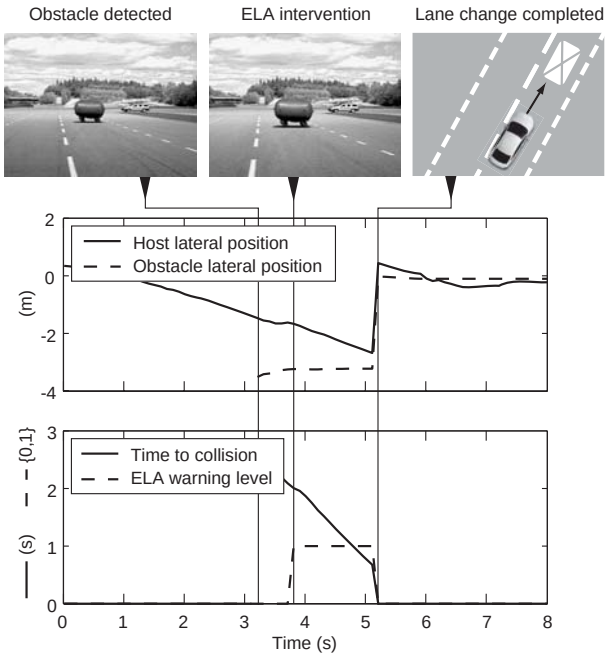


***Figure 7:*** *A typical ELA intervention sequence, the host vehicle speed is about 40 km/h. Note that in this case only the decision algorithm is evaluated, the actual intervention module has been deactivated. By disabling the interventions and actually colliding with the dummy, the logged data can be used for off-line tuning of the decision algorithm since no steering intervention interferes with the data. When the lane change is completed, the ELA warning level is deactivated. See Section 6.2 for an explanation of this behaviour.*

has been tested on a subset of 2 000 km, chosen such that a representative variety of driving conditions have been kept. From these tests we learned that in practice, the issue of intentional late avoidance manoeuvres is not really a problem. Not a single false intervention has been detected due to such driving behaviour. Furthermore, if the system is disabled in situations with extremely poor or ambiguous lane markings, not a single false alarm has been experienced, which is an encouraging result.

# 7 Conclusions

The main result of this work is the development of the Emergency Lane Assist concept and that it has a high potential to reduce the number of accidents in major accident categories while simultaneously reducing false alarms and problems of misuse with conventional lane guidance systems. Of course, since ELA is a preventive system, it needs to intervene when there is still time to avoid a collision. Thus, in theory there is still a risk of false alarms.

The performance has been evaluated, both in a controlled test environment where interventions were triggered, and in real traffic situations where no interventions are desired. From these results it is concluded that the outlook of reaching sufficient performance for the proposed active safety function regarding false alarms and intervention failure looks promising.

Future work include evaluating and developing the decision algorithm further, for instance using artificial environments with multiple objects.

# Appendix A: Accident categories

These are the accident categories and subcategories. As mentioned in Section 2.2, these accident categories were created to reflect important issues in potential active safety systems, but not with a particular active safety function in mind. Note that the vehicle marked with an “H” in each scenario refers to the host vehicle which is equipped with the active safety function. Each row consist of the main category and its subcategories, *e.g.*, 11, 12, 13 are subcategories of 1x.

Category 1x
Unintentional lane departure

Category 11
Run-off-road

Category 12
Collision with vehicle in opposite direction

Category 13
Collision with infrastructure

Category 2x
Collision with object in same lane

Category 21
Vehicle in same lane

Category 22
Other object in same lane

Category 3x
Lane change accident

Category 31
Blind spot related accident

Category 32
Collision with faster moving vehicle

Category 33
Collision with slower moving vehicle

Category 4x
Loss of grip

Category 41
Entering curve too fast

Category 42
Loss of grip due to ice, snow, etc.

Category 5x
Accident at intersection

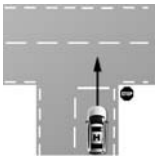

Category 51
Approaching a give-way situation too fast

Category 52
Other accident at intersection

Category 6x
Overtaking in two-way traffic

Category 7x
Miscellaneous. Parking, reversing, etc.

Category 71
Leaving car park

Category 72
Other accidents related to parking, reversing, etc.

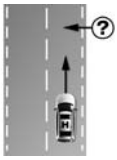

Category 8x
Obstacle enters lane

Category 81
Wildlife

Category 82
Pedestrian

Category 82
Cyclist

## Appendix B: Potential active safety functions

This is a very brief description of the active safety functions as evaluated in Chapter 2. Some of these systems have been presented elsewhere and some of them are new.

**Lane Keeping Aid (LKA)** Includes a vision system for lane detection and uses a steering wheel actuator to prevent the vehicle from leaving the lane (Pohl and Ekmark, 2003).

**Lane Change Aid (LCA)** Assists during lane changes by activating a warning light if another vehicle is in the blind spot. This system is currently on the market.

**Collision Mitigation by Braking (CMbB)** Automatic braking when forward collision is unavoidable (Jansson, 2002).

**Collision Mitigation by Braking (CMbB2):** Same as CMbB but also includes a road friction detector to be able to brake earlier during bad road conditions.

**Collision Mitigation by Braking (CMbB3)** Collision Mitigation by Braking with friction detection and a system for detecting drowsy or distracted drivers, thus allowing for earlier braking.

**Curvature Warning (CW)** A warning is activated if the host vehicle approaches a sharp curve too fast.

**Lane Assist Systems (LAS)** Combination of Lane Keeping Aid and Lane Change Aid. Does not use steering wheel actuator, only a warning sound.

**Lane Assist System (LAS2)** Same as above, but also monitoring traffic which is not necessarily in the blind spot but still poses a threat. Audio warning on a dangerous lane change.

**Emergency Lane Assist (ELA)** Same as Lane Assist System 2 but also monitors oncoming traffic. This system uses a steering wheel actuator to prevent dangerous lane departure.

**Give Way Warning (GWW)** The system warns if the host vehicle approaches a crossroads too fast, *e.g.*, at a red light or a stop sign too fast.

**Wildlife scanner (WLS)** Wildlife warning system. Warns if a large animal enters the road ahead of the host vehicle.

**Pedestrian & Bicycle scanner (PBS)** Searches for pedestrians/bicycles in front of the vehicle (Grubb et al., 2004, Gavrila et al., 2004). Automatic braking.

**Overtaking Guidance System (OGS)** Warns the driver of dangerous overtaking situations already commenced and informs of coming overtaking opportunities.

**True Collision Avoidance by Steering (True CAbS)** A system which actually steers around a threat when a pure braking manoeuvre is insufficient. Includes Emergency Lane Assist + Collision Mitigation by Braking 3.

# References


Beji, L. and Bestaoui, Y. (2005). Motion generation and adaptive control method of automated guided vehicles in road following. *IEEE Transactions on Intelligent Transportation Systems*, 6(1):113–123.

Chaib, S., Netto, M. S., and Mammar, S. (2004). $H_\infty$, adaptive, PID and fuzzy control: A comparison of controllers for vehicle lane keeping. In *Proceedings of the IEEE Intelligent Vehicles Symposium*, pages 139–144, Parma, Italy.

Chen, M., Jochen, T., and Pomerleau, D. (1995). AURORA: A vision-based roadway departure warning system. In *Proceedings of IEEE Symposium on Intelligent Robots and Systems*, pages 243–248.

Citroën (2005). An innovation award for the LDWS. Press release, `www.citroen.com/CWW/en-US/NEWS/NEWSRELEASES/ArchivesNewsReleases/200506/23032005\_PRIXAFIL.htm`.

Dellaert, F. and Thorpe, C. (1997). Robust car tracking using Kalman filtering and Bayesian templates. In *Proceedings of the SPIE conference on Intelligent Transportation Systems*, volume 3207.

Dickmanns, E. D. and Zapp, A. (1987). Autonomous high speed road vehicle guidance by computer vision. In *Selected Papers from the 10th Triennial World Congress of the International Federation of Automatic Control*, pages 221–226, Munich, Germany. Pergamon.

EACS (1996). European accident causation survey. web page, European Automobile manufacturers Association (ACEA) and the European Commission, `http://www.erso.eu/data/content/eacs.htm`.

Eidehall, A. and Gustafsson, F. (2004). Combined road prediction and target tracking in collision avoidance. In *Proceedings of the IEEE Intelligent Vehicles Symposium*, pages 619–624, Parma, Italy.

Gavrila, D. M., Giebel, J., and Munder, S. (2004). Vision-based pedestrian detection: The protector system. In *Proceedings of the IEEE Intelligent Vehicles Symposium*, pages 13–18, Parma, Italy.

González-Mendoza, M., Jammes, B., Hernández-Gress, N., Titli, A., and Estève, D. (2004). A comparison of road departure warning systems on real driving conditions. In *Proceedings of IEEE Intelligent Transportation Systems*, pages 349–354, Washington, D.C., USA.

Grubb, G., Zelinsky, A., Nilsson, L., and Rilbe, M. (2004). 3D vision sensing for improved pedestrian safety. In *Proceedings of the IEEE Intelligent Vehicles Symposium*, pages 19–24, Parma, Italy.

Hessburg, T. and Tomizuka, M. (1991). A fuzzy rule-based controller for automotive vehicle guidance. PATH research report UCB-ITS-PRR-91-18, California Partners for Advanced Transit and Highways.

Ishida, S. and Gayko, J. E. (2004). Development, evaluation and introduction of a lane keeping assistance system. In *Proceedings of the IEEE Intelligent Vehicles Symposium*, pages 943–344, Parma, Italy.

Isomoto, K., Niibe, T., Suetomi, T., and Butsuen, T. (1995). Development of a lane-keeping system for lane departure avoidance. In *Proceedings of the 2nd World Congress on ITS*, pages 1266–1271, Yokahama, Japan.

Jansson, J. (2002). Tracking and decision making for automotive collision avoidance. Licentiate thesis 965, Department of Electrical Engineering, Linköping University.

Jansson, J. (2005). *Collision Avoidance Theory with Application to Automotive Collision Mitigation*. PhD thesis, Linköping University, Linköping University, 581 83 Linköping, Sweden.

LeBlanc, D. J., Johnson, G. E., Venhovens, P. J., Gerber, G., DeSonia, R., Ervin, R. D., Lin, C.-F., Ulsoy, A. G., and Pilutti, T. E. (1996). CAPC: An implementation of a road-departure warning system. In *Proceedings of IEEE International Conference on Control Applications*, pages 590–595, Dearborn, MI, USA.

Lee, S. and Kwon, W. (2001). Robust lane keeping from novel sensor fusion. In *Proceedings of IEEE International Conference on Robotics and Automation*, pages 3704–3709, Seoul, Korea.

Mammar, S., Glaser, S., and Netto, M. (2006). Time to line crossing for lane departure avoidance: A theoretical study and an experimental setting. *IEEE Transactions on Intelligent Transportation Systems*, 7(2):226–241.

Naab, K. and Reichart, G. (1994). Driver assistance systems for lateral and longitudinal vehicle guidance. In *Proceedings of AVEC'94*, pages 449–454, Tsukuba, Japan.

Naranjo, J. E., González, C., García, R., Pedro, T. d., and Haber, R. E. (2005). Power-steering control architecture for automatic driving. *IEEE Transactions on Intelligent Transportation Systems*, 6(4):406–415.

NHTSA (2000). Automotive collision avoidance system field operational test. web page, National Highway Traffic Safety Administration, `www.nhtsa.dot.gov/people/injury/research/pub/ACAS/ACAS-fieldtest`.

Petersson, L., Fletcher, L., Barnes, N., and Zelinsky, A. (2004). An interactive driver assistance system monitoring the scene in and out of the vehicle. In *Proceedings of IEEE International Conference on Robotics and Automation*, pages 3475–3481, New Orleans, LA, USA.

Pilutti, T. and Ulsoy, A. G. (2003). Fuzzy-logic-based virtual rumble strips for road departure warning systems. *IEEE Transactions on Intelligent Transportation Systems*, 4(1):1–12.

Pohl, J. and Ekmark, J. (2003). Development of a haptic intervention system for unintended lane departure. In *Proceedings of the 2003 SAE World Congress*, Detroit, MI, USA.

Polychronopoulos, A., Scheunert, U., and Tango, F. (2004). Centralized data fusion for obstacle and road borders tracking in a collision warning system. In *Proceedings of the 7th International Conference on Information Fusion*, pages 760–767, Stockholm, Sweden.

Rugh, W. J. (1996). *Linear System Theory*. Information and system sciences series. Prentice Hal, Upper Saddle River, New Jersey, 2 edition.

Thorpe, C. E. (1990). *Vision and Navigation: the Carnegie Mellon Navlab*. Kluwer Academic Publishers.

van Winsum, W., Brookhuis, K. A., and de Ward, D. (2000). A comparison of different ways to approximate time-to-line crossing (TLC) during car driving. In *Accident Analysis and Prevention 32*, pages 47–56.

Zomotor, Z. and Franke, U. (1997). Sensor fusion for improved vision based lane recognition and object tracking with range-finders. In *Proceedings of the IEEE Conference on Intelligent Transportation Systems*.

# Paper B

# Joint road geometry estimation and vehicle tracking

**Authors:** Andreas Eidehall, Jochen Pohl and Fredrik Gustafsson

Extended version of “Combined road prediction and target tracking in collision avoidance”. In *Proceedings of the IEEE Intelligent Vehicles Symposium 2004*, pages 619-624.

Provisionally accepted for publication in *Control Engineering Practice*, 2006.

Preliminary version published as Technical Report LiTH-ISY-R-2755, Department of Electrical Engineering, Linköping University, Linköping, Sweden.

# Joint road geometry estimation and vehicle tracking

Andreas Eidehall[⋆§], Jochen Pohl[§] and Fredrik Gustafsson[⋆]

[⋆]Department of Electrical Engineering
Linköping University
SE–581 83 Linköping, Sweden

[§]Vehicle Dynamics and Active Safety
Volvo Car Corporation
SE–405 31 Göteborg, Sweden

**Abstract**

Detection and tracking of other vehicles and estimation of lane geometry will be required for many intelligent driver assistance systems in the future. By combining the processing of these two features into a single filter, better utilisation of the available information can be achieved. For instance, it is demonstrated that it is possible to improve the road shape estimate by including information about the lateral movement of leading vehicles.

Statistical evaluation is done by comparing the estimated parameters to true values in varying road and weather conditions. The performance is also related to typical requirements of active safety applications such as Adaptive Cruise Control and a new safety function called Emergency Lane Assist.

# 1 Introduction

In the future, many automotive active safety systems such as Adaptive Cruise Control (ACC), collision avoidance or lane guidance will require detailed knowledge about the vehicle surroundings. Typically, the position of surrounding objects and the shape of the road is needed. Road or lane shape information is usually obtained from a vision system and other vehicles are often detected by radar. Functions such as ACC, and also a new safety function called Emergency Lane Assist (ELA) (Eidehall et al., 2006), are dependent on lane assignment, *i.e.*, determining which lanes tracked vehicles are currently occupying, something which relies on accurate information about both road shape and object positions.

Integrated object and road geometry tracking is a fairly new research area. The concept was introduced by Zomotor and Franke (1997) and Dellaert and Thorpe (1997) and the idea is to try to improve the road geometry estimate by studying the motion of other vehicles and vice versa. The interconnection comes from assuming that observed, leading vehicles are likely to keep following their lane, *i.e.*, in relation to the lane, their lateral position is constant. Thus, the movement of these can be used to support the road shape estimate. This is particularly important during poor visibility since vision-based lane trackers are very sensitive to changed visibility conditions, *e.g.*, caused by changes in weather or by driving on a road with lots of hills, and also by worn lane markings in general. This is achieved by modelling the motion of surrounding vehicles in relation to the road, *i.e.*, assuming that the movement of vehicles is connected to the shape of the road. The road geometry and the positions of all objects are then treated in a single, centralised filter. A similar approach is presented by NHTSA (2000) where the trails of tracked vehicles are analysed separately and then used as input into the road shape estimation process. The concept was further developed and evaluated by Gern et al. (2001). A related topic is introduced by Melo et al. (2006) in which surveillance system detects highway lanes using vehicle trails only, which is possible as the surveillance application obtains many samples of the same road segment. In our application, relying solely on vehicle motion for lane shape estimation pushes the assumption a bit too far.

Other techniques to improve road geometry estimates have also been suggested. Trzebiatowski et al. (2004) suggests visually detecting reflex posts as additional information of the road shape, and Ma et al. (2000) and Polychronopoulos et al. (2004) both suggests supporting the road shape estimate by tracking road-side objects such as guard rails or pavement by radar.

This article evaluates to what extent the motion of leading vehicles can be used to improve the performance of road shape estimation. It is compared to decoupled filtering, where road shape and vehicles are treated in different filters. In addition, different road models are compared and some statistical properties of the resulting estimate are examined. This is then related to typical requirements that the ELA and ACC functions apply to the road shape estimate.

The sensor configuration that has been studied is a radar in combination with a monovision system. The radar is of the type typically used for adaptive cruise control applications: a 77 GHz doppler radar with a range of approximately 150 metres and a field of view of about 15°. The vision system is an off-the-shelf single, black and white camera solution that delivers distances to the lane markings, heading angle and road curvature

based on image processing. However, the methods derived in this article are general and could be used with other types of sensors.

The new ELA safety function, and other potential applications, are briefly discussed in Section 2. For more details on ELA, readers are referred to Eidehall et al. (2006). Section 3 presents a derivation of the road model and the road-aligned coordinate system. Section 4 introduces the tracking system, including theoretic derivation of the models and filtering methods. Finally, Section 5 presents evaluation and results of the tracking system.

# 2 Applications

## 2.1 Emergency Lane Assist

Different types of lane guidance systems have recently been presented by several car manufacturers. Lane guidance systems try to prevent lane departure and the motivation is that many accidents occur due to a distracted or drowsy driver departing from a lane and colliding with a road-side object or an oncoming vehicle. There are two major problems with such technology. The first is false alarms when crossing the lane markings intentionally. The second is misuse. A system that uses a steering wheel to prevent lane departure could be used as an autopilot by the driver while carrying out distractive tasks.

Honda has proposed a solution of the misuse problem by only applying 80% of the torque required to keep the vehicle in the lane (Ishida and Gayko, 2004). uThis is in order to keep the driver in the loop at all times. Pilutti and Ulsoy (2003) investigate a way to make false alarms less intrusive by trying to mimic the sound or vibration of so called "rumble strips", *i.e.*, the grooved lane markings that are sometimes found on motorways. A similar system has also been put into production by Citroën (2005).

Emergency Lane Assist (ELA) provides another alternative when it comes to reducing false alarms and misuse problems associated with conventional lane guidance systems. This is achieved by only trying to prevent *dangerous* lane departure. The system monitors adjacent lanes and as long as there are no other vehicles approaching, the lane markings can be crossed without ELA intervention, but as soon as a commenced lane change manoeuvre is considered dangerous, for example with respect to an oncoming vehicle, a torque is applied to the steering wheel in order to prevent lane departure. The risk level of a lane change manoeuvre is assessed based on the position and motion of vehicles in the adjacent lanes. In addition, road edges, barriers or even solid lane markings could also be used to activate intervention. This approach makes ELA a pure safety system rather than a comfort/convenience system. Figure 1 shows critical ELA situations.

A prerequisite is that ELA must never prevent an avoidance manoeuver, *i.e.*, if the driver is trying to avoid an obstacle in the current lane, ELA must never apply a steering wheel torque to direct the vehicle towards this threat. Avoidance manoeuvres can be detected by looking for threats in the lane of the host vehicle for example, but also by using a driver-interpretation module to analyse the strength and speed of the steering wheel manoeuvre. The driver interpretation module is at this point not included in the presented system. To further ensure that the system does not intervene in a way that conflicts with the intentions of the driver, only allow a fairly low torque will be allowed

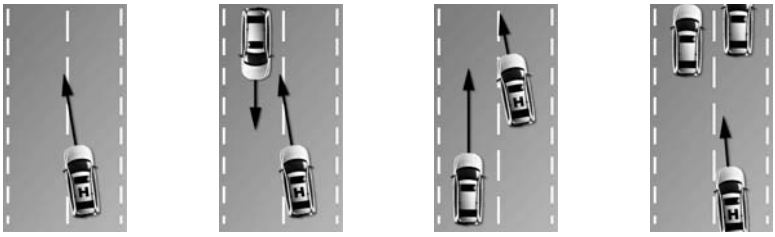

No ELA intervention since there is no threat in the adjacent lane. | ELA intervention. | ELA intervention. | No ELA intervention since there is a threat also in the own lane.

***Figure 1:*** *Critical ELA situations. The letter "H" indicates the ELA host vehicle.*

to be applied to the steering wheel. Thus, the driver can always override the steering intervention by a resolute steering manoeuvre in the desired direction.

## 2.2 Adaptive Cruise Control

Adaptive Cruise Control (ACC) is a new type of cruise control that is starting to appear on the market. When there are no other vehicles near, ACC works like a standard cruise control which controls the accelerator in order to keep the speed at a preset level. As soon as a slower-moving leading vehicle is approached, ACC automatically reduces the speed in order to maintain a preset time gap. It is then crucial to assign leading vehicles to the correct lane in order to adapt the speed to the correct vehicle.

## 2.3 Requirements on the tracking performance

A number of important requirements on the tracking system can be pointed out. In ELA, once the decision to intervene has been taken, the host vehicle needs to be guided back to the centre of its original lane. To do this, the lateral position relative to the lane needs to be known, and usually, a modern off-the-shelf lane tracker provides this information with good enough accuracy.

Furthermore, the lateral position of other objects needs to be known, or more specifically, their position relative to the lane, *i.e.*, lane assignment. For example, in ELA, if an oncoming vehicle is mistakenly judged by the tracking system to be in the adjacent lane, but is really positioned in the same lane as the host vehicle, it is undesirable to make the decision to steer the host vehicle back into this lane. Similarly, ACC needs accurate lane assignment in order to adapt the speed to the correct leading vehicle. This puts tough requirements, both on the tracking of objects, but also on the long range road geometry tracking. This is discussed further and quantified in Section 5.4.

Thirdly, accurate range and range rate information of other objects is needed. However, with the use of long range Doppler radar, this is usually not a problem.

# 3 Geometric road model

## 3.1 Overview

The position on the road for each vehicle is denoted $(x, y)$ in a road-aligned coordinate system, where $x$ is the driven distance along the road and $y$ the lateral position in the lane. This needs to be related to a Cartesian coordinate system $(\tilde{x}, \tilde{y})$ which is attached to the host vehicle, see Figure 4. The purpose of Section 3.2 is to find this transformation $T : (x, y) \rightarrow (\tilde{x}, \tilde{y})$. For this derivation, a model of the road is needed, which is obtained from a general model describing the road curvature as $c(x) = c_0 + c_1 x$. This describes a clothoid curve which is a commonly used parametrisation in automotive tracking applications. However, the trigonometric formulas that arise do not give an explicit expression for $T(x, y)$. If such an expression is needed, either the trigonometric functions can be Taylor expanded, or a simpler model with $c_1 = 0$ can be used (constant curve radius). These approximations are treated in Section 3.3.

## 3.2 Model derivation

### Curved coordinate system

A two-dimensional coordinate transformation $T$ is first derived, from the road-aligned coordinate system $(x, y)$ to a cartesian coordinate system $(\tilde{x}, \tilde{y})$ which is attached to the host vehicle is first derived, see Figure 2. The derivation starts with a planar curve $\mathbf{r}(x)$, where $x$ is the distance along a curve. Assume the curvature along the curve is given by $c = c(x)$, *i.e.*, the radius is $r(x) = 1/c(x)$. Now, if $\hat{\mathbf{t}}(x)$ is the tangent vector to the curve, where the hat means that it is unit length, *i.e.*, $\|\hat{\mathbf{t}}(x)\| = 1$, the normal vector $\mathbf{n}(x)$ is defined as

$$\mathbf{n}(x) = \frac{d\hat{\mathbf{t}}}{dx}(x). \tag{1}$$

Vector analysis gives an alternative expression for $\mathbf{n}(x)$ where it is given that it is perpendicular to $\hat{\mathbf{t}}(x)$ and that its length is precisely $c(x)$. In addition, $c(x)$ is defined to be positive for left turns and negative for right turns. The normal can thus be written $\mathbf{n}(x) = -c(x)\mathbf{R}(-\frac{\pi}{2})\hat{\mathbf{t}}(x) = c(x)\mathbf{R}(\frac{\pi}{2})\hat{\mathbf{t}}(x)$ where $\mathbf{R}(\alpha)$ is a $\alpha$-radian, counterclockwise rotational matrix, *i.e.*,

$$\mathbf{R}(\alpha) \triangleq \begin{pmatrix} \cos\alpha & -\sin\alpha \\ \sin\alpha & \cos\alpha \end{pmatrix}. \tag{2}$$

Thus, the differential equation

$$\frac{d\hat{\mathbf{t}}}{dx}(x) = c(x)\mathbf{R}(\frac{\pi}{2})\hat{\mathbf{t}}(x) \tag{3}$$

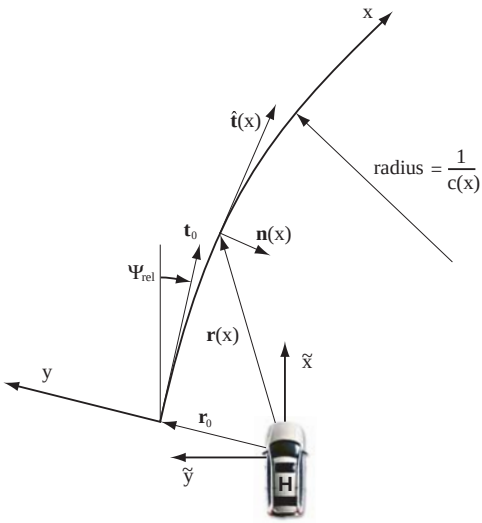


***Figure 2:*** *The vectors used in the derivation of $T$.*

is obtained, which has the solution

$$\hat{\mathbf{t}}(x) = \exp\left(\mathbf{R}(\frac{\pi}{2})\int_0^x c(\tau)d\tau\right)\hat{\mathbf{t}}_0 = \mathbf{R}\left(\int_0^x c(\tau)d\tau\right)\hat{\mathbf{t}}_0, \tag{4}$$

where $\hat{\mathbf{t}}_0$ is an arbitrary initial condition, *i.e.*, $\hat{\mathbf{t}}(x) = \hat{\mathbf{t}}_0$, with the condition $\|\hat{\mathbf{t}}_0\| = 1$. The last equality is proved in the appendix. This can then be used to obtain an expression for the position:

$$\mathbf{r}(x) = \int_0^x \hat{\mathbf{t}}(\tau)d\tau + \mathbf{r}_0 = \int_0^x \mathbf{R}\left(\int_0^{\tau_1} c(\tau_2)d\tau_2\right)d\tau_1\hat{\mathbf{t}}_0 + \mathbf{r}_0, \tag{5}$$

where the free parameter $\mathbf{r}_0$ is used to describe an offset perpendicular to $\hat{\mathbf{t}}_0$ and with length $y_{\text{off}}$:

$$\mathbf{r}_0 = \mathbf{R}(-\Psi_{\text{rel}})\begin{pmatrix} 0 \\ -y_{\text{off}} \end{pmatrix}. \tag{6}$$

This is used to model the host vehicle's lateral offset from the centre of the lane and is shown in Figure 2.

To construct the coordinate transformation $T$, one of the coordinates is defined to be the distance along the curve: $T(x, 0) = \mathbf{r}(x)$. To define the other coordinate, $T$ is required to be orthogonal. A natural choice is to simply extend a straight line at $T(x, 0)$ along $\mathbf{R}(\frac{\pi}{2})\hat{\mathbf{t}}(x)$. This choice will also give us a positively oriented transformation. $T$

will look like

$$\begin{pmatrix}\tilde{x}\\ \tilde{y}\end{pmatrix} = T(x,y) = \mathbf{r}(x) + \mathbf{R}(\frac{\pi}{2})\hat{\mathbf{t}}(x)y. \tag{7}$$

### Road curvature function

The road is often modelled as segments of straight lines, arcs and clothoids (Dickmanns and Zapp, 1986, Gern et al., 2000). Clothoids are segments for which the curvature changes linearly with the distance along the curve. According to Swedish road authorities (Vägverket, 1994), this agrees well with how roads are constructed. The function

$$c(x) = c_0 + c_1 x \tag{8}$$

will suffice for all these cases. Of course, when approaching a curve, there might be situations for example where the section 0 - 50 metres of the field of view is a straight line and the section 50 - 100 metres is a clothoid, a case that cannot be modelled with a linear curvature law.

Inserting (8) into (4) and using

$$\hat{\mathbf{t}}_0 = \begin{pmatrix}\cos(-\Psi_{\text{rel}})\\ \sin(-\Psi_{\text{rel}})\end{pmatrix}, \tag{9}$$

the following expression is obtained:

$$\hat{\mathbf{t}}(x) = \mathbf{R}(c_0 x + c_1 x^2/2)\begin{pmatrix}\cos(-\Psi_{\text{rel}})\\ \sin(-\Psi_{\text{rel}})\end{pmatrix} = \mathbf{R}(-\Psi_{\text{rel}})\begin{pmatrix}\cos(c_0 x + c_1 x^2/2)\\ \sin(c_0 x + c_1 x^2/2)\end{pmatrix}. \tag{10}$$

The last simplification is proved in the appendix. Equation (10) gives the second term of (7). In order to get an expression for the first term, (10) needs to be integrated, which cannot be done analytically. Instead, some sort of approximation is needed.

## 3.3 Coordinate transformation approximations

In order to obtain a closed form expression of the position $\mathbf{r}(x)$, the expression (10) for $\hat{\mathbf{t}}(x)$ needs to be simplified. After that, the new $\hat{\mathbf{t}}(x)$ and $\mathbf{r}(x)$ are inserted into (7) in order to obtain the coordinate transformation. Three different approximations are here derived and compared.

### Approximation A: Omitting the clothoid parameter

Using $c_1 = 0$ in (10) the following expression is obtained:

$$\hat{\mathbf{t}}(x) = \mathbf{R}(-\Psi_{\text{rel}})\begin{pmatrix}\cos(c_0 x)\\ \sin(c_0 x)\end{pmatrix},$$

which, used in (5) gives

$$\mathbf{r}(x) = \mathbf{R}(-\Psi_{\text{rel}})\begin{pmatrix}\sin(c_0 x)\\ 1-\cos(c_0 x)\end{pmatrix}\frac{1}{c_0} + \mathbf{R}(-\Psi_{\text{rel}})\begin{pmatrix}0\\ -y_{\text{off}}\end{pmatrix},$$

and the coordinate transformation (7) becomes

$$\begin{aligned} T_a(x,y) &\triangleq \mathbf{r}(x) + \mathbf{R}(\frac{\pi}{2})\mathbf{t}(x)y \\ &= \mathbf{R}(-\Psi_{\text{rel}}) \begin{pmatrix} (1-c_0 y)\sin(c_0 x) \\ 1-(1-c_0 y)\cos(c_0 x) - c_0 y_{\text{off}} \end{pmatrix} \frac{1}{c_0} \end{aligned} \tag{11}$$

### Approximation B: Linearising the trigonometric functions

If $\sin\tau \approx \tau$ and $\cos\tau \approx 1$ is used, then (10) becomes

$$\hat{\mathbf{t}}(x) = \mathbf{R}(-\Psi_{\text{rel}}) \begin{pmatrix} 1 \\ c_0 x + c_1 x^2/2 \end{pmatrix}.$$

Inserting this into (5) gives

$$\mathbf{r}(x) = \mathbf{R}(-\Psi_{\text{rel}}) \begin{pmatrix} x \\ c_0 x^2/2 + c_1 x^3/6 \end{pmatrix} + \mathbf{R}(-\Psi_{\text{rel}}) \begin{pmatrix} 0 \\ -y_{\text{off}} \end{pmatrix},$$

and from (7), the coordinate transformation becomes

$$T_b(x,y) \triangleq \mathbf{R}(-\Psi_{\text{rel}}) \begin{pmatrix} x - y(c_0 x + c_1 x^2/2) \\ y - y_{\text{off}} + c_0 x^2/2 + c_1 x^3/6 \end{pmatrix}. \tag{12}$$

### Approximation C: As B, plus further approximations

Some further approximation steps are carried out:

$$\begin{aligned} T_b(x,y) &\approx \mathbf{R}(-\Psi_{\text{rel}}) \begin{pmatrix} x \\ y - y_{\text{off}} + c_0 x^2/2 + c_1 x^3/6 \end{pmatrix} \approx \\ &\approx \begin{pmatrix} 1 & \Psi_{\text{rel}} \\ -\Psi_{\text{rel}} & 1 \end{pmatrix} \begin{pmatrix} x \\ y - y_{\text{off}} + c_0 x^2/2 + c_1 x^3/6 \end{pmatrix} = \\ &= \begin{pmatrix} x + \Psi_{\text{rel}}(y - y_{\text{off}} + c_0 x^2/2 + c_1 x^3/6) \\ -\Psi_{\text{rel}} x + y - y_{\text{off}} + c_0 x^2/2 + c_1 x^3/6 \end{pmatrix} \approx \\ &\approx \begin{pmatrix} x \\ y - y_{\text{off}} - \Psi_{\text{rel}} x + c_0 x^2/2 + c_1 x^3/6 \end{pmatrix} \triangleq T_c(x,y). \end{aligned} \tag{13}$$

This is a commonly used approximation (Dickmanns and Zapp, 1987, Gern et al., 2001). Note that the road geometry effect in the $x$ component has been completely ignored, *i.e.*, $x = \tilde{x}$.

### Geometric comparison

In order to give a feeling of the errors these approximations represent, a typical road shape with the different approximations is generated. Vägverket (1994) gives the following guidelines for road construction. For a 50 km/h road, the minimum radius is 140 metres and for a 90 km/h road it is 550 metres. The recommended maximum clothoid parameters for these curves are given by the formula

$$c_1^{\max} = \frac{k}{v^3},$$

where $k = 0.45$ (m/s$^3$) which is the maximum "jerk" and $v$ the velocity, giving the clothoid $1.7 \cdot 10^{-4}$ and $2.9 \cdot 10^{-5}$ (1/m$^2$) for the 50 (km/h) and the 90 (km/h) curve, respectively. In Figure 3, the approximations are compared with the exact transformation. Note that on straight stretches and on pure circle segments, $T_a$ coincides with the exact transformation. The fact that the curve effect in the $x$ coordinate has been ignored in Approximation C can be seen by the horizontal line at the top of the shape.

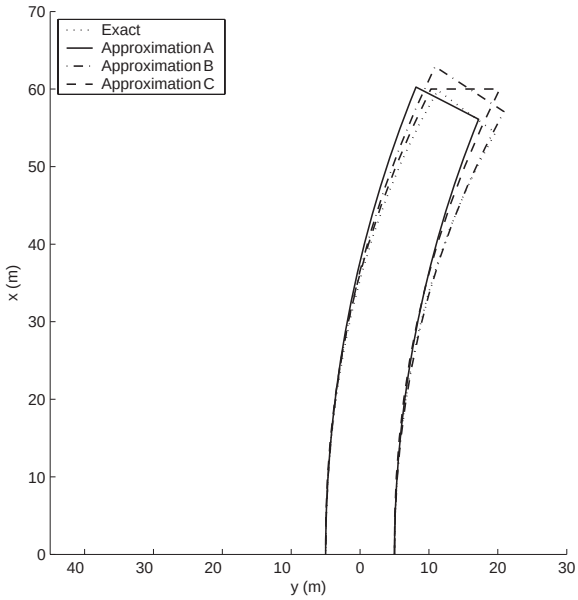


***Figure 3:*** *Illustration of the different approximations* (11) - (13)*. A road with edges at $y = -5$ and $y = 5$ has been transformed with the three approximations and with the true transformation, based on a typical 50 km/h curve.*

# 4 Filtering

One of the advantages of the road-aligned coordinate system is that the motion of surrounding vehicles can be modelled very easily since the fact that they turn when entering curves are already captured by the road model. Another advantage is that vehicle position prediction also becomes more accurate since it is predicted that they will follow the shape of the road, not just their current tangent.

A drawback with the introduced coordinate system is that it generates nonlinear measurement equations which increases the complexity of the filter. In addition, since the road model becomes interconnected with the positions of vehicles in the filter, an error in the road model estimate will result in an error in the position estimates of other vehicles and vice versa. However, this is not a problem in the presented application since it is

dependent on both the road estimate and the vehicle position estimates and can thus not benefit from accurate information in one of the estimates if the other has a large error.

To be able to use a Kalman filter, three state space models are used, based on the approximations from the previous section. The filters based on Approximation A, B and C will be referred to as Filter A, B and C. The states for the host vehicle are shown in Figure 4. In addition, even though $c_1$ is not included in Approximation A it is still observable and is needed in the filter for dynamic reasons as it affects the dynamics of $c_0$. Observed vehicles will have the states $x_i$, $\dot{x}_i$ and $y_i$, where $i$ runs through all tracked objects. Note that this section presents an example of a dynamic model that has been used in the evaluation. The geometric model from the previous section is general and can be used with higher order motion models, such as the bicycle model (Gillespie, 1992).

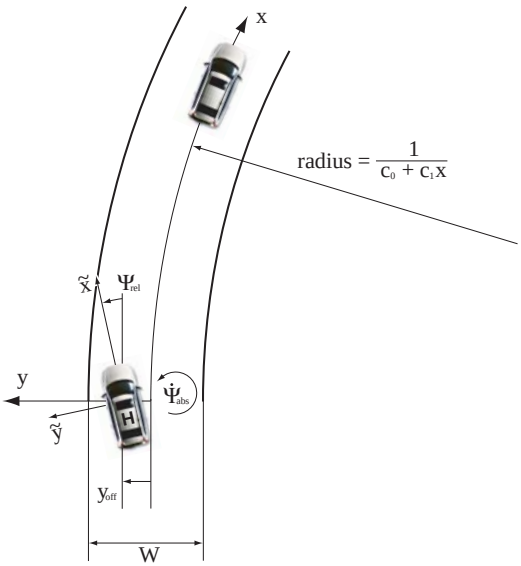


***Figure 4:*** *$W$, $y_{\text{off}}$, $\Psi_{\text{rel}}$, $c_0$ and $c_1$ are the host vehicle states. The mapping $T$ transforms from the coordinate system $(x, y)$ to the coordinate system $(\tilde{x}, \tilde{y})$.*

## 4.1 Motion model

The coordinates $x$ and $y$ denote the position in the curved coordinate system that is aligned with the road according to Figure 4. In these coordinates, the motion model for the other vehicles can be greatly simplified. For instance, the equation $\dot{y}^i = 0$ can be used, which means that the other vehicles will keep following their own lanes. The longitudinal model is simply $\ddot{x}^i = 0$. Note that this is relative velocity and acceleration. This means that if the host vehicle acceleration is available, the tracking performance could be improved by using this as an input signal. Hence, for tracked vehicles, the following motion model is

obtained:

$$\dot{x}^i = v^i, \tag{14a}$$

$$\dot{v}^i = 0, \tag{14b}$$

$$\dot{y}^i = 0, \tag{14c}$$

where $v^i$ is the longitudinal relative velocity of object $i$, *i.e.*, the time derivative of $x^i$.

A dynamic model for the shape of the road is also needed. Two parametrisation are used in the derivation, $C(X)$ is a global curvature model and $c(x)$ is a local model around the host vehicle. A common assumption is that the shape of the road consists of elements of so called clothoid curves, *i.e.*, segments where the curvature changes linearly with the distance, also discussed Section 3.1. This means, that along such a segment, the curvature changes as

$$C(X) = C_0 + C_1 X, \tag{15}$$

where $X$ is the current driven distance along the segment, see Figure 5. For now, it is

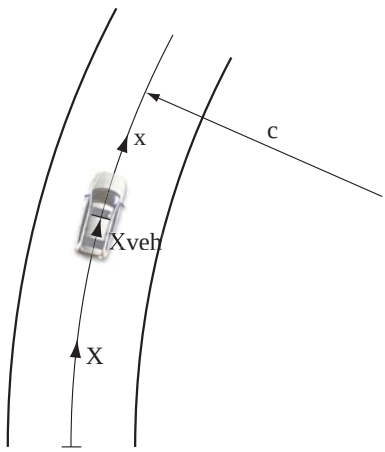


***Figure 5:*** *Here, the relationship between the local and the global curvature model is shown.*

assumed that $C_0$ and $C_1$ are constants describing the shape of the road. This can also be expressed locally around the current position of the host vehicle as

$$c(x) = c_0 + c_1 x. \tag{16}$$

If the local coordinate $x$ is defined as

$$X = X_{\text{veh}} + x, \tag{17}$$

where $X_{\text{veh}}$ is the position of the host vehicle around which the local model is expressed. Inserting (17) into (15) the following expression for the local model is obtained:

$$\begin{aligned} c(x) &= C(X_{\text{veh}} + x) = C_0 + C_1(X_{\text{veh}} + x) \\ &= C_0 + C_1 X_{\text{veh}} + C_1 x. \end{aligned} \tag{18}$$

The terms of the local model (16) can now be identified as

$$c_0 = C_0 + C_1 X_{\text{veh}} \tag{19a}$$

$$c_1 = C_1 \tag{19b}$$

As the host vehicle moves, this local parametrisation will change according to

$$\dot{c}_0 = \underbrace{\dot{C}_0}_{=0} + \underbrace{\dot{C}_1}_{=0} X_{\text{veh}} + C_1 \dot{X}_{\text{veh}} = c_1 v \tag{20a}$$

$$\dot{c}_1 = \dot{C}_1 = 0 \tag{20b}$$

which follows from the assumption that $C_0$ and $C_1$ are constant. The velocity of the host vehicle is denoted $v$. These equations will be used as the dynamic model for $c_0$ and $c_1$. The derivation started with the assumption that $C_0$ and $C_1$ were constant. The fact that they only are only piecewise constant with jumps when switching from one clothoid element to another is handled by introducing process noise to the discrete time versions of (20). For the width of the lane, the model $\dot{W} = 0$ will be used. To summarise, the dynamic model for the road is

$$\dot{W} = 0, \tag{21a}$$

$$\dot{c}_0 = v c_1, \tag{21b}$$

$$\dot{c}_1 = 0. \tag{21c}$$

For the host vehicle parameters it is first clarified that $\Psi_{\text{rel}}$ is the angle between the host vehicle and the lane, and $\Psi_{\text{abs}}$ is the angle between the host vehicle and some fix reference. Thus

$$\Psi_{\text{abs}} = \Psi_{\text{rel}} + \gamma \Leftrightarrow \Psi_{\text{rel}} = \Psi_{\text{abs}} - \gamma \tag{22}$$

were $\gamma$ is the angle between the road and the fixed reference. A relationship between $\Psi_{\text{rel}}$ and $\Psi_{\text{abs}}$ can be obtained by differentiating (22):

$$\dot{\Psi}_{\text{rel}} = \dot{\Psi}_{\text{abs}} - \dot{\gamma} = \dot{\Psi}_{\text{abs}} - \frac{v}{r} = \dot{\Psi}_{\text{abs}} - c_0 v, \tag{23}$$

where $r$ is the current road radius and, since the host vehicle by definition is located at $x = 0$ in (16), $r = 1/c_0$. $\dot{\Psi}_{\text{abs}}$ can typically be measured with a yaw rate sensor. Furthermore, $y_{\text{off}} = \sin(\Psi_{\text{rel}})v \approx \Psi_{\text{rel}} v$. To summarise, the motion of host vehicle is modelled as

$$y_{\text{off}} = v \Psi_{\text{rel}}, \tag{24a}$$

$$\dot{\Psi}_{\text{rel}} = -v c_0 + \dot{\Psi}_{\text{abs}}. \tag{24b}$$

The discrete-time dynamics is then given by the sampling formula (Rugh, 1996) and assuming piecewise constant input, and sampling time $T_s$. Furthermore, adding stochastic process noise, the discrete-time motion equations for the objects become

$$x^i_{t+1} = x^i_t + T_s v^i_t + w^i_{1,t}, \tag{25a}$$

$$v^i_{t+1} = v^i_t + w^i_{2,t}, \tag{25b}$$

$$y^i_{t+1} = y^i_t + w^i_{3,t}. \tag{25c}$$

For the host vehicle it is

$$y_{\text{off},t+1} = y_{\text{off},t} + vT_s\Psi_{\text{rel},t} - v^2T_s^2c_{0,t}/2 - v^3T_s^3c_{1,t}/6 + vT_s^2\dot{\Psi}_{\text{abs},t}/2 + w_{4,t}, \quad (26a)$$

$$\Psi_{rel,t+1} = \Psi_{\text{rel},t} - vT_sc_{0,t} - v^2T_s^2c_{1,t}/2 + T_s\dot{\Psi}_{\text{abs},t} + w_{5,t}, \quad (26b)$$

and for the road

$$W_{t+1} = W_t + w_{6,t}, \quad (27a)$$

$$c_{0,t+1} = c_{0,t} + vT_sc_{1,t} + w_{7,t}, \quad (27b)$$

$$c_{1,t+1} = c_{1,t} + w_{8,t}. \quad (27c)$$

The variables $\{w_{i,t}\}_{i=1}^{8}$ are white, zero-mean Gaussian process noise, with covariance matrices $Q_{\text{road}}$, $Q_{\text{host}}$ and $Q_{\text{obj}}$ for the road, host and object states, respectively.

## 4.2 Measurement model

The measurements for the host vehicle are $\Psi_{\text{rel}}^m$, $c_0^m$, $L^m$ and $R^m$, where the two latter are the distances to the left and right lane marking, see Figure 4. Superscript $m$ denotes measured quantities. For the other vehicles the position $\tilde{x}^m$ and $\tilde{y}^m$ is measured, which is expressed in the Cartesian coordinate system attached to the vehicle. These relate to the states as

$$L_t^m = W_t/2 - y_{\text{off},t} + e_{1,t}, \quad (28a)$$

$$R_t^m = -W_t/2 - y_{\text{off},t} + e_{2,t}, \quad (28b)$$

$$\Psi_{\text{rel},t}^m = \Psi_{\text{rel},t} + e_{3,t}, \quad (28c)$$

$$c_{0,t}^m = c_{0,t} + e_{4,t}, \quad (28d)$$

$$\begin{bmatrix} \tilde{x}_t^{i,m} \\ \tilde{y}_t^{i,m} \end{bmatrix} = T(x_t^i, y_t^i) + \begin{bmatrix} e_{5,t} \\ e_{6,t} \end{bmatrix}^i, \quad (28e)$$

where the variables $\{e_{i,t}\}_{i=1}^{6}$ denote white, zero-mean Gaussian measurement noise with covariance matrices $R_{\text{host}}$ and $R_{\text{obj}}$ for the host and object states, respectively. $T$ is one of the approximations from Section 3.3.

## 4.3 Decoupled model

The performance of Filters A, B and C is also compared to a decoupled filter, where tracking of host/road and objects is done separately. The decoupled filter is based on (26), (27) and (28a)-(28d) only, and is consequently not affected by the movement of leading vehicles. The decoupled filter is thus the same as Filters A, B and C, but with the difference that the measurement equation of object positions is removed.

## 4.4 Extended Kalman Filter

According to the previous sections, the state-space model used in this application is nonlinear. Hence, the problem of recursively estimating the state variable in a nonlinear

state-space model needs to be handled. A general model with nonlinear measurement equation can be written:

$$\mathbf{z}_{t+1} = \mathbf{A}_t \mathbf{z}_t + \mathbf{B}_t \mathbf{u}_t + \mathbf{w}_t, \tag{29a}$$

$$\mathbf{y}_t = \mathbf{h}(\mathbf{z}_t) + \mathbf{e}_t, \tag{29b}$$

Here, $\mathbf{z}_t$ denotes the state vector, which in our model consist of the states $W$, $y_{\text{off}}$, $\Psi_{\text{rel}}$, $c_0$, $c_1$ as defined in Figure 4 and the three states $x$, $v$ and $y$, defined in (14), repeated once for each object. This means that the size of the state vector, and thus also model equations, will vary with the number of objects. The matrices $\mathbf{A}_t$ and $\mathbf{B}_t$ consist of the combined motion model from (25), (26) and (27) and the measurement equation $\mathbf{h}$ is a combination of (28a)-(28e) where (28e) is repeated once for each object. The signal $\mathbf{u}_t$ consist of the yaw-rate signal $\dot{\Psi}_{\text{abs}}$ only.

The extended Kalman filter has a long tradition in automotive applications. For details of the Kalman Filter and the extended Kalman filter, see Kalman (1960), Kay (1998), Gustafsson (2000) or Kailath et al. (2000). Data association in the filter is done with a standard method that can be found in the literature (Blackman, 1986). The method consists of sequentially associating the track-measurement pair with the minimum distance and also involves basic dead-reckoning mechanisms.

# 5 Evaluation

## 5.1 Accuracy of the road shape estimate

The evaluation is carried out by running the filters and comparing the estimated parameters to the true values. The sensor setup that is used during the evaluation is the camera and radar combination discussed in the introduction. In order to be able to rerun the filters with different tuning settings, the evaluation has mainly been done off-line, on recorded sensor data. The true values of the lane geometry parameters are obtained from a detailed map that is reconstructed from the sensor data (Eidehall and Gustafsson, 2006). Four filters are evaluated: the three filters referred to as A, B and C, based on the approximations derived in Section 3.3, plus the decoupled filter in Section 4.3.

## 5.2 Filter tuning

Tuning the filter involves adjusting the "$Q$" and "$R$" matrices in the Kalman filter, referred to as process and measurement noise covariance. If these are constrained to be diagonal, 14 parameters have to be tuned. Here, the tuning was started by first using "physical" intuition in order to try to judge errors in measurements and change rates in different states. This was then used as a starting point for manual tuning in order to obtain acceptable performance from all three filters. After that, semi-optimisation was carried out by tuning the performance along lines in the parameter space. For instance, an important parameter is the process noise of tracked vehicles' lateral movements. This is defined as $Q_{\text{lat}} = E[(w^i_{3,t})^2] = (Q_{obj})_{3,3}$. This parameter controls how much the lateral movement of tracked vehicles is tied to the lane. A low value of $Q_{\text{lat}}$ means that vehicles are very likely to keep following the lane, and there is thus a strong connection between lateral

movement of tracked vehicles and the road shape parameters. Conversely, a high value $Q_{\text{lat}}$ means that vehicles are more likely to move laterally in relation to the lane and thus loosens the connection to the road shape.

The result from this is shown in Figure 6, where the Root Mean Square Error (RMSE) during a five minute test drive has been computed for various values of $Q_{\text{lat}}$. The advantage of using information from leading vehicles is here clearly visible, which has also been indicated by Zomotor and Franke (1997) and Gern et al. (2000).

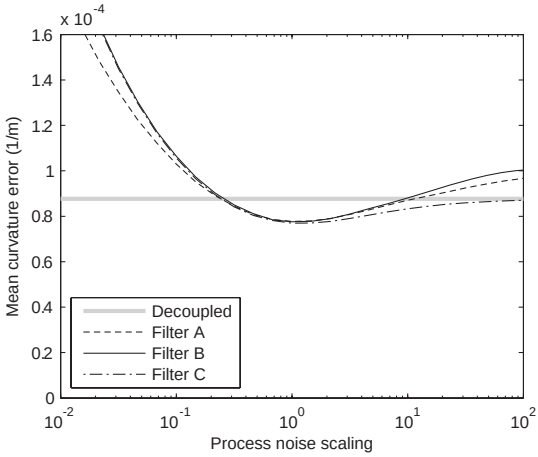


***Figure 6:*** *An example where the design variable $Q_{lat}$ is scaled from $10^{-2}$ to $10^{2}$ around a nominal value. The plot shows the curvature RMSE for the different filters. The decoupled filter from Section 4.3 is also included, which is unaffected by the changes in the lateral process noise. The advantage of using information from leading vehicles is here clearly visible.*

***Figure 7:*** *This is a video clip from data sequence 1. Snow reduces the visibility.*

When the filters are run on different data sequences, it is interesting to note that the optimal value for $Q_{\text{lat}}$ is about the same, which indicates that this is a property which is

independent of road and weather conditions.

## 5.3 Mean estimation error

In order to evaluate the performance, the filters have been executed on three different data sequences with varying road and weather conditions:

**Sequence 1** American motorway with very gentle curves and with low curvature. Snow reduces the visibility of the vision system.

**Sequence 2** German motorway with many hills, which reduces the visibility of vision system. The sequence contains a lot of curves and curves with relatively high curvature. Weather conditions are fine.

**Sequence 3** German motorway, also with many curves. Visibility of the vision system is good since there are almost no slopes and good weather conditions.

Each sequence is 5 minutes long and all three contains plenty of other vehicles that can be used to support the road geometry estimate. The performance has been compared by computing the Root Mean Square Error (RMSE) for each filter on the three sequences. For reference, the error of the unfiltered measurements of road curvature, taken directly from the image processing unit, has also been computed. The results are shown in Table 1. Using the method in Section 5.2, a scale factor of about one for $Q_{\text{lat}}$ was chosen as a common optimum for all three sequences. It can be seen that an important improvement in accuracy compared to the unfiltered measurements comes from the Kalman filter for the host vehicle and road states only, *i.e.*, the decoupled filter. However, also adding information about leading vehicles, which is done in Filter A, B and C, further improves performance.

Table 1 reveals on examination that Filter A, B and C (the performance is similar) reduces the RMSE 7 - 13 percent compared to the decoupled filter and 35 - 80 percent compared to the unfiltered measurements. Most of the improvement in Filter A, B and C originates from curve entries and exits. This is rather small subset of the data sequences, which means that the improvement during these specific events is much higher. For an illustration of this, consider the curvature estimate plotted in Figure 8. Filter B has been compared to the decoupled filter for a short section of data sequence 3. It can be seen that during the actual changes in curvature there is a time delay in the decoupled filter, which is reduced significantly in Filter B.

It is interesting to note that the error in the measurements is significantly higher in sequence 1 and 2, which were with lower visibility. However, the improvement achieved by the filters in sequence 1 is much higher which is probably due to the fact that the curves are very gentle in this sequence. In particular, the curve entries and exits are much longer. Using information from leading vehicles is probably not needed in sequence 1 since the error in the decoupled filter alone is very small. From this particular experiment, it is difficult to conclude that one of the approximations has an advantage compared to the others since the performance is very similar.

| | Sequence 1 | Sequence 2 | Sequence 3 |
|---|---|---|---|
| Measurements | $5.28 \cdot 10^{-4}$ | $4.98 \cdot 10^{-4}$ | $2.72 \cdot 10^{-4}$ |
| Decoupled | $1.22 \cdot 10^{-4}$ | $3.36 \cdot 10^{-4}$ | $2.03 \cdot 10^{-4}$ |
| Filter A | $1.10 \cdot 10^{-4}$ | $3.12 \cdot 10^{-4}$ | $1.78 \cdot 10^{-4}$ |
| Filter B | $1.10 \cdot 10^{-4}$ | $3.13 \cdot 10^{-4}$ | $1.77 \cdot 10^{-4}$ |
| Filter C | $1.08 \cdot 10^{-4}$ | $3.12 \cdot 10^{-4}$ | $1.78 \cdot 10^{-4}$ |

***Table 1:*** *Curvature RMSE (1/m). Using the method in Section 5.2, a scale factor close to one for $Q_{lat}$ was chosen as a common optimum for all three sequences.*

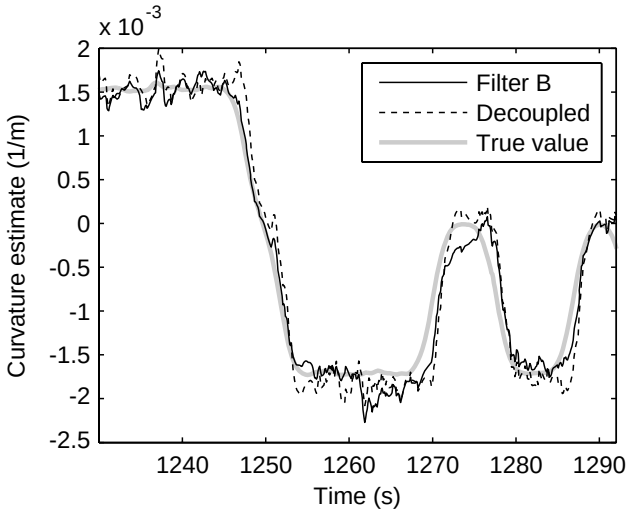


***Figure 8:*** *In this zoomed in section of data sequence 3 it can be seen that the decoupled filter has a time delay which is reduced by taking the movement of leading vehicles into account, as is illustrated by Filter B.*

### 5.4 Lane assignment

The problem of deciding which lane each tracked vehicles is currently occupying is usually referred to as the lane assignment problem. This is where the quality of the lane geometry estimate becomes vitally important; even the slightest error in the road shape parameters will result in a significant lateral error for distant vehicles, for instance at 70 - 100 metres.

In order to quantify the importance of the curvature parameter the $\tilde{y}$-part of (28e) is approximated using a second order Taylor expansion around $\Psi_{\text{rel}} = y = y_{\text{off}} = 0$,

$$\tilde{y} = (\cos(c_0 x) - 1)\frac{1}{c_0} \approx (1 - \frac{(c_0 x)^2}{2} - 1)\frac{1}{c_0} = c_0 \frac{x^2}{2}. \tag{30}$$

This implies that for small changes in $c_0$,

$$\Delta\tilde{y} \approx \frac{x^2}{2}\Delta c_0, \tag{31}$$

which means that for a leading vehicle 100 metres away from the host vehicle, a small error, say $5 \cdot 10^{-4}$ (1/m) in $c_0$ will result in an error of 2.5 metres in $\tilde{y}$. Such an error is enough to assign a leading vehicle to the wrong lane, which is a very serious error for the applications discussed in Section 2.

### 5.5 Statistical properties

Since the true curvature value is available, a statistical distribution of the error can be computed. In Figure 9, a histogram for the error is shown for data sequence 3. The error level $5 \cdot 10^{-4}$ (1/m) from the previous section has also been indicated, which is a requirement for making correct lane assignments at long distances. For quantification, the period of time that the error is above this level has been computed for all filters and all data sequences, as displayed in Table 2. This is an important property and any reduction of this number reduces the probability of error in a potential application.

In this experiment, the improvement of Filters A, B and C compared to the decoupled filter is obvious. Using Filter A, the reduction of the time where the error is above the threshold, compared to the decoupled filter, is 30 percent for data sequence 2 and 60 percent for sequence 3. The performance in sequence 1 is very good from all filters, including the decoupled filter, as was also discussed in Section 5.3. In fact, in Filters A, B and C the error is below the threshold in the entire sequence, and the decoupled filter is only above the threshold for 0.171 percent of the time, or approximately one sample every 60 seconds. The best performance in sequence 2 and 3 is obtained by Filter A and B, respectively. In Filters B and C, the clothoid parameter $c_1$ also affects the lane assignment, but it can be shown that its influence is negligible.

## 6 Conclusions

It is clear that combined lane prediction and target tracking can give better road shape estimates and thus improve the performance of automotive applications such as Emergency Lane Assist and Adaptive Cruise Control. The improvement is achieved by using

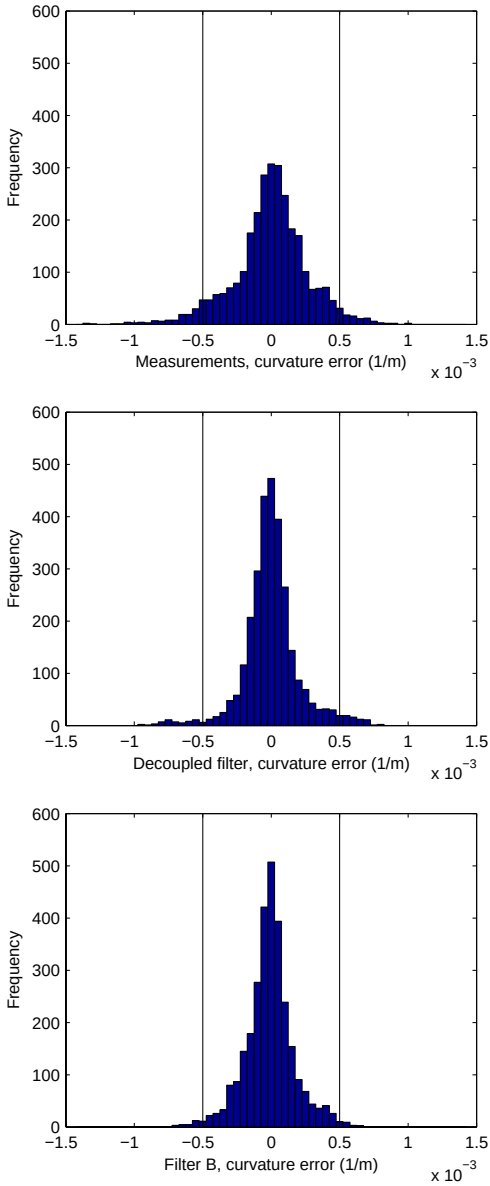


***Figure 9:*** *Error distribution in data sequence 3. The error level* $5 \cdot 10^{-4}$ *(1/m) is a requirement for making correct lane assignments at long distances.*

| | Sequence 1 | Sequence 2 | Sequence 3 |
|---|---|---|---|
| Measurements | 26.2% | 25.7% | 7.54% |
| Decoupled | 0.171% | 11.3% | 4.48% |
| Filter A | 0.0% | 7.86% | 1.78% |
| Filter B | 0.0% | 8.16% | 1.50% |
| Filter C | 0.0% | 8.03% | 1.88% |

***Table 2:*** *The period of time that the error is above the level* $5 \cdot 10^{-4}$*, expressed as a percentage of the total time.*

already available information, and thus no extra sensors or hardware is needed, although the computational cost is higher since the Kalman filter includes more states.

Three different road models have been evaluated, but none of them stands out as much better or worse than the others. Since Filter A, which does not include the clothoid parameter $c_1$, has similar performance to the other two filters, it is concluded that this parameter is not crucial in the measurement model. The advantage of Filter C is that the computational load can be reduced using a separate filter for the longitudinal dynamics of other tracked vehicles, thus reducing the number of states in the Kalman filter.

Other information that could be included to improve the performance is GPS with map data (Weigel et al., 2006) or a vision system with higher resolution dedicated to road geometry prediction is probably needed.

# 7 Appendix A: Proof of (4) and (10)

In this section, it is proved that the equation

$$\exp\left(\mathbf{R}(\frac{\pi}{2})\int_0^x c(\tau)d\tau\right)\hat{\mathbf{t}}_0 = \mathbf{R}\left(\int_0^x c(\tau)d\tau\right)\hat{\mathbf{t}}_0 \tag{32}$$

holds. The expression holds if, for any scalar $\lambda$

$$\exp\left(\mathbf{R}(\frac{\pi}{2})\lambda\right) = \mathbf{R}(\lambda) \tag{33}$$

In order to evaluate the left hand side, diagonalisation of the argument is used:

$$\mathbf{R}(\frac{\pi}{2})\lambda = \begin{pmatrix} 0 & -1 \\ 1 & 0 \end{pmatrix}\lambda = VD\lambda V^* \tag{34}$$

where

$$V = \frac{1}{\sqrt{2}}\begin{pmatrix} 1 & 1 \\ -i & i \end{pmatrix} \quad \text{and} \quad D = \begin{pmatrix} i & 0 \\ 0 & -i \end{pmatrix} \tag{35}$$

Then, since $V$ is orthonormal, $V^{-1} = V^*$ and thus

$$\exp(VD\lambda V^*) = V\exp(D\lambda)V^* = V\begin{pmatrix} \exp(i\lambda) & 0 \\ 0 & \exp(-i\lambda) \end{pmatrix}V^*$$

Now, these three matrices are multiplied:

$$\begin{aligned}\exp(\mathbf{R}(-\frac{\pi}{2})\lambda) &= \exp(VD\lambda V^*)\\ &= \frac{1}{2}\begin{pmatrix}\exp(i\lambda)+\exp(-i\lambda) & i\exp(i\lambda)-i\exp(-i\lambda)\\ -i\exp(i\lambda)+i\exp(-i\lambda) & \exp(i\lambda)+\exp(-i\lambda)\end{pmatrix}\\ &= \begin{pmatrix}\cos\lambda & -\sin\lambda\\ \sin\lambda & \cos\lambda\end{pmatrix} = \mathbf{R}(\lambda). \end{aligned} \tag{36}$$

This is the same expression as (33) and thus (32) holds. Finally, it is shown that

$$\begin{aligned}\mathbf{R}(\alpha)\begin{pmatrix}\cos\beta\\ \sin\beta\end{pmatrix} &= \begin{pmatrix}\cos\alpha & -\sin\alpha\\ \sin\alpha & \cos\alpha\end{pmatrix}\begin{pmatrix}\cos\beta\\ \sin\beta\end{pmatrix} = \begin{pmatrix}\cos\beta\cos\alpha-\sin\beta\sin\alpha\\ \cos\beta\sin\alpha+\sin\beta\cos\alpha\end{pmatrix}\\ &= \begin{pmatrix}\cos\beta & -\sin\beta\\ \sin\beta & \cos\beta\end{pmatrix}\begin{pmatrix}\cos\alpha\\ \sin\alpha\end{pmatrix} = \mathbf{R}(\beta)\begin{pmatrix}\cos\alpha\\ \sin\alpha\end{pmatrix}.\end{aligned}$$

# References


Blackman, S. S. (1986). *Multiple-Target Tracking with Radar Applications*. Artech House, Inc.

Citroën (2005). An innovation award for the LDWS. Press release, `www.citroen.com/CWW/en-US/NEWS/NEWSRELEASES/ArchivesNewsReleases/200506/23032005\_PRIXAFIL.htm`.

Dellaert, F. and Thorpe, C. (1997). Robust car tracking using Kalman filtering and Bayesian templates. In *Proceedings of the SPIE conference on Intelligent Transportation Systems*, volume 3207.

Dickmanns, E. D. and Zapp, A. (1986). A curvature-based scheme for improving road vehicle guidance by computer vision. In *Proceedings of the SPIE conference on Mobile Robots*.

Dickmanns, E. D. and Zapp, A. (1987). Autonomous high speed road vehicle guidance by computer vision. In *Selected Papers from the 10th Triennial World Congress of the International Federation of Automatic Control*, pages 221–226, Munich, Germany. Pergamon.

Eidehall, A. and Gustafsson, F. (2006). Obtaining reference road geometry parameters from recorded sensor data. In *Proceedings of the IEEE Intelligent Vehicles Symposium*, pages 256–260, Tokyo, Japan.

Eidehall, A., Pohl, J., Gustafsson, F., and Ekmark, J. (2006). Towards autonomous collision avoidance by steering. *IEEE Transactions on Intelligent Transportation Systems*.

Gern, A., Franke, U., and Levi, P. (2000). Advanced lane recognition - fusing vision and radar. In *Proceedings of the IEEE Intelligent Vehicles Symposium*, Dearborn, MI, USA.

Gern, A., Franke, U., and Levi, P. (2001). Robust vehicle tracking fusing radar and vision. In *Proceeding of The International Conference on Multisensor Fusion and Integration for Intelligent Systems*, pages 323–328.

Gillespie, T. D. (1992). *Fundamentals of Vehicle Dynamics*. Society of Automotive Engineers, Inc.

Gustafsson, F. (2000). *Adaptive Filtering and Change Detection*. John Wiley & Sons, Ltd.

Ishida, S. and Gayko, J. E. (2004). Development, evaluation and introduction of a lane keeping assistance system. In *Proceedings of the IEEE Intelligent Vehicles Symposium*, pages 943–344, Parma, Italy.

Kailath, T., Sayed, A. H., and Hassibi, B. (2000). *Linear estimation*. Prentice Hall.

Kalman, R. E. (1960). A new approach to linear filtering and prediction problems. *Transactions of the ASME-Journal of Basic Engineering*, 82:35–45.

Kay, S. K. (1998). *Fundamentals of Statistical Signal Processing, Volume 1: Detection Theory*. Prentice Hall Signal Processing. Prentice Hall, Upper Saddle River, New Jersey.

Ma, B., Lakshmanan, S., and Hero, III, A. O. (2000). Simultaneous detection of lane and pavement boundaries using model-based multisensor fusion. *IEEE Transactions on Intelligent Transportation Systems*, 1(3):135–147.

Melo, J., Naftel, A., Bernardino, A., and Santos-Victor, J. (2006). Detection and classification of highway lanes using vehicle motion trajectories. *IEEE Transactions on Intelligent Transportation Systems*, 7(2):188–200.

NHTSA (2000). Automotive collision avoidance system field operational test. web page, National Highway Traffic Safety Administration, `www.nhtsa.dot.gov/people/injury/research/pub/ACAS/ACAS-fieldtest`.

Pilutti, T. and Ulsoy, A. G. (2003). Fuzzy-logic-based virtual rumble strips for road departure warning systems. *IEEE Transactions on Intelligent Transportation Systems*, 4(1):1–12.

Polychronopoulos, A., Amditis, A., Floudas, N., and Lind, H. (2004). Integrated object and road border tracking using 77 ghz automotive radars. In *Proceeding of the IEE Radar, Sonar and Navigation*, volume 151, pages 375–381.

Rugh, W. J. (1996). *Linear System Theory*. Information and system sciences series. Prentice Hal, Upper Saddle River, New Jersey, 2 edition.

Trzebiatowski, M. S. v., Gern, A., Franke, U., Kaeppeler, U.-P., and Levi, P. (2004). Detecting reflection posts - lane recognition on country roads. In *Proceedings of the IEEE Intelligent Vehicles Symposium*, pages 304–309, Parma, Italy.

Vägverket (1994). Vägutformning 94 version s-2. Technical report, Swedish National Road Administration.

Weigel, H., Cramer, H., Wanielik, G., Polychronopoulos, A., and Saroldi, A. (2006). Accurate road geometry estimation for a safe speed application. In *Proceedings of the IEEE Intelligent Vehicles Symposium*, pages 516–521, Japan.

Zomotor, Z. and Franke, U. (1997). Sensor fusion for improved vision based lane recognition and object tracking with range-finders. In *Proceedings of the IEEE Conference on Intelligent Transportation Systems.*

# Paper C

# Lane departure detection for improved road geometry estimation

**Authors:** Andreas Eidehall, Thomas Schön and Fredrik Gustafsson

Published in *Proceedings of the IEEE Intelligent Vehicles Symposium 2006*, pages 546–551, Tokyo, Japan.

# Lane departure detection for improved road geometry estimation

Andreas Eidehall[⋆§], Thomas Schön[⋆] and Fredrik Gustafsson[⋆]

[⋆]Department of Electrical Engineering
Linköping University
SE–581 83 Linköping, Sweden

[§]Vehicle Dynamics and Active Safety
Volvo Car Corporation
SE–405 31 Göteborg, Sweden

**Abstract**

This paper presents a method for detecting lane departures, including lane changes, of surrounding vehicles in an automotive tracking application. This information is used to adapt the dynamic models used in the estimation algorithm in order to accommodate for the fact that a lane departure is in progress. The goal is to improve the accuracy of the road geometry estimates, which is affected by the motion of surrounding vehicles. The significantly improved performance is demonstrated using sensor data from authentic traffic environments.

# 1 Introduction

This paper is concerned with the problem of simultaneously estimating the position of surrounding vehicles and the road geometry. The position of the surrounding vehicles is measured using a vision system and a radar, whereas the shape of the road is measured using vision only. It has been shown that integrating the tracking of other vehicles with the tracking of the road geometry parameters can give better performance than treating these problems separately (NHTSA, 2000, Dellaert and Thorpe, 1997, Eidehall and Gustafsson, 2004, Zomotor and Franke, 1997). A fundamental assumption is that leading vehicles will keep following their lane, and their lateral movement can thus be used to support the otherwise difficult process of road geometry prediction. For example, when entering a curve as in Figure 1 it can be seen that the vehicles ahead all start moving to the right and thus there is a high probability that the road is turning to the right. This information can be used to significantly improve the rather crude road geometry estimates provided by the vision system. The assumption introduced above can mathematically be represented as

***Figure 1:*** *When entering a curve, all vehicles start moving in the lateral direction. This information can be used to support the road geometry estimate.*

$\dot{y}^i = 0$, where $y^i$ is the lateral position of vehicle $i$. Note that $y^i$ is the position in relation to the lane, not the position in global Cartesian coordinates or coordinates attached to the host vehicle. In order to efficiently handle this, a road-aligned, curved coordinate system is employed. It is important to note that the assumption of zero lateral velocity of the leading vehicles does not hold when they depart from the lane. This is typically accounted for in the model by adding white noise to the equation. The amount of noise, parameterised by the covariance matrix $Q_{\text{lat}}$, that should be used is a compromise. On the one hand it needs to be small enough for the lateral movement of the tracked vehicles to in fact improve the road prediction. On the other hand, it needs to be large enough so that every lane departure of a leading vehicle is not misinterpreted as a curve entry. This exemplifies the fundamental compromise present in all recursive estimation problems, the trade-off between noise attenuation and tracking accuracy. This compromise is illustrated in Figure 2, where the estimated road curvature, one of the road geometry parameters, using two different filters is plotted. One filter with a high value of $Q_{\text{lat}}$ and one filter with a low. For reasons of comparison, the true values for the road curvature which is obtained from the sensor data (Eidehall and Gustafsson, 2006) and the raw measurements from the

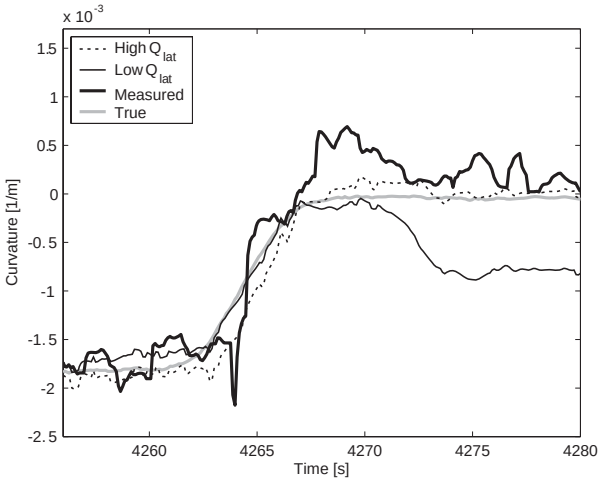


***Figure 2:*** *Comparison of estimation performance from two filters, one with a large $Q_{lat}$ and one with a small $Q_{lat}$. The raw measurement signal from the image processing unit and the reference signal are also included. Comparing the raw vision measurement to the result from the filters clearly illustrates the power of a model based sensor fusion approach.*

vision system are also included. It is interesting to compare the raw vision measurements to the result from the filter. This clearly illustrates the power of a model based sensor fusion approach.

In Figure 2, an exit phase of a curve where the curvature drops from about $1.8 \cdot 10^{-3}$ $[m^{-1}]$ to zero can be seen. In this particular scenario there are two leading vehicles that can support the curvature estimate, see Figure 1. It can be seen that the filter with a low value of $Q_{\text{lat}}$ performs much better during the curve exit and this is how we would really like to tune the filter. However, at a later stage the performance of this filter deteriorates. If the recorded video is studied, see Figure 3, it can be seen that this performance degradation coincide exactly with a lane change of one of the leading vehicles. The filter with a higher value of $Q_{\text{lat}}$ does not suffer from this problem, but on the other hand it has a time delay in the estimate during the curve exit.

The aim of this paper is to detect harmful lane departures of the leading vehicles and adapt the models accordingly, in order to obtain an improved road geometry estimate. When the lane departures have been detected, the compromise discussed above can systematically be resolved. This is accomplished by using a small $Q_{\text{lat}}$ when the assumption $\dot{y}_i = 0$ is valid and only increase $Q_{\text{lat}}$ during lane departure maneuvers.

Detection of lane departures and other model changes in automotive tracking has previously been studied, for example by Kaempchen et al. (2004) and Weiss et al. (2004), where Interacting Multiple Models (IMM) are used. However, their purpose is to improve the position estimates of the surrounding objects, rather than the road geometry parameters. Another approach is presented by Yen et al. (2004), where a neural network is used

to detect lateral movement in a vision based system. The method we propose is different and based on the standard *cumulative sum* (CUSUM) algorithm (Page, 1954, Gustafsson, 2000), which is augmented with a module for correcting the error caused by using the wrong model during the detection phase.

The paper is structured as follows. First, the dynamic model and the estimation algorithm are briefly reviewed in Section 2. This is followed by a discussion on how to detect lane departures of leading vehicles and how this information can be used to obtain better estimates. In Section 4 it is discussed how the error caused by using the wrong model during the detection phase can be corrected. Finally, we provide a discussion on alternative methods in Section 5 and state our conclusion in Section 6.

## 2 Estimation Problem

The dynamic model is based on a curved, road-aligned coordinate system, defined in Figure 4, where $x$ is the longitudinal position along the road and $y$ is the lateral position perpendicular to $x$. For instance, this means that if $y^i$ is the lateral position of object $i$, then $y^i = 0$ simply means that object $i$ is at the centre of our own lane, irrespective of road shape. For the lateral dynamics, a constant position model is used, i.e., $\dot{y}^i = 0$, and for the longitudinal dynamics a constant velocity model is used. Other states in the model are lane width $W$, host vehicle lateral position $y_{\text{off}}$, host vehicle heading angle relative to the lane $\Psi_{\text{rel}}$, road curvature parameter $c_0$, which is defined as the inverse road radius and finally the road clothoid parameter $c_1$, i.e. the curvature change rate. The vision system delivers estimates of $W$, $y_{\text{off}}$, $\Psi_{\text{rel}}$ and $c_0$, which are used as measurements in our estimation problem. Furthermore, the radar provides measurements of the relative position of objects resolved in the coordinate system $(\tilde{x}, \tilde{y})$, attached to the host vehicle. The dynamic model is discussed in more detail in the Appendix and the resulting estimation problem and its solution is treated elsewhere (Eidehall and Gustafsson, 2004, Eidehall et al., 2005). Tuning of the process and measurement noise will not be discussed in detail, except for the process noise of $y^i$. The discrete-time dynamic model describing the evolution of $y^i$

***Figure 3:*** *A snapshot from the video just after time 4270 [s], where the lane change of the tracked vehicle commences.*

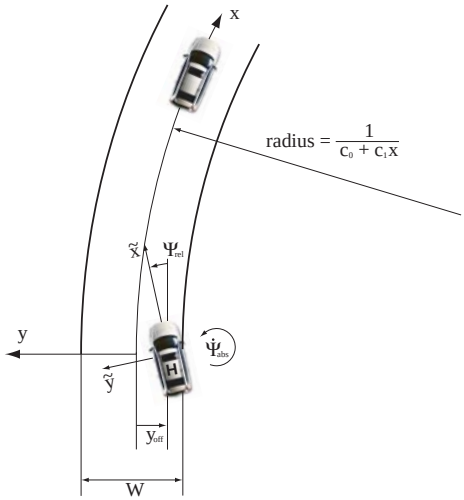


***Figure 4:*** *The surrounding vehicles are conveniently modelled and tracked using a curved, road-aligned coordinate system* $(x, y)$.

over time is given by

$$y_{t+1}^i = y_t^i + w_t^i, \tag{1}$$

where $w_t^i$ is zero mean white Gaussian noise, with variance $Q_{\text{lat}}$. In applying an Extended Kalman Filter (EKF), the tuning parameter $Q_{\text{lat}}$ describes to what degree it is believed that vehicles will keep driving at the same lateral position in relation to the lane.

# 3 Detecting Lane Departures

The approach employed for improving the road geometry estimates based on detecting lane departures is illustrated in Figure 5. This is a standard approach within the area of

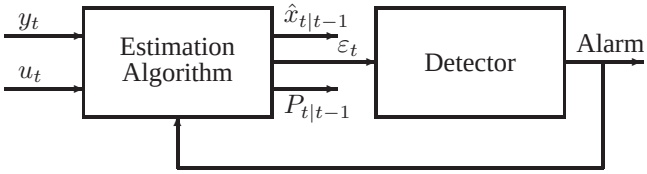


***Figure 5:*** *The estimation algorithm delivers residuals, which are used in the detector to decide whether a change has occurred or not. If a change is detected this information is fed back for use in the estimation algorithm. Note that in this application, one detector for each tracked vehicle is needed.*

change detection, which is a well established research area (Gustafsson, 2000, Basseville and Nikiforov, 1993, Kay, 1998). The aim of the detector in Figure 5 is to detect lane departures based on the information available in the residuals $\varepsilon_t = y_t - \hat{y}_t$ from the estimation algorithm. When a lane departure is detected this is indicated by an alarm from the detector, which is used to temporarily change model for the vehicle performing the lane departure. This implies that the estimation algorithm can provide a better estimate, simply due to the fact that a more accurate model is used. This section is concerned with devising the detection algorithm illustrated with the detection box in Figure 5. The estimation algorithm used in the present studies is based on the extended Kalman filter (Eidehall, 2004, Eidehall and Gustafsson, 2004). The basic components of a change detection algorithm are illustrated in Figure 6.

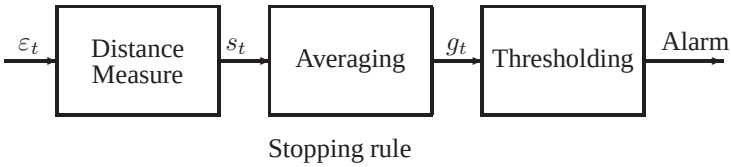


***Figure 6:*** *The components of the detector are a distance measure, and a stopping rule, where the latter consists of an averaging and a thresholding procedure.*

## 3.1 Distance Measure

The distance measure is used to gage whether a change has occurred or not. It is an important design variable, that should be chosen with the application in mind. Common standard choices are to use the residuals $s_t = \varepsilon_t$ or the squared residuals $s_t = \varepsilon_t^2$. However, in the present application this would provide poor detection performance. The reason is that the residuals only contain angular information. This would imply that the distance measure implicitly depend on the longitudinal distance to the leading vehicle, whereas for detecting lane departures we are only interested in lateral distances. If the longitudinal distance to the leading vehicle is small, a small change of its lateral position would lead to a large angular change. If the same change of lateral position would be observed for a vehicle further away, the angular change would be smaller. Hence, we need a distance measure that is invariant to the distance to the leading vehicle. The most natural choice in this respect is provided by lateral displacement of the leading vehicle, approximately given by

$$s_t = |\varepsilon_t r_t|, \tag{2}$$

where $r_t$ denotes the distance to the leading vehicle, available from the estimation algorithm, primarily based on the radar measurements. The reason for using $|\varepsilon_t r_t|$ and not just $\varepsilon_t r_t$ in (2) is that we want to be able to detect both left and right lateral displacements, using a one-sided test.

## 3.2 Stopping Rule

The stopping rule is used to give an alarm when an auxiliary test statistic $g_t$ exceeds a certain threshold. One of the most powerful tools for obtaining a good stopping rule in change detection problems is provided by the *CUSUM-test*, introduced by Page (1954).

*ALGORITHM 1 (CUSUM-test).*

1. $g_t = \max(g_{t-1} + s_t - \nu, 0)$.
2. Alarm if $g_t > h$.

After an alarm, reset $g_t = 0$.

## 3.3 Application and Result

When the CUSUM-test gives an alarm this is fed back to the estimation algorithm, where an increased $Q_{\text{lat}}$ is employed for the vehicle performing the lane departure. Since this model better describes the lane departure it will result in better estimates, which also is clear from Figure 7. This lane departure model is used for 2 seconds, the approximate time of a typical lane departure. After this we switch back to the original model. The

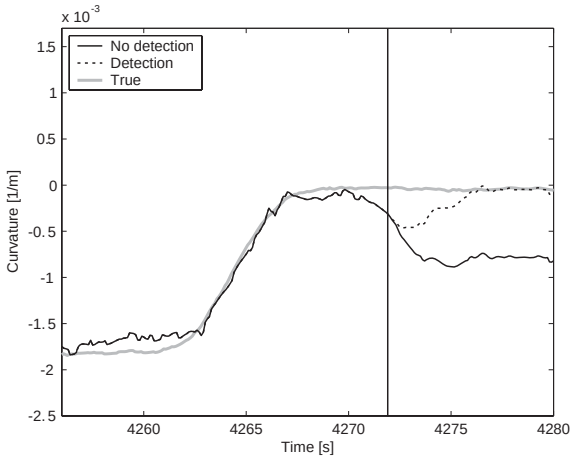


***Figure 7:*** *Illustrating how the estimation performance is improved using lane departure detection. This is the same data using in Figure 2, but the estimates from the filter based on change detection is also included.*

idea outlined above has been tested using 35 minutes of authentic traffic data. The detection performance is detailed in Table 1. For the present application a missed detection is much worse than false detection. A missed detection clearly degrades the estimation performance substantially, see Figure 7, whereas a false detection merely implies a slight performance degradation, since more noise than necessary is used in the model. Hence,

***Table 1:*** *Detection performance, based on* $35$ *minutes of authentic traffic data.*

| | |
|---|---|
| Correct detections | 35 |
| Missed detections | 3 |
| False detections | 27 |

the $27$ false detections are not that serious. It is interesting, and perhaps not too surprising, to note that most of the false detections are due to sharp road turns. If these could be isolated, most of the false detections could probably be eliminated. However, since the false detections does not significantly degrade the performance this has not been investigated further.

# 4 Further enhancement

In most signal based detection algorithms, there is a detection delay, *i.e.*, a time delay between the actual event, for example the start of a lane change manoeuvre, and the detection. In the CUSUM-test, the detection delay is the time it takes for $g_t$ to reach the threshold $h$. This means that when an alarm is triggered, the actual event took place a certain time ago, which in this application means that, even if the model is changed at the time of the alarm, the wrong model has been used during the detection phase.

In this section, a way of correcting for the error that is made by using the wrong model during the detection phase is introduced. The idea is to store old measurements $y_t$, input signals $u_t$, estimates $\hat{x}_{t|t}$ and covariance matrices $P_{t|t}$ in a memory. If the time when an event, such as a lane change, occurs is defined as $t_0$ and the average time delay for detection is $t_{\text{delay}}$, then the time when the detection is made is on average $t_0 + t_{\text{delay}}$. We

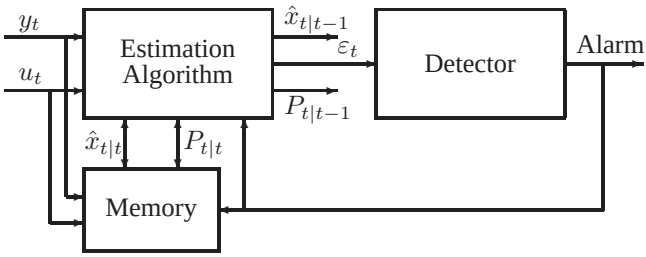


***Figure 8:*** *The change from Figure 5 is that a memory block has been included. The memory block stores the recent history of the measurements, input signals, estimates and their covariance.*

propose a *refiltering* scheme, that on detection at time $t_0 + t_{\text{delay}}$, the filter is rerun with the correct model between times $t_0$ and $t_0 + t_{\text{delay}}$ in order to correct for the error that is caused by using the wrong model. The estimate at time $t_0 + t_{\text{delay}}$ is then replaced with the one that has been obtained with the correct model. A schematic illustration of this idea is given in Figure 8.

In our application, this means that $Q_{\text{lat}}$ is increased a certain time *before* the detection and then kept high according to the previous section so that the total time equals the time of a typical lane change. A result of this is typically a jump in the estimate at the detection times. Two detailed examples of the behaviour of the enhanced algorithm are illustrated in Figure 9 and Figure 10. The performance for a five minute data set is shown in Figure 11.

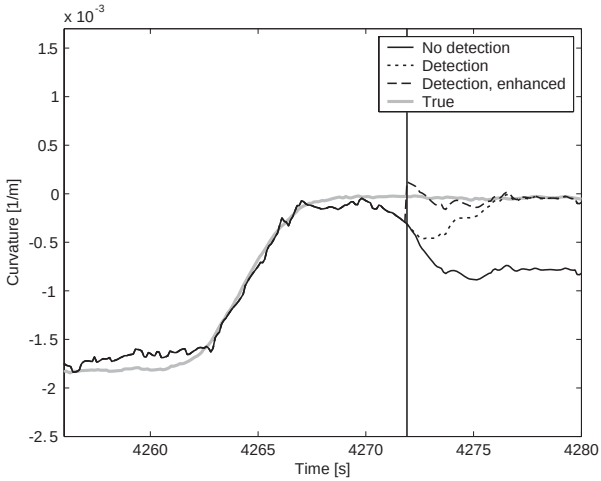


***Figure 9:*** *The behaviour of the three approaches when the lane change is detected. The filter with no detection scheme deteriorates, the filter with detection converges when switching to the correct model, and the enhanced detection algorithm jumps to the value it would have had if it had used the correct model from the beginning of the lane change.*

# 5 Alternative methods

Weiss et al. (2004) discuss the use of a filter based on interacting multiple models (IMM) for detecting lane changes. The goal of their work is to improve the position estimates of surrounding vehicles, rather than road geometry. Of course, the same approach could be used in an integrated road geometry and object tracking model as the one proposed in this article in order to also improve road geometry estimation.

In an IMM approach, two or more models are run simultaneously and they are each given a probability, of being the "correct model", based on their residuals. The final estimate is then formed as a weighted average, using the probabilities as weights. We believe that the methods we propose here, based on the CUSUM-test, have several advantages. Firstly, a lane change is a distinct event, so either one or the other model is valid, not something in between. This means that conceptually, it is preferable to switch models completely rather than averaging two models. Secondly, the CUSUM-test provides a

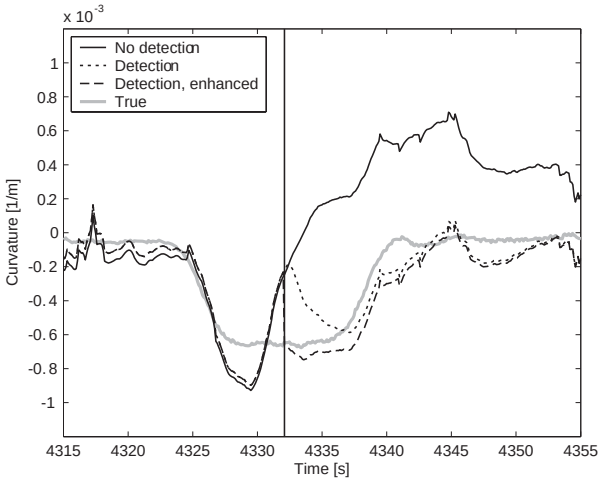


***Figure 10:*** *Same plots as in Figure 9 but for a different time interval.*

clear indication that something has happened, rather than a continuous change in probabilities and this indication can be used to take appropriate countermeasures. For example, this is necessary for initiating the refiltering scheme presented in Section 4.

Other methods that could be interesting to investigate is to use a two-sided test. In the proposed method, the absolute value of the residuals was used in combination with a one-sided test. An alternative could be to use the signed residuals and a two-sided test, which might eliminate some of the false alarms. The reason is that an alarm could be triggered by a driver who is "wobbling" in the lane but actually not changing lanes. On the other hand, it could be argued that we would benefit from detecting any kind of lateral movement, not just lateral movement related to a lane change.

# 6 Conclusion

By detecting behaviour that deviates from the model in a tracking system, we can rely more on the model when it in fact is accurate. In the present application, this means that the road geometry estimate, which is supported by the motion of surrounding vehicles, can be significantly improved. A CUSUM-test is used, which has the advantage of giving a distinct alarm when a change has occurred. It is also concluded that the method of correcting for the error that was caused by using the wrong model during the detection phase does give further improvements of the estimation accuracy.

# 7 Acknowledgment

The authors would like to thank the program SEnsor Fusion for Safety systems (SEFS), part of the larger Intelligent Vehicle Safety Systems (IVSS) program and Volvo Car Cor-

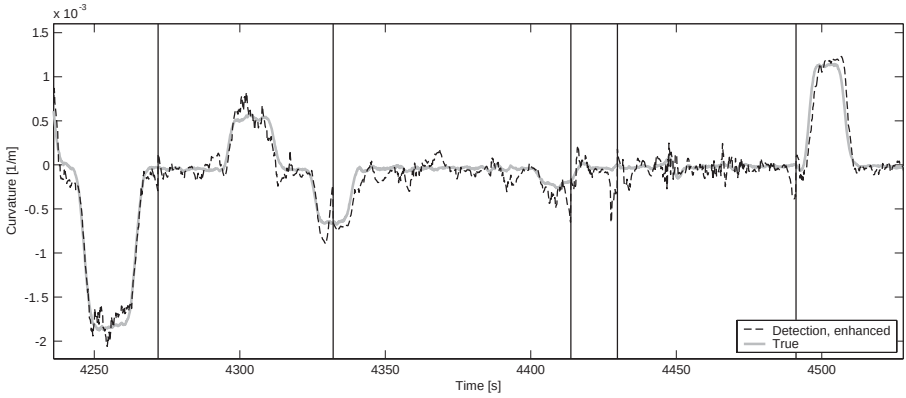


***Figure 11:*** *This figure shows the curvature estimate for a five minute data set collected in an authentic traffic environment, compared to the true curvature value. The vertical lines indicates detection of lane changes. It is interesting to note that in the last curve, around time 4500 [s], there is a time delay in the filter which is not present in any of the other curves. This is due to the fact that there are no vehicles to support the estimate and thus the curve can only be detected robustly once we have entered it.*

poration for supporting this work.

# Appendix A: Dynamic Model

In this appendix the underlying dynamic model that is used throughout the paper is discussed in more detail. The derivation is performed in continuous-time. The discrete-time dynamic is obtained using the standard sampling formula (Rugh, 1996), under the assumption of piecewise constant input signals.

## System Model

The coordinates $x$ and $y$ denote the position in the curved coordinate system, which is attached to the road according to Figure 4. The longitudinal coordinate $x$ is relative, i.e., $x$ is the longitudinal distance between the host vehicle and the tracked object. The motion model for the surrounding vehicles is greatly simplified in using the curved, rather than a Cartesian coordinate system. For example, it allows us to use the equation $\dot{y}^i = 0$, to model the assumption that the surrounding vehicles will follow their own lanes. In the longitudinal direction $\ddot{x}^i = -a\cos(\Psi_{\text{rel}})$ will be used, where $a$ is the measured acceleration of the host vehicle, if available. Hence, we have the following motion model:

$$\dot{x}^i = v^i, \tag{3a}$$
$$\dot{v}^i = -a\cos(\Psi_{\text{rel}}), \tag{3b}$$
$$\dot{y}^i = 0, \tag{3c}$$

where $v^i$ is the longitudinal relative velocity of object $i$, i.e., the time derivative of $x^i$. It is affected by the host vehicle acceleration since it is the *relative* velocity that is modelled. For the road geometry parameters we first clarify that $\Psi_{\text{rel}}$ is the angle between the host vehicle and the lane, see Fig 4, whereas $\Psi_{\text{abs}}$ is the angle to some fix reference. A relationship between the two can be obtained by differentiating $\Psi_{\text{rel}}$ w.r.t. time,

$$\Psi_{\text{rel}} = \Psi_{\text{abs}} + \gamma \quad \Rightarrow \tag{4a}$$
$$\dot{\Psi}_{\text{rel}} = \dot{\Psi}_{\text{abs}} + \dot{\gamma} = \dot{\Psi}_{\text{abs}} + \frac{v}{r} = \dot{\Psi}_{\text{abs}} + c_0 v, \tag{4b}$$

where $r$ is the current road radius, $v$ the velocity and $\gamma$ denotes the angle between the lane and some fix reference. $\dot{\Psi}_{abs}$ is typically measured using a yaw rate sensor. Furthermore,

$$\dot{y}_{off} = \sin(\Psi_{\text{rel}})v \approx \Psi_{\text{rel}} v. \tag{5}$$

Using $\dot{W} = 0$ and $\dot{c}_1 = 0$ continuous-time motion equations for the road model can be written

$$\dot{W} = 0, \tag{6a}$$
$$\dot{c}_0 = v c_1, \tag{6b}$$
$$\dot{c}_1 = 0, \tag{6c}$$

and for the motion of host vehicle we have

$$\dot{y}_{off} = v\Psi_{\text{rel}}, \tag{7a}$$
$$\dot{\Psi}_{\text{rel}} = v c_0 + \dot{\Psi}_{\text{abs}}. \tag{7b}$$

To account for uncertainties in the model we add zero mean white Gaussian noise to the corresponding discrete-time equations. The covariance matrices are $Q_{\text{road}}$, $Q_{\text{host}}$ and $Q_{\text{obj}}$ for the road, host and object states, respectively. Note that $Q_{\text{lat}}$, defined in Section 1 is the diagonal component of $Q_{\text{obj}}$ corresponding to (3c), the lateral movement of the tracked vehicles.

## Measurement Model

The measurements for the host vehicle are $\Psi^m_{\text{rel}}$, $c^m_0$, $L^m$ and $R^m$, where the two latter are the distances to the left and right lane marking, see Figure 4. Superscript $m$ is used to denote measured quantities. The (relative) position $(\tilde{x}^m,\ \tilde{y}^m)$ of the surrounding vehicles is measured using radar. Note that the radar delivers measurements resolved in the

Cartesian coordinate system, which is attached to the vehicle. The resulting measurement model is,

$$L^m = W/2 - y_{\text{off}}, \tag{8a}$$
$$R^m = -W/2 - y_{\text{off}}, \tag{8b}$$
$$\Psi^m_{\text{rel}} = \Psi_{\text{rel}}, \tag{8c}$$
$$c^m_0 = c_0, \tag{8d}$$
$$\begin{pmatrix} \tilde{x}^{i,m} \\ \tilde{y}^{i,m} \end{pmatrix} = \frac{R(-\Psi_{\text{rel}})}{c_0} \begin{pmatrix} (1 + c_0 y^i)\sin(c_0 x^i) \\ (1 + c_0 y^i)\cos(c_0 x^i) - 1 - c_0 y_{\text{off}} \end{pmatrix}, \tag{8e}$$

where $R(-\Psi_{\text{rel}})$ is a rotational matrix performing clockwise rotation of $\Psi_{\text{rel}}$ radians. Furthermore, zero mean Gaussian white measurement noise is added to (8). The covariance matrices are $R_{\text{host}}$ and $R_{\text{obj}}$ for the host/road and object states, respectively.

## References


Basseville, M. and Nikiforov, I. V. (1993). *Detection of abrupt changes theory and applications.* Information and systems sciences series. Prentice Hall, Englewood Cliffs, NJ, USA.

Dellaert, F. and Thorpe, C. (1997). Robust car tracking using Kalman filtering and Bayesian templates. In *Proceedings of the SPIE conference on Intelligent Transportation Systems*, volume 3207.

Eidehall, A. (2004). An automotive lane guidance system. Licentiate Thesis 1122, Department of Electrical Engineering, Linköping University.

Eidehall, A. and Gustafsson, F. (2004). Combined road prediction and target tracking in collision avoidance. In *Proceedings of the IEEE Intelligent Vehicles Symposium*, pages 619–624, Parma, Italy.

Eidehall, A. and Gustafsson, F. (2006). Obtaining reference road geometry parameters from recorded sensor data. In *Proceedings of the IEEE Intelligent Vehicles Symposium*, pages 256–260, Tokyo, Japan.

Eidehall, A., Schön, T. B., and Gustafsson, F. (2005). The marginalized particle filter for automotive tracking applications. In *Proceedings of the IEEE Intelligent Vehicle Symposium*, pages 369–374, Las Vegas, USA.

Gustafsson, F. (2000). *Adaptive Filtering and Change Detection.* John Wiley & Sons, Ltd.

Kaempchen, N., Weiss, K., Schaefer, M., and Dietmayer, K. C. J. (2004). IMM object tracking for high dynamic driving maneuvers. In *Proceedings of IEEE Intelligent Vehicles Symposium*, pages 825–830, Parma, Italy.

Kay, S. K. (1998). *Fundamentals of Statistical Signal Processing, Volume 1: Detection Theory*. Prentice Hall Signal Processing. Prentice Hall, Upper Saddle River, New Jersey.

NHTSA (2000). Automotive collision avoidance system field operational test. web page, National Highway Traffic Safety Administration, `www.nhtsa.dot.gov/people/injury/research/pub/ACAS/ACAS-fieldtest`.

Page, E. S. (1954). Continuous inspection schemes. *Biometrika*, 41(1/2):100–115.

Rugh, W. J. (1996). *Linear System Theory*. Information and system sciences series. Prentice Hal, Upper Saddle River, New Jersey, 2 edition.

Weiss, K., Kaempchen, N., and Kirchner, A. (2004). Multiple-model tracking for the detection of lane change maneuvers. In *Proceedings of the IEEE Intelligent Vehicles Symposium*, pages 937–942, Parma, Italy.

Yen, P.-S., Fang, C.-Y., and Chen, S.-W. (2004). Motion analysis of nearby vehicles on a freeway. In *Proceedings of IEEE International Conference on Networking, Sensing & Control*, pages 903–908, Taipei, Taiwan.

Zomotor, Z. and Franke, U. (1997). Sensor fusion for improved vision based lane recognition and object tracking with range-finders. In *Proceedings of the IEEE Conference on Intelligent Transportation Systems*.

# Paper D

# Statistical threat assessment for general road scenes using Monte Carlo sampling

**Authors:** Andreas Eidehall and Lars Petersson

Extended version of “Threat assessment of general road scenes using Monte Carlo sampling”. In *Proceedings of the IEEE Intelligent Transportation Systems 2006*, pages 1173-1178.

Submitted to *IEEE Transactions on Intelligent Transportation Systems*, 2006.

Preliminary version published as Technical Report LiTH-ISY-R-2756, Department of Electrical Engineering, Linköping University, Linköping, Sweden.

# Statistical threat assessment for general road scenes using Monte Carlo sampling

Andreas Eidehall[⋆§] and Lars Petersson[†]

[⋆]Department of Electrical Engineering
Linköping University
SE–581 83 Linköping, Sweden

[§]Vehicle Dynamics and Active Safety
Volvo Car Corporation
SE–405 31 Göteborg, Sweden

[†] Vision Science, Technology and Applications
National ICT Australia Limited
Canberra, ACT 0200, Australia

**Abstract**

This article presents a threat assessment algorithm for general road scenes. A road scene consists of a number of objects that are known and the threat level of the scene is based on their current positions and velocities.

The future driver inputs of the surrounding objects are unknown, and are modelled as random variables. In order to capture realistic driver behaviour, a dynamic driver model is implemented as a probabilistic prior, which computes the likelihood of a potential manoeuvre. A distribution of possible future scenarios can then be approximated using Monte Carlo sampling. Based on this distribution, different threat measures can be computed, *e.g.*, probability of collision or time to collision.

Since the algorithm is based on Monte Carlo sampling, it is computationally demanding, and several techniques are presented to increase the performance without increasing computational load. The algorithm is intended both for on-line safety applications in a vehicle, and for off-line data analysis.

# 1 Introduction

While most research within automotive collision warning and avoidance is carried out on sensor technology, *e.g.*, radar, laser and vision systems, threat assessment is gaining more and more interest. Threat assessment algorithms are currently moving from deterministic models towards stochastic models which take many possible scenarios into account.

## 1.1 Deterministic threat assessment

Deterministic threat assessment refers to methods that predict a single future trajectory for all objects and uses these to compute various threat measures, for instance time to collision (Labayrade et al., 2005, Dagan et al., 2004, NHTSA, 2000), predicted minimum distance, predicted time to minimum distance (Polychronopoulos et al., 2004) etc. Note that the predicted trajectories are often based on statistical estimation methods such as the Kalman filter, but only a point estimate is then used in the threat assessment.

Jansson (2005) provides an overview of different deterministic threat assessment methods. An approach when systematically choosing warning thresholds in different deterministic methods is presented by Yang et al. (2003).

## 1.2 Stochastic threat assessment

A stochastic threat assessment algorithm is demonstrated by Jansson (2005) in a Collision Mitigation by Braking System. The estimated probability density from the Kalman filter is predicted using Kalman filter time updates, thus also predicting the distribution, and then using this distribution to find the future point in time where the probability of collision equals one. However, this method is only suitable for short time predictions since the uncertainty quickly increases. Polychronopoulos et al. (2004) suggests using several different models for prediction, representing possible future manoeuvres. The different possibilities are then condensed into a single prediction without considering them as distinct possibilities. Broadhurst et al. (2005) takes this one step further and considers many (thousands) different possibilities for all objects by trying to approximate the true probability density function (PDF) of the predictions with Monte Carlo sampling. The current state of all objects is assumed known, and the control inputs that determine the future trajectories are modelled as stochastic variables which can then be used to compute a PDF for the future positions.

Our work is based on the framework presented by Broadhurst *et al.* , with some modifications, and uses this to define a new threat assessment method. One of the contributions is a new way to create a more efficient use of the samples. This is achieved by using a dynamic model that is designed with the Monte Carlo sampling in mind, but also by an iterative sampling process which removes and replaces samples that generate collisions at an early stage. We have also added visibility constraints to highlight the fact that drivers have most of their attention focused forward and thus are less likely to detect and consider objects in other regions.

The main goal of the threat assessment algorithm is to detect general threats, *i.e.*, threats that are not necessarily connected to a particular safety function. For example, an extension compared to most conventional safety systems is the ability to detect *indirect*

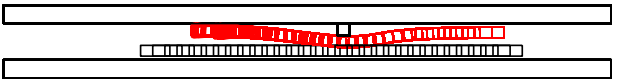

***Figure 1:*** *In this situation, the host vehicle (black) is moving from the left to right in a straight line, and an oncoming vehicle (red) is moving from the right to the left. The system predicts that it is likely that the oncoming vehicle will have to swerve left in order to avoid the obstacle, and thus becomes a threat to the host vehicle.*

*threats.* These are threats from objects that may not be on a direct collision course, but are forced into a collision course by other elements in the traffic situation. An example illustrating this is when an oncoming vehicle has to swerve to avoid an obstacle and because of that becomes a threat to the host vehicle. The vehicles may not be on a direct collision course from the beginning, but the situation still poses a threat because of the obstacle. This example is illustrated in Figure 1. Another example is a tailgating situation. Again, the vehicles are not on a collision course from the beginning, but in this case there is a certain probability that the leading vehicle will brake.

In order to be able to use the threat assessment algorithm with general road scenes, a demonstration is provided showing how it can be combined with a road-aligned, curved coordinate system. This significantly simplifies the model when the road bends. Another contribution is a modified dynamic model which allows accelerations and dynamic forces to be accurately computed directly in the curved coordinate system. Using this, acceleration limitations due to road friction or engine torque can be incorporated without having to switch to Cartesian coordinates.

The result is an algorithm that currently runs off-line in Matlab and has been evaluated, both using a small set of simulated scenarios, and using a large set of recorded sensor data. The intended use is both for on-line safety applications with execution at every time update of the system, but also for off-line analysis of recorded sensor data.

The statistical model is formulated in Section 2 and the road-aligned coordinate system is presented in Section 2.5. Implementation aspects, such as time discretisation and collision detection are discussed in Section 4. Results and conclusions are given in Section 5 and Section 6, respectively.

# 2 Model

## 2.1 Stochastic model

The future paths of other objects are determined by their current position and their future control inputs such as steering, braking, etc. In a real application, their current positions can be measured using a sensor, or a combination of sensors. However, their future control inputs are unknown, and that is why in this paper, they are modelled using a stochastic variable

$$\mathcal{U} = [\mathbf{u}_1, \ldots, \mathbf{u}_m]$$

which consists of the control input for $m$ number of objects in the scene. $\mathbf{u}_i$ contains the control input for a time interval $I_t = [0, T_{\text{max}}]$ for object $i$, *i.e.*, $\mathbf{u}_i = (u_1(t), \ldots, u_{n_c}(t))_i$. $T_{\text{max}}$ is the prediction horizon, *i.e.*, the period of time when the predictions are made and $n_c$ is the number of control inputs for each object. This means that, given a control input $\mathcal{U}$, the entire system can be simulated, using motion models for all objects, to reach a state $X(\mathcal{U})$. $X(\mathcal{U})$ will contain the position and other states for all objects for the entire time interval $I_t$, given the control input $\mathcal{U}$, and can be written

$$X(\mathcal{U}) = [\mathbf{x}_1(\mathbf{u}_1), \ldots, \mathbf{x}_m(\mathbf{u}_m)].$$

In this paper, a prior distribution $\pi(\mathcal{U})$ is used to model driver preference, *i.e.*, that certain manoeuvres are more likely than others. Details are given in Section 2.3.

This framework is inspired by the work done by Broadhurst et al. (2005) in that the control inputs of other objects are considered stochastic and that we also use Monte Carlo sampling to compute the threat quantities. However, the method suggested by Broadhurst *et al.* does not consider the fact that almost always, drivers try to avoid colliding with other objects. This is further addressed in Section 3.

## 2.2 Dynamic model

### Cars/Bicycles

A car or a bicycle is geometrically described as a rectangle[1] and two control inputs $(u_1, u_2)$ are used for longitudinal and lateral control respectively.

The evaluation of (28) is based on discrete samples of $\mathcal{U}$. In any Monte Carlo application, there is a trade off between computational performance and accuracy. More samples means higher accuracy, but also higher computational load. In this application, the samples will be spread out over an interval of the control inputs, and we claim that it is important to have the sampling process in mind at an early stage when choosing the dynamic model.

For instance, Broadhurst et al. (2005) propose using steering wheel angles as control input. However, for high velocities, the limiting factor for lateral movement is not the steering angle, but rather tyre-to-road friction. In order to deal with this, Broadhurst *et al.* proposes to simply remove samples with higher lateral acceleration than what is physically allowed. We believe that better results could be obtained by distributing samples according to this maximum level from the beginning and thus, get a higher concentration of samples within the allowed control input set.

A simple friction model is used, where the maximal friction force is proportional to the normal force and thus limits the acceleration. To simplify the model, the accelerations in the lateral and longitudinal directions are treated separately. The model that will be

used is

$$\dot{x} = v\cos\theta \tag{1a}$$

$$\dot{y} = v\sin\theta \tag{1b}$$

$$\dot{v} = \begin{cases} u_1 a_f & \text{if } v \leq v_{\text{long}} \\ u_1 \frac{k/v + a_f}{2} + \frac{k/v - a_f}{2} & \text{if } v > v_{\text{long}} \end{cases} \tag{1c}$$

$$\dot{\theta} = \begin{cases} v\sin(\varphi_{\text{max}} u_2)/L & \text{if } v \leq v_{\text{lat}} \\ a_f u_2 / v & \text{if } v > v_{\text{lat}} \end{cases} \tag{1d}$$

where $(x, y)$ is the position, $v$ the velocity and $\theta$ the heading angle of the modelled vehicle. Furthermore, the maximum acceleration due to road friction is denoted $a_f$, $\varphi_{\text{max}}$ is the maximum steering angle, $L$ is the wheelbase and $k$ is a parameter describing engine power. $v_{\text{long}}$ and $v_{\text{lat}}$ are the breakpoint velocities at which the limit of the longitudinal acceleration switches from tyre-to-road friction to engine power, and from maximum steering angle to tyre-to-road friction[1]. Using this model, the control input sets $u_1, u_2 \in [-1, 1]$ can be used for all velocities.

### Pedestrians

The motion model for pedestrians is a simple constant acceleration model:

$$\begin{aligned} \dot{x} &= v_x \\ \dot{y} &= v_y \\ \dot{v}_x &= a_f u_1 \\ \dot{v}_y &= a_f u_2 \end{aligned}$$

The input set $u_1, u_2 \in [-1, 1]$ can also be used in this case.

### Obstacles

To emulate other obstacles and road boundaries, general convex polygons will be used. Each polygon also has a motion vector, which allows moving objects to be generated.

## 2.3 Prior distribution

The prior distribution $\pi(\mathcal{U})$ is used to model the fact that drivers have a goal with their driving. For instance, they want to get from point $A$ to point $B$ and maintain desired velocity. Typically, drivers also strive for a comfortable ride by minimising acceleration forces in all directions. Broadhurst et al. (2005), suggest a driver preference distribution that models four different aspects:

[1]Figures for a typical car: The size is $1.8 \times 4.8$ [m], $L = 2.4$ [m], $\varphi_{\text{max}} = 0.5$ [rad], $a_f = 9.1$ [ms$^{-2}$] and $k = 66.6$ [m$^2$s$^{-3}$]. This gives $v_{\text{lat}} = 6.76$ [m/s] and $v_{\text{long}} = 7.32$ [m/s]. For a bicycle, the size is $0.6 \times 2$ [m], $L = 1.6$ [m], $\varphi_{\text{max}} = 0.5$ [rad], $a_f = 4$ [ms$^{-2}$] and $k = 0.75$ [m$^2$s$^{-3}$]. This gives $v_{\text{lat}} = 3.7$ [m/s] and $v_{\text{long}} = 0.2$ [m/s].

1. Distance to intended path
2. Deviation from desired velocity
3. longitudinal acceleration
4. steering angle

We use the same distribution, except that the steering angle is replaced with lateral acceleration, which seems to be a more relevant measure. The distribution is defined as:

$$\pi(\mathcal{U}) = ae^{-f(\mathcal{U},X(\mathcal{U}))}, \tag{2}$$

where $a$ is a normalising constant and

$$f(\mathcal{U}, X(\mathcal{U})) = \sum_{i=1}^{m} \omega_i g(\mathbf{u}_i, \mathbf{x}_i(\mathbf{u}_i)). \tag{3}$$

The sum runs over all objects in the scene, *i.e.*, $f$ is the total cost of the manoeuvres of all objects. The weights $\omega_i$ can be used to prioritise the prior driver preference between different objects, something that is utilised when implementing the visibility constraints in Section 2.4. We then define

$$g(\mathbf{u}_i, \mathbf{x}_i(\mathbf{u}_i)) = \int_{I_t} [(l_x x(t) + l_y y(t) - l_z)^2 \lambda_1 + \tag{4}$$

$$(v(t) - v_0)^2 \lambda_2 + a_{\text{long}}(t)^2 \lambda_3 + a_{\text{lat}}(t)^2 \lambda_4] dt \tag{5}$$

which represents the cost of a manoeuvre for a single object over the entire time interval $I_t$, where $l_x x(t) + l_y y(t) - l_z$ measures the distance to the line $l = (l_x, l_y, l_z)$, and $v_0$ is the initial (desired) velocity. The line $l$ represents the desired path and can be any line, but usually it coincides with the tangent of the object at time $t = 0$. Note, that for the pedestrian object class, $v(t)$ has to be computed from $v_x(t)$ and $v_y(t)$. The signals $a_{\text{lat}}(t)$ and $a_{\text{long}}(t)$ are computed from the control inputs. The weights $\lambda_i$ are chosen to balance the costs of these different behavioural aspects in (4), and have so far been calibrated by visually inspecting the distributions[2]. These values are significantly higher than those presented by Broadhurst et al. (2005) which gives a narrower distribution. In order to avoid numerical problems at the "tails" of the distribution, a logarithmic representation of $\pi(\mathcal{U})$ has been implemented. A more systematic approach to calibrating these parameters, for example, by adapting the distribution to authentic recorded data, would certainly be interesting, and this may lie ahead in our future work.

## 2.4 Visibility constraints

In this section, a method is formulated for incorporating the fact that drivers have most of their attention directed forward and are more likely to detect other objects in this region.

[2] $\lambda_1 = 60/T_{\text{max}}$, $\lambda_2 = 0.5/T_{\text{max}}/(1 + |v_0|)$, $\lambda_3 = 1/T_{\text{max}}/a_f^2$, $\lambda_4 = 75/T_{\text{max}}/\varphi_{\text{max}}$ where $T_{\text{max}}$ is the length of the time interval $I_t$.

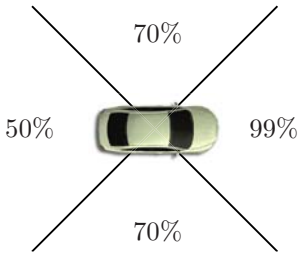


***Figure 2:*** *The probability that the host vehicle will observe/regard a vehicle within different regions.*

Furthermore, drivers are much more inclined to adapt their driving behaviour with respect to other vehicles in front of them rather than behind. For example, in Figure 3, if vehicle 1 approaches vehicle 2 from behind with a high relative velocity, then vehicle 1 is much more likely to change course in order to avoid colliding with vehicle 2, compared to vehicle 2 changing course in order to let vehicle 1 pass, even though this might have been a more comfortable manoeuvre for both vehicles overall.

The first step is to define regions around each object and then assign an attention level to each region. The regions and corresponding attention levels we have chosen are shown in Figure 2. These values are just an example and are not scientifically justified, the main contribution here is the way these constraints can be implemented. A matrix $\mathbf{V}$ is constructed which contains the visibility levels within all object pairs, where element $\mathbf{V}_{ij}$ indicates how well object $i$ can be seen or how much it is registered by object $j$. The example in Figure 3 will generate the following $\mathbf{V}$ matrix:

| | $j=1$ | $j=2$ | $j=3$ |
|---|---|---|---|
| $i=1$ | - | 50% | 99% |
| $i=2$ | 99% | - | 70% |
| $i=3$ | 99% | 70% | - |

The weights $\omega_i$ in (3) are then chosen as

$$\omega_i = \sum_{j \neq i} \hat{\mathbf{V}}_{ij} \tag{6}$$

where $\hat{\mathbf{V}}$ is a normalised version of $\mathbf{V}$, *i.e.*, the sum of all elements equals one. For instance, this means that in a situation where one vehicle follows another, the leading

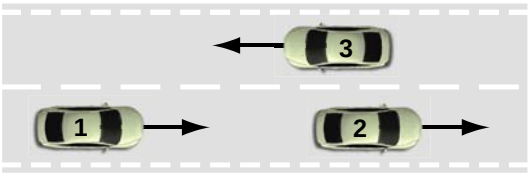


***Figure 3:*** *This scenario is used as an example to illustrate the method for incorporating visibility constraints.*

vehicle will have a high weight in order to represent the fact that this vehicle is more likely to follow its own preferences rather than adapting its behaviour to the vehicle approaching from behind.

## 2.5 Road-aligned coordinates and tracking

Many automotive tracking systems recently presented have proposed using a curved, road-aligned coordinate system for tracking (Polychronopoulos et al., 2004, Eidehall and Gustafsson, 2004, Zomotor and Franke, 1997). Such a curved coordinate system would also be very suitable to use with the threat assessment algorithm proposed in this article. For instance, if the road boundaries of a curved road are to be modelled in a Cartesian coordinate system, they would either have to be approximated with a number of polygon shapes, or a more general class of obstacles with curved edges would have to be introduced. If a road-aligned coordinate system is used, the road boundary could be modelled as a straight line instead. Furthermore, the driver preference function, represented by the prior in Section 2.3, could also be greatly simplified. The straight line representing the desired path, would automatically follow the curved road in such a coordinate system.

However, before the threat assessment algorithm can be implemented, the effects of the curved coordinate system on the physical limitations of the vehicle and the dynamic model need to be investigated. For example, when driving along a curve, a certain amount of the lateral force available is already used just to follow the road, thus reducing the amount of remaining friction force in that direction. This is not automatically incorporated and how to handle this is analysed in Section 2.5.

### Tracking

The position of objects in the road coordinates is often already available since tracking is typically done in that frame of reference. It has been shown that tracking in curved, road-aligned coordinates has many advantages (Eidehall and Gustafsson, 2004, Zomotor and Franke, 1997). The main feature is that the estimate of the road shape can be improved by studying the motion of leading vehicles and using a model of their motion in relation to the road. There are also other advantages when it comes to modelling and prediction. In the system presented, a road model with the shape of a circle segment is used (Eidehall and Gustafsson, 2004).

The positions of objects are expressed in $(x, y)$ coordinates, where $x$ is the longitudinal position along the road and $y$ is the lateral position measured from the centre of the host vehicle lane. In order to carry out tracking, these positions need to be related to the coordinate systems of the sensors attached to the host vehicle, which is why a host vehicle coordinate system $(\tilde{x}, \tilde{y})$ is introduced, see Figure 4.

A relationship between $(x, y)$ and $(\tilde{x}, \tilde{y})$ can be expressed as

$$\begin{pmatrix} \tilde{x} \\ \tilde{y} \end{pmatrix} = \mathbf{R}(-\Psi_{\text{rel}}) \begin{pmatrix} (1+cy)\sin(cx) \\ (1+cy)\cos(cx) - 1 - cy_{\text{off}} \end{pmatrix} \frac{1}{c}$$

where $\mathbf{R}$ is a rotational matrix, *i.e.*,

$$\mathbf{R}(\alpha) = \begin{pmatrix} \cos\alpha & -\sin\alpha \\ \sin\alpha & \cos\alpha \end{pmatrix}$$

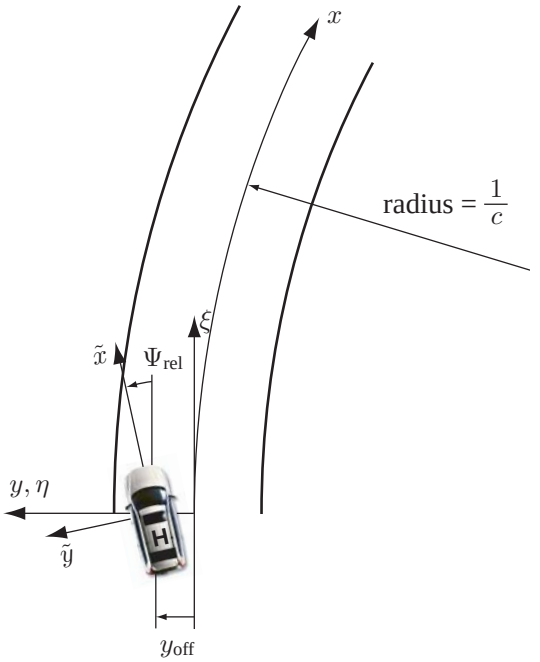


***Figure 4:*** *Definition of the coordinate systems* $(x, y)$*,* $(\tilde{x}, \tilde{y})$ *and* $(\xi, \eta)$ *and the parameters* $c$*,* $y_{\text{off}}$ *and* $\Psi_{\text{rel}}$*.*

and the other variables are defined in Figure 4. This relationship is then used to construct a measurement equation in an extended Kalman filter. For the purpose of tracking, a simpler dynamic model than the one described in Section 2.2 is used. One of the advantages of the road-aligned coordinate system is that modelling motion in relation to the road becomes greatly simplified. For example, the equation $\dot{y} = 0$ can be used to express the fact that vehicles will keep to their lanes, even if the road bends. For longitudinal dynamics, the equation $\ddot{x} = 0$ is used, *i.e.*, constant velocity.

### Vehicle dynamics in curved coordinates

In this section, the effects from the curved coordinate system on the dynamics of the vehicles are analysed, which is one of the main contributions of this work. A problem with a non-Cartesian frame of reference is that Newton's laws of motion cannot be directly applied. Instead, they need to be applied in a Cartesian coordinates, and then transformed to the curved space. Thus, we introduce Cartesian coordinates $(\xi, \eta)$ which are attached at the centre of the host vehicle lane and coincide with $(x, y)$ at the origin, see Figure 4. Then the accelerations $\ddot{x}$ and $\ddot{y}$ as functions of $\ddot{\xi}$ and $\ddot{\eta}$ are computed. The physical limits in the $(\xi, \eta)$ space can then be translated to the $(x, y)$ space. Starting with $\xi$, the relationship for

velocity is found as

$$\dot{\xi} = \frac{\partial \xi}{\partial x}\dot{x} + \frac{\partial \xi}{\partial y}\dot{y}.$$

Acceleration can then be obtained as

$$\begin{aligned}\ddot{\xi} =& \frac{d}{dt}\left(\frac{\partial \xi}{\partial x}\dot{x} + \frac{\partial \xi}{\partial y}\dot{y}\right) = \\ & \left(\frac{\partial^2 \xi}{\partial x^2}\dot{x} + \frac{\partial^2 \xi}{\partial x \partial y}\dot{y}\right)\dot{x} + \frac{\partial \xi}{\partial x}\ddot{x} + \left(\frac{\partial^2 \xi}{\partial x \partial y}\dot{x} + \frac{\partial^2 \xi}{\partial y^2}\dot{y}\right)\dot{y} + \frac{\partial \xi}{\partial y}\ddot{y} = \\ & \frac{\partial^2 \xi}{\partial x^2}\dot{x}^2 + \frac{\partial^2 \xi}{\partial y^2}\dot{y}^2 + 2\frac{\partial^2 \xi}{\partial x \partial y}\dot{x}\dot{y} + \frac{\partial \xi}{\partial x}\ddot{x} + \frac{\partial \xi}{\partial y}\ddot{y} = \\ & \mathbf{v}^T \mathbf{H}_\xi \mathbf{v} + \mathbf{J}_\xi \mathbf{a},\end{aligned} \tag{7}$$

where $\mathbf{v}$ and $\mathbf{a}$ represent the velocity and acceleration in the $(x, y)$ coordinates, *i.e.*,

$$\mathbf{v} = \begin{pmatrix}\dot{x} \\ \dot{y}\end{pmatrix}, \quad \mathbf{a} = \begin{pmatrix}\ddot{x} \\ \ddot{y}\end{pmatrix},$$

$\mathbf{J}_\xi$ is the Jacobian

$$\mathbf{J}_\xi = \begin{pmatrix}\frac{\partial \xi}{\partial x} & \frac{\partial \xi}{\partial y}\end{pmatrix}$$

and $\mathbf{H}_\xi$ is the Hessian matrix

$$\mathbf{H}_\xi = \begin{pmatrix}\partial^2 \xi / \partial x^2 & \partial^2 \xi / \partial x \partial y \\ \partial^2 \xi / \partial x \partial y & \partial^2 \xi / \partial y^2\end{pmatrix}.$$

The $\eta$ coordinate can be treated analogously:

$$\ddot{\eta} = \mathbf{v}^T \mathbf{H}_\eta \mathbf{v} + \mathbf{J}_\eta \mathbf{a}. \tag{8}$$

(7) and (8) is a general relationship between accelerations in two coordinate systems. A circular road segment has the following coordinate transformation:

$$\begin{pmatrix}\xi \\ \eta\end{pmatrix} = \begin{pmatrix}(1 + cy)\sin(cx) \\ (1 + cy)\cos(cx) - 1\end{pmatrix}\frac{1}{c}$$

Inserting this into (7) and (8), preferably using a symbolic software package, and collecting the trigonometric terms gives

$$\begin{aligned}\ddot{\xi} = \sin(cx)[\ \ddot{y} - c\dot{x}^2(1 + cy)\ ] + \\ \cos(cx)[\ (1 + cy)\ddot{x} + 2c\dot{x}\dot{y}\ ]\end{aligned} \tag{9}$$

$$\begin{aligned}\ddot{\eta} = \cos(cx)[\ \ddot{y} - c\dot{x}^2(1 + cy)\ ] - \\ \sin(cx)[\ (1 + cy)\ddot{x} + 2c\dot{x}\dot{y}\ ]\end{aligned} \tag{10}$$

The movement of objects along the $y$ axis is small (about $\pm 5$ [m]) compared to the typical road radius (typically above $100$ [m]) which implies that $|cy| \ll 1$ and thus $1 + cy \approx 1$. Furthermore, (9) and (10) can jointly be expressed as a rotation, again using the rotational matrix $\mathbf{R}$:

$$\begin{pmatrix} \ddot{\xi} \\ \ddot{\eta} \end{pmatrix} = \mathbf{R}(-cx) \begin{pmatrix} \ddot{x} + 2c\dot{x}\dot{y} \\ \ddot{y} - c\dot{x}^2 \end{pmatrix} \Leftrightarrow$$

$$\begin{pmatrix} \ddot{x} \\ \ddot{y} \end{pmatrix} = \mathbf{R}(cx) \begin{pmatrix} \ddot{\xi} \\ \ddot{\eta} \end{pmatrix} + \begin{pmatrix} -2c\dot{x}\dot{y} \\ c\dot{x}^2 \end{pmatrix} \tag{11}$$

However, $\ddot{x}$ and $\ddot{y}$ do not necessarily coincide with the longitudinal and lateral direction for the individual vehicles. That is why a rotation of the accelerations $\ddot{x}$ and $\ddot{y}$ with $\theta$ radians is needed, where $\theta$ is the heading angle of the vehicle relative to the road, as explained in Section 2.2. The Cartesian accelerations $\ddot{\xi}$ and $\ddot{\eta}$ also need to be rotated for the same reason, since the acceleration limitations are expressed in the vehicle reference frame. These needs to be rotated, first with $cx$ radians to be align with the road, $cx$ being the angle between the $x$ axis and the $\xi$ axis, and then with an additional $\theta$ radians to become aligned with the vehicle. The following variables are introduced:

$$\begin{pmatrix} a_{\text{long}} \\ a_{\text{lat}} \end{pmatrix} = \mathbf{R}(\theta) \begin{pmatrix} \ddot{x} \\ \ddot{y} \end{pmatrix} \tag{12}$$

$$\begin{pmatrix} a'_{\text{long}} \\ a'_{\text{lat}} \end{pmatrix} = \mathbf{R}(\theta + cx) \begin{pmatrix} \ddot{\xi} \\ \ddot{\eta} \end{pmatrix} \tag{13}$$

where “long” and “lat” refer to the longitudinal and lateral direction of vehicle modelled. To explain the notation, $a_{\text{long}}$ and $a_{\text{lat}}$ are accelerations in the curved coordinate system and $a'_{\text{long}}$ and $a'_{\text{lat}}$ are the corresponding accelerations in a fixed Cartesian coordinate system, where Newton’s laws of motion can be applied. Multiplying (11) with $\mathbf{R}(\theta)$ immediately gives

$$\begin{pmatrix} a_{\text{long}} \\ a_{\text{lat}} \end{pmatrix} = \begin{pmatrix} a'_{\text{long}} \\ a'_{\text{lat}} \end{pmatrix} + \mathbf{R}(\theta) \begin{pmatrix} -2c\dot{x}\dot{y} \\ c\dot{x}^2 \end{pmatrix} \tag{14}$$

and by introducing the variables

$$\begin{pmatrix} a_{\text{long,off}} \\ a_{\text{lat,off}} \end{pmatrix} = \mathbf{R}(\theta) \begin{pmatrix} -2c\dot{x}\dot{y} \\ c\dot{x}^2 \end{pmatrix} \tag{15}$$

(14) can be rewritten as

$$\begin{cases} a_{\text{long}} = a'_{\text{long}} + a_{\text{long,off}} \\ a_{\text{lat}} = a'_{\text{lat}} + a_{\text{lat,off}} \end{cases} \tag{16}$$

The subscript “off” suggests that these act as an offset on the accelerations to compensate for the fact that the coordinate system is non-Cartesian. Using $\dot{x} = v\cos\theta$ and $\dot{y} = v\sin\theta$ the acceleration offsets can be computed by evaluating (15):

$$a_{\text{long,off}} = -\cos^2\theta\sin\theta c v^2 \tag{17}$$

$$a_{\text{lat,off}} = (\cos^3\theta - 2\cos\theta\sin^2\theta) c v^2 \tag{18}$$

To illustrate these offsets, consider a special case where a vehicle drives along a curve and stays at a constant lateral position in relation to the lane. In this case $\dot{y} = \theta = 0$ and thus $a_{\text{long,off}} = 0$ and $a_{\text{lat,off}} = cv^2$. $cv^2$ acts as an acceleration offset in the lateral direction, exactly describing the phenomenon in the example mentioned earlier, *i.e.*, when negotiating a curve, a certain amount of the available friction force in one direction is already used to stay in the lane, thus reducing the remaining room for manoeuverability in the same direction. According to typical guidelines for road construction (Vägverket, 1994), a 90 km/h road has a minimum radius of 550 metres which gives $a_{\text{off}}$ = 1.25 m/s$^2$. A road of 50 km/h has a minimum radius of 140 metres, which gives $a_{\text{off}}$ = 1.38 m/s$^2$. Thus, under good road conditions, the offset can be up to about 15% of the lateral acceleration available, which indicates that this effect should not be neglected.

The minimum turning radius is also affected by the fact that the coordinates are curved. A similar offset for the turning rate is thus introduced:

$$\dot{\theta} = \dot{\theta}' + \dot{\theta}_{\text{off}} \tag{19}$$

where $\dot{\theta}$ is the turning rate in the curved coordinates $\dot{\theta}'$ is the turn rate in the fixed Cartesian coordinates. First define

$$\mathbf{v}' = \begin{pmatrix} \dot{\xi} \\ \dot{\eta} \end{pmatrix} \quad \text{and} \quad v' = |\mathbf{v}'| \tag{20}$$

The following well-known relationships between turn rate and acceleration under circular motion in the two reference frames are used:

$$a_{\text{lat}} = v\dot{\theta} \quad \text{and} \quad a'_{\text{lat}} = v'\dot{\theta}' \tag{21}$$

Note that $a'_{\text{lat}}$ can be computed from $a_{\text{lat}}$ using (16). In order to find $v'$ the Jacobian is evaluated:

$$\mathbf{J}_{\xi,\eta} = \begin{pmatrix} \mathbf{J}_{\xi} \\ \mathbf{J}_{\eta} \end{pmatrix} = \begin{pmatrix} (1+cy)\cos(cx) & \sin(cx) \\ -(1+cy)\sin(cx) & \cos(cx) \end{pmatrix} \tag{22}$$

Again using $1 + cy \approx 1$, it is noted that $\mathbf{J}_{\xi,\eta} \approx \mathbf{R}(-cx)$. Thus, the following relationship holds:

$$\mathbf{v}' = \mathbf{J}_{\xi,\eta}\mathbf{v} \approx \mathbf{R}(-cx)\mathbf{v} \quad \Rightarrow \quad v = |\mathbf{v}| \approx |\mathbf{v}'| = v'. \tag{23}$$

Using this, and inserting (21) into (19) gives

$$a_{\text{lat}}/v = a'_{\text{lat}}/v + \dot{\theta}_{\text{off}}, \tag{24}$$

and thus, from the definition of $a_{\text{lat,off}}$

$$\dot{\theta}_{\text{off}} = (a_{\text{lat}} - a'_{\text{lat}})/v = a_{\text{lat,off}}/v. \tag{25}$$

The model can then be modified by adding $a_{\text{long,off}}$ to the longitudinal dynamics and $a_{\text{lat,off}}$

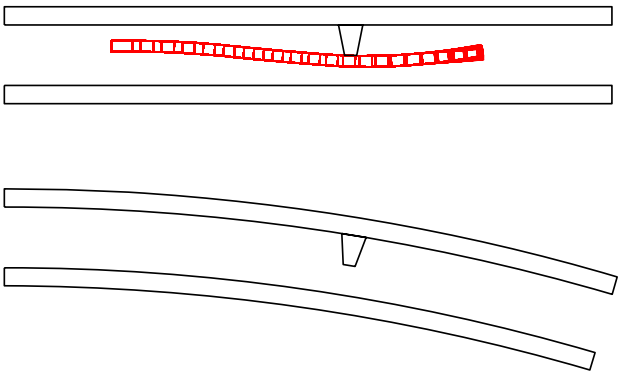

***Figure 5:*** *A vehicle approaches an obstacle at a high velocity. In the top scenario, the vehicle can barely pass the obstacle. The lower scenario has no conflict-free solution since the lateral friction force available is not sufficient to avoid the obstacle.*

and $\dot{\theta}_{\text{off}}$ to the lateral dynamics, replacing (1c) and (1d) with:

$$\dot{v} = \begin{cases} u_1 a_f + a_{\text{long,off}} & \text{if } v \leq v_{\text{long}} \\ u_1 \frac{k/v + a_f}{2} + \frac{k/v - a_f}{2} + a_{\text{long,off}} & \text{if } v > v_{\text{long}} \end{cases} \tag{26}$$

$$\dot{\theta} = \begin{cases} v \sin(\varphi_{\text{max}} u_2)/L + \dot{\theta}_{\text{off}} & \text{if } v \leq v_{\text{lat}} \\ (a_f u_2 + a_{\text{lat,off}})/v & \text{if } v > v_{\text{lat}} \end{cases} \tag{27}$$

To demonstrate how these modifications affect the model, consider the example in Figure 5. A vehicle approaches an obstacle at high velocity and has to swerve right in order to avoid it. When the road is straight, this is possible, but if the same scenario takes place on a road that bends to the right, the lateral friction force available is not sufficient.

# 3 Threat assessment

In this section, "host vehicle" refers to the vehicle equipped with the potential safety system, *i.e.*, the vehicle that is warned of potential danger. The host vehicle is modelled as a deterministic object, not in the stochastic framework. The reason for this is that even though the future actions of the host vehicle are not known, the threat of the *current* trajectory can be computed. The driver of the host vehicle can then, for example, be informed if he or she needs to act or not in order to avoid a collision.

As was discussed earlier, drivers most often try to avoid collisions, a fact which is not considered by Broadhurst et al. (2005). Trying to incorporate this, we will create a mix of two distributions. One where other vehicles try to avoid the host vehicle, and one where they do not see or consider the host vehicle. These distributions are then weighted based on the visibility relation between the host vehicle and the objects. We start by

computing the posterior distribution of $\mathcal{U}$, given that there are no collisions during $I_t$. Mathematically, a collision-free event is expressed as the complement $\mathcal{C}^c$, where $\mathcal{C}$ is the event of a collision. The posterior distribution of $\mathcal{U}$ can then be computed using Bayes theorem:

$$P(\mathcal{U}|\mathcal{C}^c) = \frac{P(\mathcal{C}^c|\mathcal{U})\pi(\mathcal{U})}{\int_{\mathcal{X}_M} P(\mathcal{C}^c|\mathcal{U})\pi(\mathcal{U})d\mathcal{U}} \tag{28}$$

where $\mathcal{X}_M$ is the set of physically allowed steering inputs, $P(\mathcal{C}|\mathcal{U}) \in \{0, 1\}$ is the probability of collision given a steering input, and $\pi(\mathcal{U})$ is the prior distribution of $\mathcal{U}$, which was explained in Section 2.3.

In order to compute the final distribution of $\mathcal{U}$, a certain risk that other objects might disregard or not see the host vehicle will be included. The following events are defined:

- $\mathcal{C}_A$ = collision between any objects, including the host vehicle, and
- $\mathcal{C}_B$ = collision between any objects, excluding the host vehicle.

A new, merged distribution for $\mathcal{U}$ is then defined as:

$$P(\mathcal{U}) = w_A P(\mathcal{U}|\mathcal{C}_A^c) + w_B P(\mathcal{U}|\mathcal{C}_B^c). \tag{29}$$

The weights are chosen based on the visibility calculations in Section 2.4 in order to capture the fact that the probability of the host vehicle being disregarded or not seen by another vehicle depends on their relative positions and orientations.

We propose the following weights, where $k$ is the object index of the host vehicle

$$w_A = \min_j \{\hat{\mathbf{V}}_{kj} : j \neq k\} \tag{30}$$

and then $w_B$ is chosen such that $w_A + w_B = 1$. This makes sense, since $w_A$ is then the minimum visibility of the host vehicle by other objects, *i.e.*, it represents the worst case of how little the host vehicle is regarded or how little it is seen by others.

Whether a situation is judged to be dangerous or not, depends on how much of the probability mass of $\mathcal{U}$ is conflict-free. This will be determined by forming a set $U_\alpha \subset \mathcal{X}_M$ which is defined to be the most likely set of control inputs with probability mass $\alpha$. Mathematically, it is obtained by first defining $U(\delta) = \{\mathcal{U} \in \mathcal{X}_M : P(\mathcal{U}) > \delta\}$, and then $\delta_\alpha = \sup\{\delta \in \mathbb{R}^+ : P(U(\delta)) > \alpha\}$. This means that $U_\alpha = U(\delta_\alpha) = \{\mathcal{U} \in \mathcal{X}_M : P(\mathcal{U}) > \delta_\alpha\}$ has $P(U_\alpha) \geq \alpha$, but depending on the behaviour of the distribution, we often actually have $P(U_\alpha) = \alpha$. Furthermore, we are guaranteed that $U_\alpha$ does not have a lesser probability than $\alpha$. The set $U_\alpha$ is illustrated in Figure 6.

A final threat level of the host vehicle can then be computed as

$$P(\mathcal{C}_B|U_\alpha) \in \{0, 1\} \tag{31}$$

by choosing $\alpha$ at an appropriate level, depending on how much probability mass to include. This can be interpreted as the amount of probability mass the host vehicle should avoid, *i.e.*, using $\alpha = 99\%$ the probability of avoiding a collision is greater than $99\%$.

If a threat is detected, *i.e.*, $P(\mathcal{C}_B|U_\alpha) = 1$, time to collision can be computed and used as a warning level for taking countermeasures or alerting the driver.

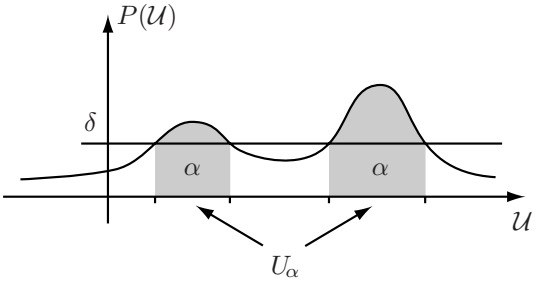


***Figure 6:*** *An illustration of how the set $U_\alpha$ is defined.*

# 4 Implementation

## 4.1 Collision detection and time discretisation

This section deals with the computation of $P(\mathcal{C}|\mathcal{U})$ in (28) or (31), *i.e.*, given a combination of control inputs $\mathcal{U}$, compute whether or not it will result in a collision. The first step is to insert the time variable $t$ using the marginalisation formula:

$$P(\mathcal{C}|\mathcal{U}) = \int_{I_t} P(\mathcal{C}|\mathcal{U}, t)P(t)dt, \tag{32}$$

where $P(t)$ is constant, since all times in $I_t$ will appear with equal probability. However, computing $P(\mathcal{C}|\mathcal{U}, t)$ for a continuous time variable $t$ is difficult, thus discretisation of the time variable is needed. First, define a sampling time $T_s$ and a time interval $I_s(n) = [nT_s, (n+1)T_s]$, then (32) can be rewritten as

$$P(\mathcal{C}|\mathcal{U}) = \sum_n \int_{I_s(n)} P(\mathcal{C}|\mathcal{U}, t)P(t)dt, \tag{33}$$

where the sampling time $T_s$ is chosen to be small enough so that the integral can be approximated as

$$\int_{I_s(n)} P(\mathcal{C}|\mathcal{U}, t)dt \approx P(\mathcal{C}|\mathcal{U}, t = nT_s). \tag{34}$$

The appropriate size of $T_s$ depends on the expected sizes and velocities of objects, if it is too large, there is a chance that objects can pass through each other and the detection of a collision is missed. In order to compute $P(\mathcal{C}|\mathcal{U}, t = nT_s)$, the system is simulated, using the dynamic model in Section 2.2, to reach time $nT_s$. Then the polygon shape of all objects is computed and a polygon intersection algorithm is applied. If a non-empty intersection between any two polygons is detected, we have $P(\mathcal{C}|\mathcal{U}, t = nT_s) = 1$.

Similarly, a time discretisation for the control input is defined, with sampling time $T_c$ and a corresponding time interval $I_c(k) = [kT_c, (k+1)T_c]$. The reason for discretising

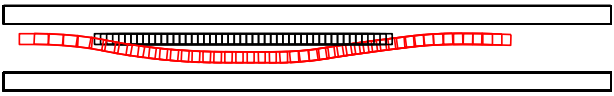

***Figure 7:*** *In this scenario two vehicles are moving from the left to the right, one approaches the other from behind with a higher velocity. The large, long rectangles are used to model road boundaries. This overtaking manoeuvre was found as the most likely path,* i.e.*, $\arg\max_{\mathcal{U}\in\mathcal{X}_M} P(\mathcal{U}|\mathcal{C}^c)$, among 1000 samples using iterative sampling with uniform sampling only.*

the control input differently is that the frequency content of a typical driver input is much lower in comparison to the sampling frequency required to detect collisions [3]. The discrete time trajectories of the dynamic model from Section 2.2 is computed using the Runge-Kutta method.

## 4.2 Monte Carlo sampling

In order to evaluate the integral (28), Monte Carlo sampling is used where $N$ samples of the control input space $\mathcal{X}_M$ are generated. The prior probability discussed in Section 2.3 is then computed and the collision detection algorithm from Section 4.1 is applied for each sample. The result is a set of samples that represent the distribution of $\mathcal{U}$, which can then be used to compute the threat quantities.

We found that uniform sampling worked well, the main reason for this is a technique referred to as iterative sampling, discussed in Section 4.3, which makes the final sample density very high. It thus becomes unnecessary to emphasise special manoeuvres or sets of the control input space, which has to be done in the method proposed by Broadhurst et al. (2005). Figure 7 shows an example of an overtaking manoeuvre that was found as the most likely path, *i.e.*, $\arg\max_{\mathcal{U}\in\mathcal{X}_M} P(\mathcal{U}|\mathcal{C}^c)$, using uniform sampling only. Typically, without the iterative sampling process, 1000 samples would not be enough to find a single collision-free sample while the iterative process generates 600 to 700 samples.

Moreover, a Monte Carlo based threat assessment algorithm, such as the one proposed, would be an ideal complement to a Monte Carlo-based filter, *i.e.*, the particle filter (Eidehall et al., 2005b, Gordon et al., 1993). In a particle filter, the distribution of the current positions of objects is already represented by samples. These samples could then be fed straight into the threat assessment algorithm, creating a seamless statistical connection between filtering and threat assessment.

## 4.3 Iterative sampling process

The straight forward approach to obtaining a set of conflict-free samples would first be to generate a random set of control inputs, secondly compute the trajectories of all objects using the dynamic model and finally apply the collision detection scheme proposed in Section 4.1. Here, we propose an iterative process which will increase the density of the

[3] We use $T_s = 0.1$ [s] and $T_c = 0.5$ [s].

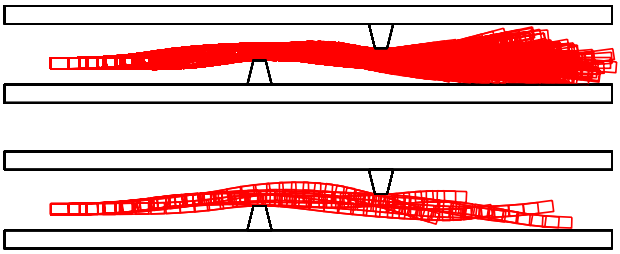

***Figure 8:*** *A set of conflict-free particles based on 500 initial samples obtained with (top) and without (bottom) iterative sampling. The iterative sampling algorithm generates much denser sample sets.*

final set of samples by iteratively removing and replacing samples that generate conflicts at an early stage in the simulation.

Let $\mathcal{X}_M$ be the set of physically allowed control inputs and let $\mathcal{X}_F^k$ be the set of inputs free from conflict at time step $k$, which refers to the time interval $I_c(k)$ as defined in Section 4.1. Formally,

$$\mathcal{X}_F^k = \{\mathcal{U} \in \mathcal{X}_M : P(\mathcal{C}|\mathcal{U}, t \in I_c(k)) = 0\}. \tag{35}$$

The algorithm starts by generating a set $U^1 \in \mathcal{X}_M$ of $N$ control inputs for time step $k = 1$. Then, for $k = 1, 2, \ldots$ repeat the following steps:

1. Simulate the system during time interval $k$ using the control inputs $U^k$.
2. Compute
$$\tilde{U}^k = U^k \cap \mathcal{X}_F^k \quad \Rightarrow \quad |\tilde{U}^k| = N_k \leq N, \tag{36}$$
i.e., remove the control inputs that will generate a conflict in time interval $k$.
3. Now form $U^{k+1}$ by resampling $\tilde{U}^k$ such that $|U^{k+1}| = N$. We propose using a mixed distribution where new samples are drawn both from a uniform distribution, and from the prior distribution. The resampling is done using replacement which means that there will be multiple copies of some elements in $U^{k+1}$. Then, new random control inputs in $\mathcal{X}_M$ for time step $k+1$ are generated and adjoined to the control inputs from $U^{k+1}$, so that even if some control inputs are repeated up to time step $k$, they are all different at time step $k+1$.

The algorithm is terminated after step 2 when the final time step has been reached. An example of the difference between iterative and non-iterative sampling can be seen in Figure 8.

# 5 Results

The results are given as the output of the threat assessment algorithm for a number of simulated and real traffic scenarios. The algorithm currently runs on a standard desktop PC in

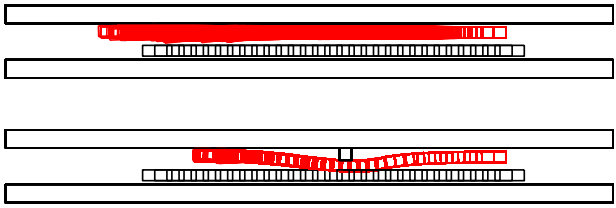

***Figure 9:*** *Revisiting the scenario in Figure 1, in these two simulations the host vehicle (black) moves from left to right in a straight line, and an oncoming vehicle (red) moves from the right to the left. In the top scenario, no danger is detected while in the bottom scenario, there is an obstacle that the oncoming vehicle has to avoid, and thus becomes a threat to the host vehicle. In the bottom scenario, a threat is detected. Time to collision is 1.4 seconds.*

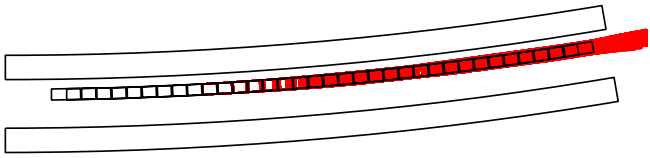

***Figure 10:*** *The host vehicle is driving extremely close to another vehicle, both moving from left to right in the image. The system recognises this as a dangerous situation, even though the vehicles have the same velocity and are thus not on a direct collision course. The reason for this is that there is a certain probability that the leading vehicle will brake. Expected time to collision is 2.8 seconds.*

non-optimised Matlab code, and the threat level of a typical scenario using 1000 samples takes two to three seconds to compute. In optimised C code, increasing performance by a factor 100 to reach 30 - 50 Hz does seem realistic. In all these experiments, 1000 samples and a prediction horizon of 3 seconds was used.

## 5.1 Simulated data

Figure 9 is a scenario where an oncoming vehicle is forced into the lane of the host vehicle by an obstacle. Figure 10 shows that the algorithm correctly identifies a situation as dangerous where the host vehicle is tailgating another vehicle. The two vehicles are not on a direct collision course, but there is a certain probability that the host vehicle will brake. Figure 11 demonstrates a situation where the host vehicle drives next to a bicycle. The bicycle passes a parked vehicle which suddenly starts to reverse, and the bicycle has to swerve and thus becomes a threat to the host vehicle. Figure 12 demonstrates the effects of the visibility constraints. Two vehicles approach a narrow passage, and the threat depends on wether the host vehicle can be expected to be seen by the other vehicle.

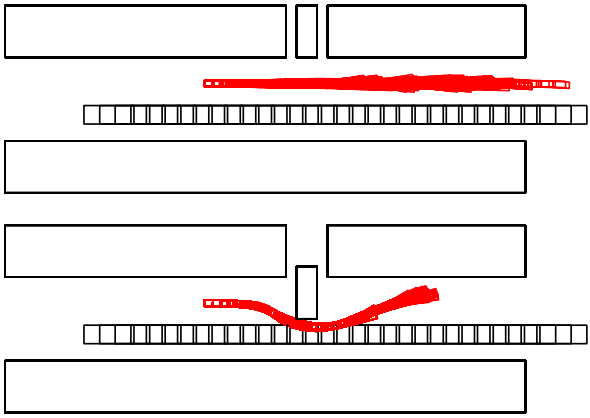

***Figure 11:*** *In this simulation, a car (black) and a bicycle (red) travels from the left to the right. In the top scenario there is no threat, but in the lower, a vehicle is reversing and the bicycle has to swerve to avoid it, and thus becomes a threat to the host vehicle. In the bottom scenario, a threat is detected by the algorithm. Time to collision is 1.5 seconds.*

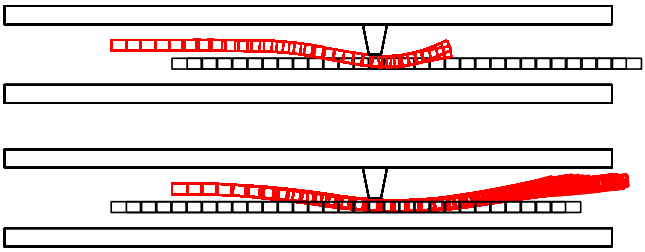

***Figure 12:*** *This simulation demonstrates the properties of the visibility constraints. The host vehicle (black) and another vehicle (red) approaches a narrow passage, moving right in the images. In the top scenario, no threat is identified since the host vehicle can be seen by the other vehicle and is likely to adapt its behaviour to avoid a collision. The result is that the other vehicle stops or slows down to let the host vehicle pass first. In the bottom scenario there is a higher probability that the host vehicle is not seen by the other vehicle and that it will steer towards the host vehicle. Here, a threat is detected and the time to collision in this scenario is 1.6 seconds.*

## 5.2 Real data

The system has been tested on recorded sensor data to evaluate the performance in authentic traffic situations. The data contains information about the host vehicle, such as velocity and yaw rate, positions of other objects obtained from a fused vision/radar system, and information about the road shape and road boundaries that is given by the vision system. The radar system is a standard 77 GHz unit mounted in the grille of the vehicle, typically used for adaptive cruise control application. The vision system is a black-and-white mono system mounted at the rear view mirror inside the windscreen. The data is filtered using an extended Kalman filter based on dynamic models of vehicles and the road (Zomotor and Franke, 1997). At present, only vehicles can be detected with the radar/vision sensor combination, *i.e.*, no other type of obstacles which somewhat limits the variation in the types of scenarios that are assessed. All data is sampled at 10 Hz.

Another "problem" is that, although we are very thankful for it, the data does not contain any accidents. Instead, the idea is to get the threat assessment algorithm to identify threatening situations, for example situations where the host vehicle is driving close to a leading vehicle or is about to change lanes in the direction of a vehicle in the adjacent lane. A correct alarm is thus defined as an alarm that coincides with a traffic situation that might not be very dangerous, but still poses some sort of threat. An alarm that does not correspond to a threatening situation is defined as a false alarm.

Figure 13 shows an example of a five minute sequence from the data set, where three threatening situations have been identified. A video clip of one of them is shown in Figure 15, a situation where the host vehicle approaches a leading vehicle at a high relative velocity. The stochastic nature of the Monte Carlo based algorithm becomes evident here. The threat value clearly has an increasing trend as the traffic scene evolves, but there is a large variance in the threat values. In fact, when applying the threat algorithm to the same scenario several times, the output threat level will vary slightly. The reason for this is the limited number of samples that are used. An example where more samples have been added is shown in Figure 14. For 10000 samples, the stochastic behaviour is significantly reduced, but of course, the computational cost is much higher; it increases linearly with the number of samples. In a real application however, these problems can be reduced by the fact that the system will have access to the threat levels from subsequent time steps. Thus, time averaging can be used to reduce noise.

For long-term performance evaluation, the algorithm has been run on a recorded data set of 4.5 hours from dense German autobahn traffic. A prediction horizon of three seconds and a sample set of 1000 samples was used. The number of alarms is shown in the first column in Table 1. The first and second row states the total number of correct and false alarms. The quantities $T_{\text{correct}}$ and $T_{\text{false}}$, the average times between correct and false alarms, are presented on the last two rows. However, many of these alarms have a relatively high time-to-collision (TTC) value, and thus does not pose a very high threat. If, for example, only alarms with TTC lower than two seconds are considered, the number of alarms will be significantly reduced, see column two of Table 1.

A limitation in this study is that there is not a lot of variation in the data set since all was taken from motorway traffic. A result of this is that all the alarms that were given can be put into three different categories:

1. The host vehicle approaches a leading vehicle at high velocity.

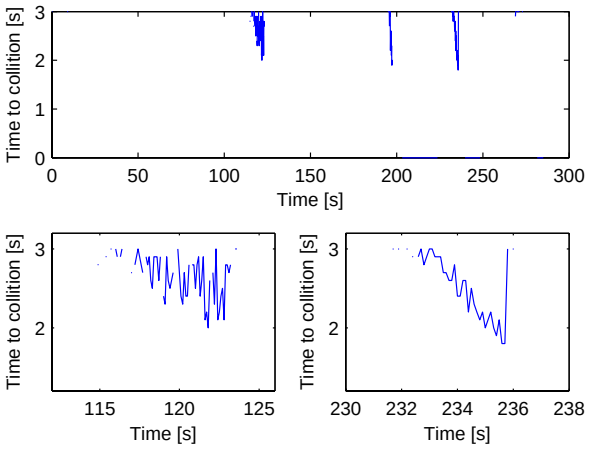


***Figure 13:*** *An example of a five minute data sequence. The top plot shows the threat levels for the entire time interval and the two bottom plots shows the detailed behaviour for two interesting time intervals.*

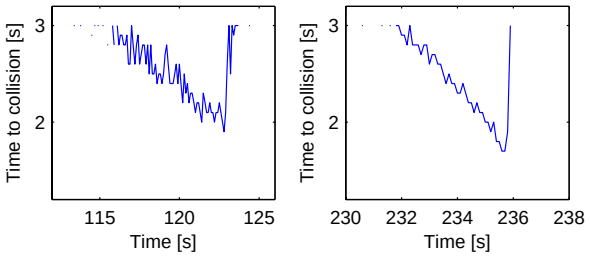


***Figure 14:*** *The two sequences from Figure 13, here run with* $10000$ *samples. The stochastic behaviour is significantly reduced, but of course, at increased computational cost.*

***Figure 15:*** *A video clip at about time 235 [s] from the data set in Figure 13. The host vehicle is approaching a leading vehicle as it is about to overtake it.*

| TTC threshold [s] | 3.0 | 2.0 |
|---|---|---|
| Correct alarms | 156 | 67 |
| False alarms | 15 | 1 |
| $T_{\text{correct}}$ [minutes] | 1.70 | 3.96 |
| $T_{\text{false}}$ [hours] | 0.29 | 4.42 |

***Table 1:*** *Long term performance.*

2. The host vehicle drives close to a leading vehicle, at about the same speed.
3. The host vehicle drifts out of its lane in the direction of a vehicle in the adjacent lane.

The false alarms are typically caused by vehicles in adjacent lanes. Their future positions are represented by a stochastic distribution, and sometimes this distribution is a bit too spread out in the lateral direction. It is interesting to note that the already existing automotive safety functions Forward Collision Warning (NHTSA, 2000) and Emergency Lane Assist (Eidehall et al., 2005a) appear as special cases within this framework. These correspond to categories 1 and 3 above.

However, the reader is reminded that this article does not suggest a new collision warning system, it merely demonstrates that the statistical framework that has been derived can be used to distinguish between threatening and non-threatening situations in some respect. In a real life application, one alarm every four minutes during normal driving is probably not acceptable.

# 6 Conclusions

A general threat assessment algorithm is proposed that is able to incorporate many future hypothesis by regarding the control inputs of other vehicles as stochastic variables. Monte Carlo sampling is then used in order to compute a threat level. A method for creating dense sample sets without increasing computational load is also presented. For example, a result of this is that it becomes unnecessary to include domain specific knowledge, such as emphasising specific manoeuvres or sets of manoeuvres for vehicles when sampling.

The algorithm was tested on both simulated data and on authentic sensor data, and successfully distinguishes between threatening and non-threatening road scenes.

It was also noted that already existing automotive safety functions such as Forward Collision Warning and Emergency Lane Assist emerge as special cases within the general framework. However, again the authors would like to stress that this article does not suggest a new collision warning system, it only demonstrates that the algorithm can be used to distinguish between threatening and non-threatening situations.

One aspect that needs further investigation is the distribution of samples. The iterative sampling process iteratively removes samples with conflicts and replaces them with copies of the conflict-free ones. Occasionally a few of the initial samples are over-represented in the final distribution. This means that even though the number of samples

in the final distribution is high, many of the samples are based on the same "parents" and thus the statistical variation can be somewhat limited. This is one of the sources of the stochastic noise in the threat level. How it is possible to reduce these problems and to create better variation in the final distributions is an interesting topic for further investigations. There are also many other possible future research topics. For example evaluating the algorithm on data with varying road and weather conditions. for instance, it would also be interesting to include "soft" obstacles to model lane markings. Another interesting topic would be to investigate if the visibility map could be improved using studies of driver behaviour.

## Acknowledgment

The authors would like to thank Intelligent Vehicle Safety Systems (IVSS) of the Swedish national road authorities and Volvo Car Corporation for sponsoring this work.

## References

Broadhurst, A. E., Baker, S., and Kanade, T. (2005). Monte carlo road safety reasoning. In *Proceedings of the IEEE Intelligent Vehicles Symposium 2005*, pages 319–324, Las Vegas, USA.

Dagan, E., Mano, O., Stein, G., and Shashua, A. (2004). Forward collision warning with a single camera. In *Proceedings of the IEEE Intelligent Vehicles Symposium 2004*, pages 37–42, Parma, Italy.

Eidehall, A. and Gustafsson, F. (2004). Combined road prediction and target tracking in collision avoidance. In *Proceedings of the IEEE Intelligent Vehicles Symposium*, pages 619–624, Parma, Italy.

Eidehall, A., Pohl, J., and Gustafsson, F. (2005a). A new approach to lane guidance systems. In *Proceedings of the IEEE Intelligent Transportation Systems 2005*, pages 108–112, Vienna, Austria.

Eidehall, A., Schön, T. B., and Gustafsson, F. (2005b). The marginalized particle filter for automotive tracking applications. In *Proceedings of the IEEE Intelligent Vehicle Symposium*, pages 369–374, Las Vegas, USA.

Gordon, N., Salmond, D., and Smith, A. (1993). A novel approach to nonlinear/non-Gaussian Bayesian state estimation. In *IEE Proceedings on Radar and Signal Processing*, volume 140, pages 107–113.

Jansson, J. (2005). *Collision Avoidance Theory with Application to Automotive Collision Mitigation*. PhD thesis, Linköping University, Linköping University, 581 83 Linköping, Sweden.

Labayrade, R., Royere, C., and Aubert, D. (2005). A collision mitigation system using laser scanner and stereovision fusion and its assessment. In *Proceedings of the IEEE Intelligent Vehicles Symposium 2005*, pages 441–446, Las Vegas, USA.

NHTSA (2000). Automotive collision avoidance system field operational test. web page, National Highway Traffic Safety Administration, `www.nhtsa.dot.gov/people/injury/research/pub/ACAS/ACAS-fieldtest`.

Polychronopoulos, A., Tsogas, M., Amditis, A., Scheunert, U., Andreone, L., and Tango, F. (2004). Dynamic situation and threat assessment for collision warning systems: the euclide approach. In *Proceedings of the IEEE Intelligent Vehicles Symposium 2004*, pages 636–641, Parma, Italy.

Vägverket (1994). Vägutformning 94 version s-2. Technical report, Swedish National Road Administration.

Yang, L., Yang, J. H., Feron, E., and Kulkarni, V. (2003). Development of a performance-based approach for a rear-end collision warning and avoidance system for automobiles. In *Proceedings of the IEEE Intelligent Vehicles Symposium 2003*, pages 316–321, Columbus, OH, USA.

Zomotor, Z. and Franke, U. (1997). Sensor fusion for improved vision based lane recognition and object tracking with range-finders. In *Proceedings of the IEEE Conference on Intelligent Transportation Systems.*

# Paper E

# The Marginalised Particle Filter for Automotive Tracking Applications

**Authors:** Andreas Eidehall, Thomas Schön and Fredrik Gustafsson

Published in *Proceedings of the IEEE Intelligent Vehicles Symposium 2005*, pages 370–375, Las Vegas, USA.

# The Marginalised Particle Filter for Automotive Tracking Applications

Andreas Eidehall[⋆§], Thomas Schön[⋆] and Fredrik Gustafsson[⋆]

[⋆]Department of Electrical Engineering
Linköping University
SE–581 83 Linköping, Sweden

[§]Vehicle Dynamics and Active Safety
Volvo Car Corporation
SE–405 31 Göteborg, Sweden

**Abstract**

This paper deals with the problem of estimating the vehicle surroundings (lane geometry and the position of other vehicles), which is needed for intelligent automotive systems, such as adaptive cruise control, collision avoidance and lane guidance. This results in a nonlinear estimation problem. For automotive tracking systems, these problems are traditionally handled using the extended Kalman filter. In this paper we describe the application of the marginalised particle filter to this problem. Studies using both synthetic and authentic data shows that the marginalised particle filter can in fact give better performance than the extended Kalman filter. However, the computational load is higher.

# 1 Introduction

Future intelligent automotive systems such as adaptive cruise control, collision avoidance and lane guidance will require detailed knowledge of the vehicle surroundings. In this paper, vehicle surroundings will refer to lane geometry and other vehicles. Typically, lane information is obtained from a vision system and other vehicles are detected using a radar.

The importance of integrating data from object tracking and road geometry tracking has quite recently been recognised (NHTSA, 2000, Eidehall and Gustafsson, 2004, Dellaert and Thorpe, 1997, Zomotor and Franke, 1997). The main idea is to try to improve the road geometry estimate by studying the motion of other vehicles and vice versa. For example, if a couple of tracked vehicles suddenly all start moving to the right, one of two things can have happened. The first is that they all started a lane change manoeuvre and the road remains straight. The other is that we are entering a curve and the vehicles are still following the centre of their lanes. These possibilities can be treated within a Bayesian framework, together with the information from the lane tracker, to build a new estimator. In order to do this we need to use a nonlinear measurement equation based on the road geometry.

The most common approach to state estimation for nonlinear problems in general, and for this application in particular, is the Extended Kalman Filter (EKF). The EKF generally gives good performance for lane tracking and not much effort has been spent on studying other alternatives. In this work, we investigate and compare the performance of the EKF to the potentially more accurate particle filter (Doucet et al., 2001a, 2000). In particular, we will study the Marginalised Particle Filter (MPF) (Doucet et al., 2000, 2001b, Schön et al., 2004). The MPF is a subtle combination of the Kalman filter and the particle filter. It can be used for nonlinear estimation problems with a conditionally linear substructure, where the conditionally linear states are estimated using Kalman filters and the nonlinear states are estimated using the particle filter. There are two advantages with MPF compared to the standard particle filter. First, for the linear states, the Kalman filter provides the optimal solution. Second, the dimensionality problem associated with the standard particle filter is reduced, since the dimension of the state variables estimated using the standard particle filter is reduced using marginalization.

Several geometric models for combined road prediction and target tracking exists. We will use a model which assumes a road consisting of circle segments, not the traditionally used clothoid approximation. It has been shown that this model can give better tracking performance (Eidehall and Gustafsson, 2004). This model is presented in Section 2. In order to solve the problem at hand, nonlinear estimation theory is needed. Hence, Section 3 is devoted to this and in particular the two algorithms EKF and MPF are discussed. These algorithms are then evaluated in Section 4. Finally, the conclusions are given in Section 5.

# 2 The combined lane tracking and object model

The difference between tracking in automotive applications and tracking in other applications, such as air traffic control or naval tracking, is that in automotive tracking it can be assumed that the motion of the tracked objects, with a certain probability, is constrained

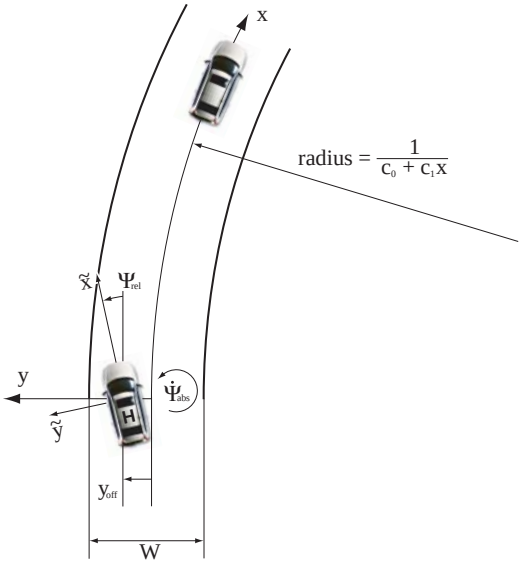


***Figure 1:*** *The coordinate systems used in deriving the dynamic motion model. Here, $(x, y)$ denotes the position in a curved coordinate system, which is attached to and follows the road. Furthermore, $(\tilde{x}, \tilde{y})$ denotes the position in a coordinate system, which is attached to the moving host vehicle.*

to the road. In order to be able to use and benefit from this fact, this section presents an appropriate dynamic model. The key idea, upon which this model is based, is the use of a curved coordinate system which is attached to and follows the road.

## 2.1 Dynamic motion model

The coordinates $x$ and $y$ denotes the position in the curved coordinate system, which is attached to the road according to Figure 1. In these coordinates, the motion model for the other vehicles can be greatly simplified. For example, it allows us to use the equation $\dot{y} = 0$, which simply means that it is assumed that the other vehicles will follow their own lanes. In the longitudinal direction we will use $\ddot{x} = -a \cos \Psi_{rel}$, where $a$ is the measured acceleration of the host vehicle and $\Psi_{rel}$ is the angle between the host vehicle and the lane. Hence, we have the following motion model:

$$\dot{x}^i = v^i, \tag{1a}$$

$$\dot{v}^i = -a \cos \Psi_{rel}, \tag{1b}$$

$$\dot{y}^i = 0, \tag{1c}$$

where $v^i$ is the longitudinal velocity of object $i$, *i.e.*, the time derivative of $x^i$. Furthermore, $\Psi_{abs}$ is the angle between the vehicle and some fix reference. We can obtain a

relationship between the $\Psi_{rel}$ and $\Psi_{abs}$ by differentiating $\Psi_{rel}$ w.r.t. time,

$$\Psi_{rel} = \Psi_{abs} + \gamma \quad \Rightarrow \tag{2a}$$

$$\dot{\Psi}_{rel} = \dot{\Psi}_{abs} + \dot{\gamma} = \dot{\Psi}_{abs} + \frac{v}{r} = \dot{\Psi}_{abs} + c_0 v, \tag{2b}$$

where $r$ is the current road radius, $v$ the velocity and $\gamma$ denotes the angle between the lane and some fix reference. $\dot{\Psi}_{abs}$ can typically be measured with a yaw rate sensor. We also have

$$\dot{y}_{\text{off}} = \sin(\Psi_{rel})v \approx \Psi_{rel} v. \tag{3}$$

Using $\dot{W} = 0$ and $\dot{c}_1 = 0$, the continuous-time motion equations for the host vehicle states can be written

$$\dot{W} = 0, \tag{4a}$$

$$\dot{y}_{\text{off}} = v\Psi_{rel}, \tag{4b}$$

$$\dot{\Psi}_{rel} = vc_0 + \dot{\Psi}_{abs}, \tag{4c}$$

$$\dot{c}_0 = vc_1, \tag{4d}$$

$$\dot{c}_1 = 0. \tag{4e}$$

The discrete-time dynamics is then given by assuming piecewise constant input signals, $[a, \dot{\Psi}_{abs}]$ (Rugh, 1996). Furthermore, adding stochastic process noise, the discrete-time motion equations for the objects become

$$x^i_{t+1} = x^i_t + T_s v^i_t - a_t \cos\Psi_{rel,t} T_s^2/2 + w^i_{1,t}, \tag{5a}$$

$$v^i_{t+1} = v^i_t - a_t \cos\Psi_{rel,t} T_s + w^i_{2,t}, \tag{5b}$$

$$y^i_{t+1} = y^i_t + w^i_{3,t}, \tag{5c}$$

and for the host vehicle

$$W_{t+1} = W_t + w_{4,t}, \tag{6a}$$

$$y_{\text{off},t+1} = y_{\text{off},t} + vT_s\Psi_{rel,t} + v^2T_s^2c_{0,t}/2 + v^3T_s^3c_{1,t}/6 + vT^2\dot{\Psi}_{abs,t}/2 + w_{5,t}, \tag{6b}$$

$$\Psi_{rel,t+1} = \Psi_{rel,t} + vT_sc_{0,t} + v^2T_s^2c_{1,t}/2 + T_s\dot{\Psi}_{abs,t} + w_{6,t}, \tag{6c}$$

$$c_{0,t+1} = c_{0,t} + vT_sc_{1,t} + w_{7,t}, \tag{6d}$$

$$c_{1,t+1} = c_{1,t} + w_{8,t}. \tag{6e}$$

The variables $\{w_{i,t}\}_{i=1}^8$ are white, zero-mean Gaussian process noise, with covariance matrices $Q_{host}$ and $Q_{obj}$ for the host and object states, respectively.

## 2.2 Measurement model

The measurements for the host vehicle, which are obtained from a vision system, are $\Psi^m_{rel}$, $c^m_0$, $L^m$ and $R^m$, where the two latter are the distances to the left and right lane

marking, see Figure 1. Superscript $m$ denotes measured quantities. For the other vehicles we use a fused radar and vision system which measures the position, $\tilde{x}^m$ and $\tilde{y}^m$, which is expressed in the Cartesian coordinate system attached to the vehicle. These relate to the states as

$$L_t^m = W_t/2 - y_{\text{off},t} + e_{1,t}, \tag{7a}$$
$$R_t^m = -W_t/2 - y_{\text{off},t} + e_{2,t}, \tag{7b}$$
$$\Psi_{rel,t}^m = \Psi_{rel,t} + e_{3,t}, \tag{7c}$$
$$c_{0,t}^m = c_{0,t} + e_{4,t}, \tag{7d}$$
$$\begin{bmatrix} \tilde{x}_t^{i,m} \\ \tilde{y}_t^{i,m} \end{bmatrix} = T(x_t^i, y_t^i) + \begin{bmatrix} e_{5,t} \\ e_{6,t} \end{bmatrix}^i, \tag{7e}$$

where the variables $\{e_{i,t}\}_{i=1}^6$ denote white, zero-mean Gaussian measurement noise with covariance matrices $R_{host}$ and $R_{obj}$ for the host and object states, respectively. $T$ is the geometric transformation from the $(x, y)$ coordinates to the $(\tilde{x}, \tilde{y})$ coordinates and $i$ is used to index the tracked objects. This transformation is given by Eidehall and Gustafsson (2004)

$$T(x, y) = R(\Psi_{rel}) \begin{bmatrix} (1 + c_0 y)\sin(c_0 x) \\ (1 + c_0 y)\cos(c_0 x) - 1 - c_0 y_{\text{off}} \end{bmatrix} \frac{1}{c_0},$$

where $R(\Psi_{rel})$ is the rotation matrix

$$R(\Psi_{rel}) = \begin{bmatrix} \cos(\Psi_{rel}) & \sin(\Psi_{rel}) \\ -\sin(\Psi_{rel}) & \cos(\Psi_{rel}) \end{bmatrix}. \tag{8}$$

# 3 Nonlinear estimation

According the previous section, the state-space model used in this application is nonlinear. Hence, we have to handle the problem of recursively estimating the state variable in a nonlinear state-space model,

$$x_{t+1} = f(x_t, u_t) + w_t, \tag{9a}$$
$$y_t = h(x_t) + e_t, \tag{9b}$$

where $x_t$ denotes the state variable, $u_t$ the input signal, $w_t$ the process noise, $y_t$ the measurements and $e_t$ the measurement noise. The solution to this problem has been known for quite some time and it can be shown to be (Jazwinski, 1970)

$$p(x_t|Y_t) = \frac{p(y_t|x_t)p(x_t|Y_{t-1})}{p(y_t|Y_{t-1})}, \tag{10a}$$
$$p(x_{t+1}|Y_t) = \int p(x_{t+1}|x_t)p(x_t|Y_t)dx_t, \tag{10b}$$

where $Y_t = \{y_i\}_{i=0}^t$. Using the probability density function $p(x_t|Y_t)$, any state estimate can be formed, *e.g.*the commonly used least-mean-squares estimator $\mathrm{E}\,(x_t|Y_t) =$

$\int x_t p(x_t|Y_t)dx_t$. However, the problem is that the multi-dimensional integrals in (10) only permit a closed form solution in rather restrictive special cases. The most commonly used special case corresponds to that $f$ and $h$ in (9) are given by linear functions and $w_t$ and $e_t$ are independent Gaussian noise sequences. In this case (10) will reduce to the standard Kalman filter (Kalman, 1960).

In the general case when there does not exist any closed form solution to (10) two different alternatives are discussed in the literature:

1. The nonlinear model (9) is approximated using a linear model, with Gaussian noise. The Kalman filter is then applied to this linearised model. This solution is referred to as the extended Kalman filter.

2. The optimal solution (10) is approximated using numerical methods, such as the particle filter.

Conceptually the second alternative provides the better solution. The reason is that it provides an approximation of the optimal solution to the original problem, rather than an optimal solution to an approximated problem. There is actually a third category of algorithms, which provides suboptimal estimates using multiple models and grid-based approximations.

The particle filter was first introduced by Gordon et al. (1993). For a thorough introduction to the standard particle filter the reader is referred to Doucet et al. (2001a) or Doucet et al. (2000). The particle filter is quite simple to implement and it is given in Algorithm 2 if steps $4a$ and $4c$ are neglected. If the model structure contains a conditionally linear substructure this can be utilised by the marginalised particle filter, which is discussed in Section 3.2. Even though the (marginalised) particle filter provides an alternative which is conceptually superior to the EKF it should be kept in mind that the computational complexity of the particle filter can be quite substantial (Karlsson et al., 2004). Furthermore, the quality delivered using the EKF is often sufficient. Still, it is interesting to solve the problem at hand using the (marginalised) particle filter, since it provides an alternative algorithm for solving the same problem. Furthermore, if more advanced measurement equations, such as the ones resulting from map information fusion, are considered the (marginalised) particle filter might be the only option. The reason is that these measurement equations simply cannot be handled within the Kalman filtering framework. However, within the particle filter framework the use of these highly nonlinear measurement equations is rather straightforward. The navigation problem for fighter aircraft, using terrain elevation maps, has been posed and solved using the marginalised particle filter (Bergman et al., 1999, Nordlund, 2002, Schön et al., 2004).

In the subsequent sections it is explained how the EKF and the marginalised particle filter can be applied to the automotive tracking problem studied in this paper, using the model described in Section 2.

## 3.1 The Extended Kalman Filter

The extended Kalman filter has a long tradition in automotive applications. For details on the Kalman Filter and the extended Kalman filter, readers are referred to the literature (Gustafsson, 2000, Kailath et al., 2000, Kalman, 1960, Kay, 1998). We will use a one-step

ahead predictor based on the EKF. The equations are given below.

$$\hat{x}_{t+1|t} = A\hat{x}_{t|t-1} + Bu_t + AK_t\left(y_t - h(\hat{x}_{t|t-1})\right), \tag{11a}$$

where the Kalman gain matrix $K_t$ is given by,

$$C_t = \left.\frac{\partial h}{\partial x}\right|_{x=\hat{x}_{t|t-1}} \tag{11b}$$

$$K_t = P_{t|t-1}C_t^T(C_tP_{t|t-1}C_t^T + R)^{-1}, \tag{11c}$$

$$P_{t+1|t} = AP_{t|t-1}A^T + Q - AK_tC_tP_{t|t-1}A^T \tag{11d}$$

Here, $Q$ and $R$ are the combined process and measurement noise covariance, *i.e.*,

$$Q = \begin{bmatrix} Q_{host} & 0 \\ 0 & I_M \oplus Q_{obj} \end{bmatrix}, \quad R = \begin{bmatrix} R_{host} & 0 \\ 0 & I_M \oplus R_{obj} \end{bmatrix},$$

were $M$ is the number of objects currently being tracked, $I_M$ is an identity matrix of size $M$ and $\oplus$ is the Kronecker product. It is worth mentioning that in the state update (11a) a data association algorithm is used. The reader is referred to *e.g.* Blackman (1986) for details regarding this matter.

## 3.2 The Marginalised Particle Filter

Let the state vector be partitioned according to

$$x_t = \begin{bmatrix} x_t^l \\ x_t^n \end{bmatrix}, \tag{12}$$

where $x_t^l$ denotes the state variables with conditionally linear dynamics and $x_t^n$ denotes the state variables with nonlinear dynamics. Using this partitioning the dynamic model derived in Section 2 can be written on the following form

$$x_{t+1}^n = A_n^n x_t^n + A_l^n x_t^l + B^n(x_t^n)u_t + w_t^n, \tag{13a}$$

$$x_{t+1}^l = A_n^l x_t^n + A_l^l x_t^l + B^l(x_t^n)u_t + w_t^l, \tag{13b}$$

$$y_t = g(x_t^n) + C(x_t^n)x_t^l + e_t, \tag{13c}$$

where $w_t^n \sim \mathcal{N}(0, Q^n)$, $w_t^l \sim \mathcal{N}(0, Q^l)$, $e_t \sim \mathcal{N}(0, R)$, and $w_t^n$ is independent of $w_t^l$. The extension to the case where $w_t^n$ and $w_t^l$ are dependent is straightforward. The linear state variables can be marginalised out and estimated using the optimal Kalman filter, whereas the nonlinear state variables are estimated using the particle filter. This technique is sometimes referred to as Rao-Blackwellization (Casella and Robert, 1996). The resulting algorithm will be referred to as the marginalised particle filter and it is thoroughly explained by *e.g.* Doucet et al. (2000), Doucet et al. (2001b) or Schön et al. (2004). It is well-known that the quality of the estimates will improve or remain unchanged when the MPF is used instead of the standard particle filter (Doucet et al., 2001b). Furthermore, is some cases the computational complexity can be decreased using the MPF (Karlsson et al., 2004).

Applying the marginalised particle filter to (13) results in Algorithm 2. A detailed derivation and discussion of this algorithm is provided by Schön et al. (2004).

*ALGORITHM 2 (The marginalised particle filter).*

1. Initialisation: For $i = 1, \ldots, N$, initialise the particles, $x_{0|-1}^{n,(i)} \sim p_{x_0^n}(x_0^n)$ and set $\{x_{0|-1}^{l,(i)}, P_{0|-1}^{(i)}\} = \{\bar{x}_0^l, \bar{P}_0\}$.

2. For $i = 1, \ldots, N$, evaluate the importance weights $q_t^{(i)} = p(y_t | X_t^{n,(i)}, Y_{t-1})$ and normalise
$$\tilde{q}_t^{(i)} = q_t^{(i)} / \textstyle\sum_{j=1}^N q_t^{(j)}.$$

3. Particle filter measurement update (resampling): Resample $N$ particles with replacement,
$$\Pr(x_{t|t}^{n,(i)} = x_{t|t-1}^{n,(j)}) = \tilde{q}_t^{(j)}.$$

4. Particle filter time update and Kalman filter:

   (a) Kalman filter measurement update,
$$\begin{aligned}
\hat{x}_{t|t}^l &= \hat{x}_{t|t-1}^l + K_t(y_t - g_t(x_t^n) - C_t \hat{x}_{t|t-1}^l), \\
P_{t|t} &= P_{t|t-1} - K_t M_t K_t^T, && \text{(14a)} \\
M_t &= C_t P_{t|t-1} C_t^T + R_t, && \text{(14b)} \\
K_t &= P_{t|t-1} C_t^T M_t^{-1}. && \text{(14c)}
\end{aligned}$$

   (b) Particle filter time update (prediction): For $i = 1, \ldots, N$, predict new particles,
$$x_{t+1|t}^{n,(i)} \sim p(x_{t+1|t}^n | X_t^{n,(i)}, Y_t).$$

   (c) Kalman filter time update
$$\begin{aligned}
\hat{x}_{t+1|t}^l &= A_l^l \hat{x}_{t|t}^l + A_n^l x_t^n + B^l(x_{t|t}^n) u_t \\
&\quad + L_t(z_t - A_l^n \hat{x}_{t|t}^l), && \text{(15a)} \\
P_{t+1|t} &= A_l^l P_{t|t} (A_l^l)^T + Q_t^l - L_t N_t L_t^T, && \text{(15b)} \\
N_t &= A_l^n P_{t|t} (A_l^n)^T + Q_t^n, && \text{(15c)} \\
L_t &= A_l^l P_{t|t} (A_l^n)^T N_t^{-1}, && \text{(15d)}
\end{aligned}$$

   where $z_t = x_{t+1}^n - A_n^n x_t^n - B^n(x_{t|t}^n) u_t$.

***Table 1:*** *The total number of states and the number of nonlinear states for $M$ objects.*

| | $M$ | 1 | 2 | 3 |
|---|---|---|---|---|
| Total | $3M+5$ | 8 | 11 | 14 |
| Nonlinear | $M+2$ | 3 | 4 | 5 |

5. Set $t := t+1$ and iterate from step 2.

In order to be able to use Algorithm 2 we need to identify the structure (13) from the dynamic model (5) – (7). Here, $x_t^n$ and $x_t^l$ consist of the following states:

$$x_t^n = \begin{bmatrix}\Psi_{rel,t} & c_{0,t} & x_t^1 & \dots & x_t^M\end{bmatrix}^T$$
$$x_t^l = \begin{bmatrix}W_t & y_{off,t} & c_{1,t} & v_t^1 & y_t^1 & \dots & v_t^M & y_t^M\end{bmatrix}^T$$

were $M$ denotes the number of tracked objects. Table 1 summaries the number of states for different numbers of tracked objects. It can be seen that the motion dynamics (5) and (6) fit the MPF structure (13) if we, for a single object, write

$$x_{t+1}^n = \underbrace{\begin{bmatrix}1 & vT_s & 0\\ 0 & 1 & 0\\ 0 & 0 & 1\end{bmatrix}}_{A_n^n} x_t^n + \underbrace{\begin{bmatrix}0 & 0 & v^2T_s^2/2 & 0 & 0\\ 0 & 0 & vT_s & 0 & 0\\ 0 & 0 & 0 & T_s & 0\end{bmatrix}}_{A_l^n} x_t^l$$
$$+ \underbrace{\begin{bmatrix}T_s & 0\\ 0 & 0\\ 0 & \cos\Psi_{rel,t}T_s^2/2\end{bmatrix}}_{B^n(x_t^n)} u_t + w_t^n \tag{16}$$

and

$$x_{t+1}^l = \underbrace{\begin{bmatrix}0 & 0 & 0\\ vT_s & v^2T_s^2/2 & 0\\ 0 & 0 & 0\\ 0 & 0 & 0\\ 0 & 0 & 0\end{bmatrix}}_{A_n^l} x_t^n + \underbrace{\begin{bmatrix}1 & 0 & 0 & 0 & 0\\ 0 & 1 & v^3T_s^3/6 & 0 & 0\\ 0 & 0 & 1 & 0 & 0\\ 0 & 0 & 0 & 1 & 0\\ 0 & 0 & 0 & 0 & 1\end{bmatrix}}_{A_l^l} x_t^l$$
$$+ \underbrace{\begin{bmatrix}0 & 0\\ vT_s^2/2 & 0\\ 0 & 0\\ 0 & \cos\Psi_{rel,t}T_s^2/2\\ 0 & 0\end{bmatrix}}_{B^l(x_t^n)} u_t + w_t^l. \tag{17}$$

Furthermore, the measurement model (7) conforms with this structure,

$$\begin{bmatrix} L_t^m \\ R_t^m \\ \Psi_{rel,t}^m \\ c_{0,t}^m \end{bmatrix} = \underbrace{\begin{bmatrix} 0 \\ 0 \\ \Psi_{rel} \\ c_{0,t} \end{bmatrix}}_{g_{host}(x_t^n)} + \underbrace{\begin{bmatrix} -1/2 & 1 & 0 & 0 & 0 \\ 1/2 & 1 & 0 & 0 & 0 \\ 0 & 0 & 0 & 0 & 0 \\ 0 & 0 & 0 & 0 & 0 \end{bmatrix}}_{C_{host}} x_t^l + e_{host,t}$$

and

$$\begin{bmatrix} \tilde{x}_t^m \\ \tilde{y}_t^m \end{bmatrix} = \underbrace{R(\Psi_{rel,t}) \begin{bmatrix} \sin(c_0 x^i) \\ \cos(c_0 x^i) - 1 \end{bmatrix}}_{g_{obj}(x_t^n)} + \underbrace{R(\Psi_{rel,t}) \begin{bmatrix} 0 & 0 & 0 & 0 & \sin(c_0 x) \\ 0 & -1 & 0 & 0 & \cos(c_0 x) \end{bmatrix}}_{C_{obj}(x_t^n)} x_t^l + e_{obj,t}.$$

Implementation of Algorithm 2 is now straightforward. Generalisation of (16) and (17) to multiple objects is accomplished by extending the system matrices and the state vector accordingly. Hence, the state dimension in the filter will change dynamically, depending on the number of objects that are tracked.

# 4 Evaluation

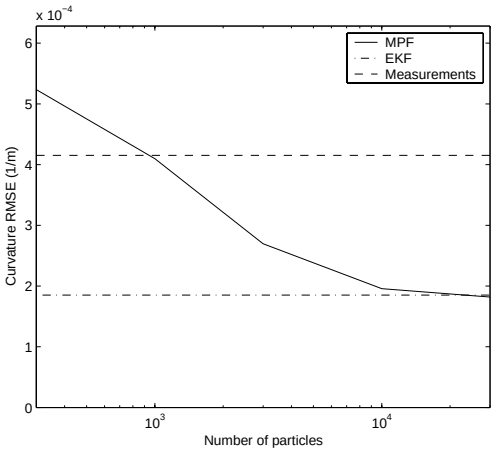


***Figure 2:*** *The curvature RMSE for different numbers of particles, using synthetic data.*

In this section we will discuss how the two filters were compared. In order to evaluate a filter, the estimated states are typically compared to the true values, if available. Here,

we have focused on the estimate of the curvature parameter $c_0$, which is crucial to many automotive applications, such as adaptive cruise control systems, collision warning or any system that rely on assigning leading vehicles to the correct lane. This is sometimes referred to as the *lane assignment problem* (Eidehall and Gustafsson, 2004, Zomotor and Franke, 1997).

In order to quantify the importance of the curvature parameter we approximate the $\tilde{y}$-part of (7e) using a second-order Taylor expansion around $\Psi_{rel} = y = y_{\text{off}} = 0$,

$$\tilde{y} = (\cos(c_0 x) - 1)\frac{1}{c_0} \approx (1 - \frac{(c_0 x)^2}{2} - 1)\frac{1}{c_0} = c_0 \frac{x^2}{2}. \tag{18}$$

This implies that for small changes in $c_0$ we have,

$$\Delta\tilde{y} \approx \frac{x^2}{2}\Delta c_0, \tag{19}$$

which means that for a leading vehicle 100 metres in front of the host vehicle, a small error of, say $5 \cdot 10^{-4}$ (1/m) in $c_0$ will result in an error of 2.5 metres in $\tilde{y}$. This is enough to assign the leading vehicle to the wrong lane.

We have compared the filters using both synthetic and authentic data. The two data sets were both run, first through the EKF and then through the MPF using different numbers of particles.

***Figure 3:*** *The data sequence was recorded during poor visibility conditions.*

## 4.1 Synthetic data

For a simulation, the true values of all parameters are readily available. Furthermore, a simulation allow us to test any filter for specific scenarios or specific disturbance environments. We have tried to create a realistic environment, but at the same time tried to challenge the filters with fast changes in the road geometry. The results from the simulation are shown in Figure 2. The plot shows the root mean square error (RMSE) of the

curvature during the simulation using different numbers of particles in the MPF. In the same plot the EKF performance and the measured curvature, $c_0^m$, are shown.

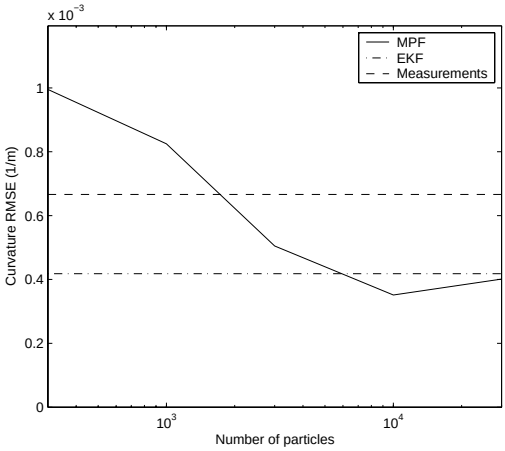


***Figure 4:*** *The curvature RMSE for different numbers of particles, using authentic data.*

Here, the MPF does not improve the estimation performance compared to the EKF. The explanation to this could be that the nonlinearities of the model are quite small and that the EKF is performing close to the Cramér-Rao lower bound (Kay, 1998).

## 4.2 Authentic data

The authentic data set was recorded in the northern parts of Sweden during the winter. From Figure 3 it is clear that the visibility of the lane markings is very low. Analogous to the simulation experiment, we have compared the EKF to the MPF using different numbers of particles. The true value of the curvature which was used to compute the magnitude of the errors was obtained from a detailed map. Figure 4 show the results of the experiment. For reference, we have also plotted the curvature and the absolute curvature error over time in Figure 5 and Figure 6, respectively. As can be seen, the MPF outperforms the EKF during high particle number settings. Why the MPF is better here, but not for synthetic data needs to be investigated further. The reason is probably that the MPF is more robust to model errors, since it does not depend on the derivatives of the measurement equations, or it is less sensitive to errors in other assumptions about noise and inputs used in the model. The fact that the curve is not monotonic in Figure 4, *i.e.*, the error is higher for the highest particle setting is due to the stochastic nature of the particle filter.

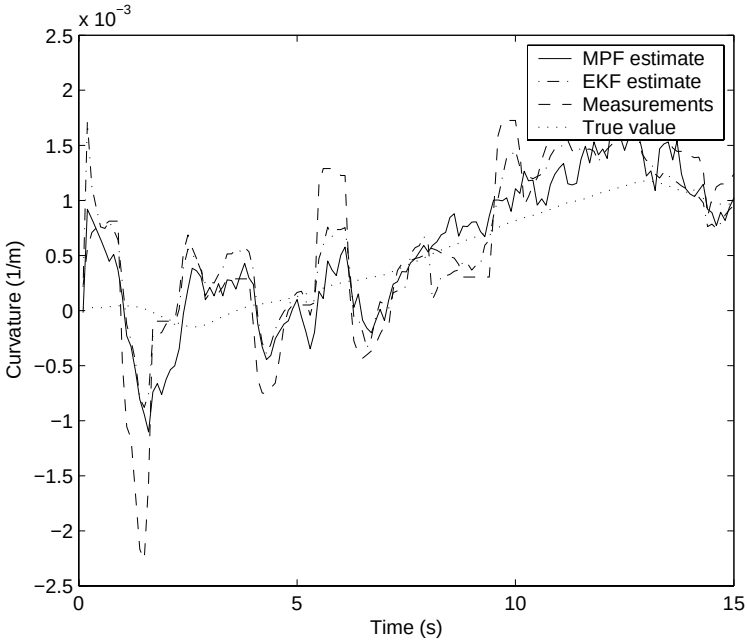


***Figure 5:*** *The true curvature, the measured curvature and the estimates from the MPF and EKF using the authentic data.*

# 5 Conclusions

We have shown that the marginalised particle filter can be implemented for automotive tracking and that it can give better performance than the traditionally used extended Kalman filter. Although the difference might not big enough to motivate the extra computational cost today, future increases in computational power will allow its implementation. Furthermore, the marginalised particle filter might be the only choice if more advanced nonlinear measurement equations, such as map information fusion, are to be used.

# References

Bergman, N., Ljung, L., and Gustafsson, F. (1999). Terrain navigation using Bayesian statistics. *IEEE Control Systems Magazine*, 19(3):33–40.

Blackman, S. S. (1986). *Multiple-Target Tracking with Radar Applications.* Artech House, Inc.

Casella, G. and Robert, C. (1996). Rao-Blackwellisation of sampling schemes. *Biometrika*, 83(1):81–94.

Dellaert, F. and Thorpe, C. (1997). Robust car tracking using Kalman filtering and

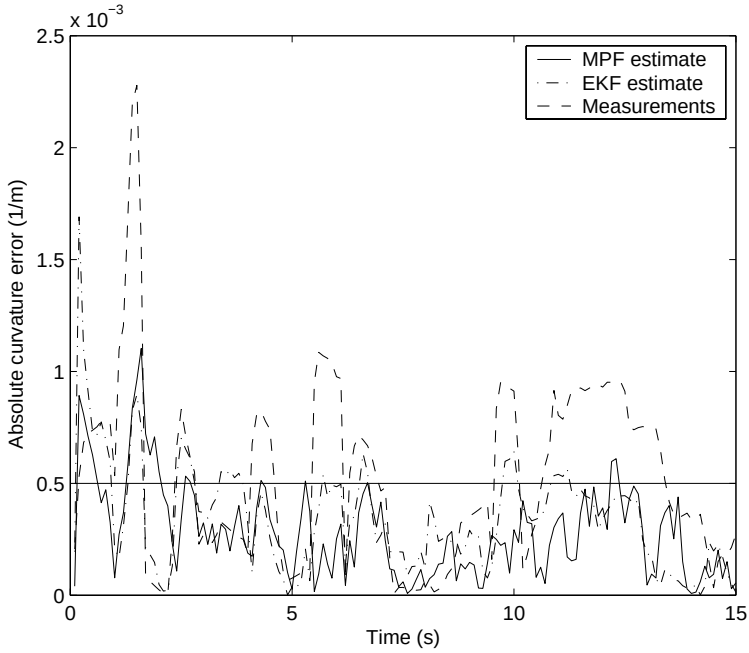


***Figure 6:*** *The absolute curvature error. Here, the level* $0.5 \cdot 10^{-3}$ *(1/m) used as a motivating example in* (19) *has been indicated. For errors above this level, leading vehicles at a distance of 100 metres are likely to be assigned to the wrong lane.*

Bayesian templates. In *Proceedings of the SPIE conference on Intelligent Transportation Systems*, volume 3207.

Doucet, A., de Freitas, N., and Gordon, N., editors (2001a). *Sequential Monte Carlo Methods in Practice.* Springer Verlag.

Doucet, A., Godsill, S., and Andrieu, C. (2000). On sequential Monte Carlo sampling methods for Bayesian filtering. *Statistics and Computing*, 10(3):197–208.

Doucet, A., Gordon, N., and Krishnamurthy, V. (2001b). Particle filters for state estimation of jump Markov linear systems. *IEEE Transactions on Signal Processing*, 49(3):613–624.

Eidehall, A. and Gustafsson, F. (2004). Combined road prediction and target tracking in collision avoidance. In *Proceedings of the IEEE Intelligent Vehicles Symposium*, pages 619–624, Parma, Italy.

Gordon, N., Salmond, D., and Smith, A. (1993). A novel approach to nonlinear/non-Gaussian Bayesian state estimation. In *IEE Proceedings on Radar and Signal Processing*, volume 140, pages 107–113.

Gustafsson, F. (2000). *Adaptive Filtering and Change Detection.* John Wiley & Sons, Ltd.

Jazwinski, A. (1970). *Stochastic processes and filtering theory.* Mathematics in science and engineering. Academic Press, New York.

Kailath, T., Sayed, A. H., and Hassibi, B. (2000). *Linear estimation.* Prentice Hall.

Kalman, R. E. (1960). A new approach to linear filtering and prediction problems. *Transactions of the ASME-Journal of Basic Engineering*, 82:35–45.

Karlsson, R., Schön, T., and Gustafsson, F. (2004). Complexity analysis of the marginalized particle filter. *Accepted for publication in IEEE Transactions on Signal Processing.*

Kay, S. K. (1998). *Fundamentals of Statistical Signal Processing, Volume 1: Detection Theory.* Prentice Hall Signal Processing. Prentice Hall, Upper Saddle River, New Jersey.

NHTSA (2000). Automotive collision avoidance system field operational test. web page, National Highway Traffic Safety Administration, `www.nhtsa.dot.gov/people/injury/research/pub/ACAS/ACAS-fieldtest`.

Nordlund, P.-J. (2002). *Sequential Monte Carlo Filters and Integrated Navigation.* Licentiate thesis, Linköping university. Thesis No. 945.

Rugh, W. J. (1996). *Linear System Theory.* Information and system sciences series. Prentice Hal, Upper Saddle River, New Jersey, 2 edition.

Schön, T., Gustafsson, F., and Nordlund, P.-J. (2004). Marginalized particle filters for mixed linear/nonlinear state-space models. *Accepted for publication in IEEE Transactions on Signal Processing.*

Zomotor, Z. and Franke, U. (1997). Sensor fusion for improved vision based lane recognition and object tracking with range-finders. In *Proceedings of the IEEE Conference on Intelligent Transportation Systems.*

# Paper F

# Obtaining reference road geometry parameters from recorded sensor data

**Authors:** Andreas Eidehall and Fredrik Gustafsson

Published in *Proceedings of the IEEE Intelligent Vehicles Symposium 2006*, pages 256–260, Tokyo, Japan.

# Obtaining reference road geometry parameters from recorded sensor data

Andreas Eidehall[⋆§] and Fredrik Gustafsson[⋆]

[⋆]Department of Electrical Engineering
Linköping University
SE–581 83 Linköping, Sweden

[§]Vehicle Dynamics and Active Safety
Volvo Car Corporation
SE–405 31 Göteborg, Sweden

**Abstract**

In many applications of tracking and sensing systems, reference data for tuning and verification of system performance is unavailable. In this article the problem of automotive on-line road shape estimation is discussed and a method for obtaining reference data for this application is presented. The reference data is based on a least squares curve which is fitted geometrically to the lane boundaries. It does not require any extra sensors or other hardware. It is also shown that the accuracy of the estimate is high enough to be used as a reference in most applications.

# 1 Introduction

During the process of tuning and validating the performance of sensor systems, including tracking and navigation algorithms, it is necessary to compare the output from the system to a reference data set. For example, when evaluating the performance of a radar for tracking air craft, the true positions of the air craft can be obtained from a GPS system. Of course, the GPS does not give the true position in theory, only a more accurate measurement. But in this case it could be argued that the error in the GPS measurement is insignificant in comparison to the error in the radar measurements.

The problem is that in many tracking and navigation examples, the true value of the data might not be available or it might be difficult or expensive to obtain. In such cases there are other techniques that can be used. For example, for a Kalman filter based tracking system, a smoothing algorithm can be applied once the entire data set has been collected. In the online application, only information from the past can be accessed, but off-line, the entire data set is available and thus also future information can be included in order to obtain a more accurate reference signal. Gustafsson (2000) or Kailath et al. (2000) provides detailed information on Kalman filtering and smoothing.

There are many other possibilities, often application specific. For example in road geometry estimation, which is a well studied field in the automotive industry, the goal is to obtain information about the shape of the road ahead of the host vehicle. This is typically done using a camera and image processing in order to analyse the shape of the white lane markings in the image. A creative solution for evaluating the accuracy of such a system was presented by Gern et al. (2000). This system uses a camera and image processing to measure the road curvature, and they want to improve the accuracy of this estimate by measuring the motion of leading vehicles with a radar. A vision based system is always sensitive to weather and visibility condition, so when evaluating the low visibility performance they drive the same road during good visibility and use that as a reference.

In this article, a new method for obtaining reference values of road geometry parameters such as road curvature is proposed. It is a geometric method based on analysing the future road trajectory and applying least squares curve fitting to a sliding window. The method does not require any extra sensors or other hardware, it only relies on information that is already available in most vehicles. An important part of this article is devoted to analysing the accuracy of the obtained values. The analysis is based on trajectory prediction precision which is evaluated on a test track with known shape.

The article first discusses different road models in Section 2 and the how to obtain the road trajectory parameters in Section 3. Next, in Section 4 the accuracy of the obtained road geometry parameters is analysed and the article ends with conclusions in Section 5

# 2 Road model

When parameterising the road shape, there are a couple of different choices of road models that can be used. A road model is expressed as a coordinate transformation $(x, y) \rightarrow (\tilde{x}, \tilde{y})$ where $(x, y)$ are points expressed in a longitudinal and lateral position relative to the road and $(\tilde{x}, \tilde{y})$ are points expressed in a Cartesian coordinate system at-

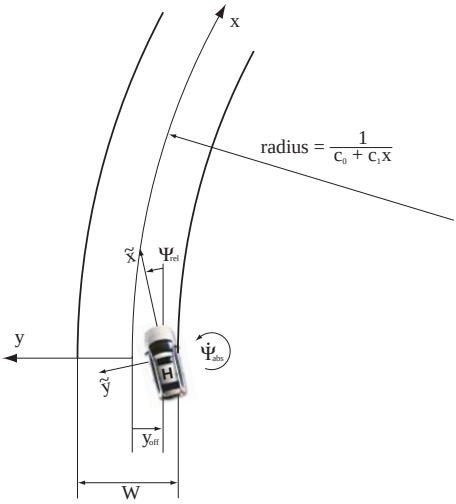


***Figure 1:*** *The road model is expressed as a mapping from the road* $(x, y)$ *coordinates to the host vehicle* $(\tilde{x}, \tilde{y})$ *coordinates.*

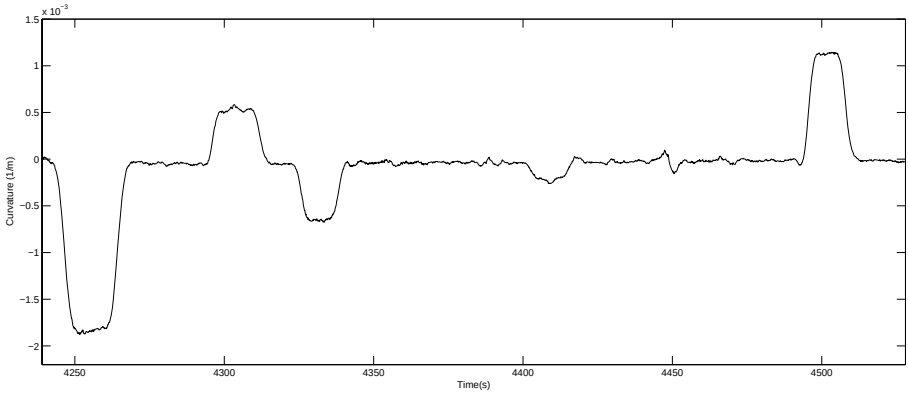


***Figure 2:*** *This plot shows a typical appearance of the road curvature parameter produced by the proposed method during a five minute test drive.*

tached to the host vehicle, see Figure 1. Typically, such models are based on a clothoid curve (Dickmanns and Zapp, 1986, Zomotor and Franke, 1997, Gern et al., 2001) which agrees well with how roads are constructed (Vägverket, 1994). A clothoid curve is a curve where the curvature changes linearly with the distance. The curvature is defined as $c(x) = 1/r(x)$ where $r(x)$ is the momentary radius at $x$ and $x$ is the distance along the curve. The radius can thus be written $r(x) = 1/c(x) = 1/(c_0 + c_1 x)$ where $c_0$ and $c_1$ is the curvature and clothoid parameter respectively. Mathematically, a road model based on an exact clothoid curve is rather complicated, which is why approximations are normally used. Different such approximations have been investigated by the authors (Eidehall and Gustafsson, 2004) and here, the most common of these will be used. This model is also most suitable for least squares curve fitting.

In mathematical form, it can be expressed as:

$$\begin{pmatrix} \tilde{x} \\ \tilde{y} \end{pmatrix} = \begin{pmatrix} x \\ y - y_{\text{off}} - \Psi_{\text{rel}} x + c_0 x^2/2 + c_1 x^3/6 \end{pmatrix}. \tag{1}$$

The variables $\Psi_{\text{rel}}$ and $y_{\text{off}}$ are defined in Figure 1. Note that this is a local model around the host vehicle at a snapshot in time. This means that as the host vehicle drive forward, the variables $y_{\text{off}}$, $\Psi_{\text{rel}}$, $c_0$ and $c_1$ will vary with time, i.e., we have $y_{\text{off}} = y_{\text{off},t}$, $\Psi_{\text{rel}} = \Psi_{\text{rel},t}$, $c_0 = c_{0,t}$ and $c_1 = c_{1,t}$. In this particular model the relationship $\tilde{x} = x$ holds, i.e., the curve effect in the $x$-direction is ignored. This line of the equation can thus be removed since it does not provide any information about the parameters to be estimated. If we also include the time varying parameters, the road model simply becomes

$$\tilde{y} = y - y_{\text{off},t} - \Psi_{\text{rel},t} x + c_{0,t} x^2/2 + c_{1,t} x^3/6. \tag{2}$$

Another possible model choice is to drop the clothoid parameter $c_1$ in (1) and thus fit a pure circle segment. Note that $\Psi_{\text{rel}}$ also is estimated, which is more a property of the driven path in relation to the road rather than a property of the road shape itself. Road models in general are discussed more thoroughly elsewhere (Eidehall and Gustafsson, 2004).

Given a set of points $(x, y)$ and $(\tilde{x}, \tilde{y})$ in both coordinate systems, i.e., $(x_{i,t}, y_{i,t})$ corresponds to $(\tilde{x}_{i,t}, \tilde{y}_{i,t})$, model (2) holds for all these points:

$$\tilde{y}_{i,t} = y_{i,t} - y_{\text{off},t} - \Psi_{\text{rel},t} x_{i,t} + c_{0,t} x_{i,t}^2/2 + c_{1,t} x_{i,t}^3/6. \tag{3}$$

These points can be obtained by the dead reckoning method described in Section 3.1. This can now be written as regression model by solving for the desired parameters $\Psi_{\text{rel},t}$, $c_{0,t}$ and $c_{1,t}$. Of course, the parameter $y_{\text{off},t}$ could also be estimated by this method, but since the direct measurement of this signal was found to be rather accurate, it was decided to be excluded in order to improve the accuracy of the other parameters. Rewriting (3)

$$\tilde{y}_{i,t} - y_{i,t} + y_{\text{off},t} = -\Psi_{\text{rel},t} x_{i,t} + c_{0,t} x_{i,t}^2/2 + c_{1,t} x_{i,t}^3/6$$

and factoring the right hand side, the expression becomes

$$\tilde{y}_{i,t} - y_{i,t} + y_{\text{off},t} = \begin{pmatrix} -x_{i,t} & x_{i,t}^2/2 & x_{i,t}^3/6 \end{pmatrix} \begin{pmatrix} \Psi_{\text{rel},t} \\ c_{0,t} \\ c_{1,t} \end{pmatrix}.$$

If we now define

$$\eta_{i,t} = \tilde{y}_{i,t} - y_{i,t} + y_{\text{off},t}, \tag{4}$$

$$\varphi_{i,t} = \begin{pmatrix} -x_{i,t} & x_{i,t}^2/2 & x_{i,t}^3/6 \end{pmatrix}, \tag{5}$$

$$\theta_t = \begin{pmatrix} \Psi_{\text{rel},t} \\ c_{0,t} \\ c_{1,t} \end{pmatrix}, \tag{6}$$

the structure

$$\eta_{i,t} = \varphi_{i,t}\theta_t \tag{7}$$

is obtained.

# 3 Parameter estimation

## 3.1 Symmetric sliding window

### Overview

In order to estimate the road parameters, information about the shape of the road is needed. This is obtained by dead reckoning the position of the host vehicle using the yaw rate and velocity sensors and at the same time compensating for the host vehicle lateral position in the lane. Of course, this is dependent on that the error in these signals is sufficiently small. This is investigated in Section 4. The reason for compensating for the lateral position in the lane, which can be measured with the vision system, is that the goal is to estimate the shape of the lane, not the path that the host vehicle is driven.

One of the design choices in the proposed method is the length of the window that is used to estimate the road parameters. A long window will give a more stable but sometimes too slow estimate, for example during curve entry, while a shorter trajectory will be faster but sometimes more noisy due to imperfections in the lane markings and in the measurements of these.

A method that have worked well in our tests is to use a time based length of about five to six seconds. This makes the trajectory longer at high speeds which is more suitable for slower changes in curvature and shorter for slower speeds which is more suitable for faster changes in curvature, which agrees with how roads are constructed. Note that when using this method, a lower limit on the host vehicle speed has to be used in order to assure that the problem remains well conditioned.

### Dead reckoning

The signals from the vehicle that are used in the dead reckoning are $\dot{\Psi}_t$, $v_t$ and $y_{\text{off},t}$ which are sampled with sample time $T_s$. $\dot{\Psi}_t$ and $v_t$ is used to compute the path of the host vehicle and $y_{\text{off},t}$ is used to, based on the host vehicle path, extract the shape of the lane.

First some preliminary definitions. For each time instant $t$ where the curve fitting process will be carried out, the interval set $I = \{-L/2, \ldots, 0, \ldots, L/2\}$ will be used,

centred around $t$. Note that the length of $I$ is really $L+1$. Furthermore, if $p$ and $q$ are integers with $p < q$ a backwards sum is defined as

$$\sum_{i=q}^{p} a_i = -\sum_{i=p}^{q} a_i, \tag{8}$$

and also, if $p = q$ the sum

$$\sum_{i=p}^{q} a_i = 0 \tag{9}$$

can be defined. First the angle of the host vehicle at time $t+i$ relative to the angle at time $t$ is computed:

$$\Psi_{i,t} = \sum_{\tau=0}^{i} \dot{\Psi}_{t+\tau} T_s, \; i \in I. \tag{10}$$

Using (8) and (9) above, this expression is defined for negative values of $i$, for example, it also means that $\Psi_{0,t} = 0$. The subscript $i,t$ refers to the angle of the host vehicle at time $i+t$ relative to, and extrapolated from, the angle at time $t$. The host vehicle path can then be computed geometrically as

$$\tilde{x}_{i,t}^{\text{veh}} = \sum_{\tau=0}^{i} \cos(\Psi_{\tau,t}) v_{t+\tau} T_s, \; i \in I, \tag{11}$$

$$\tilde{y}_{i,t}^{\text{veh}} = \sum_{\tau=0}^{i} \sin(\Psi_{\tau,t}) v_{t+\tau} T_s, \; i \in I. \tag{12}$$

Similarly, subscript $i,t$ means the position of the host vehicle at time $t+i$ relative to, and extrapolated from, the position at time $t$. The path of the centre of the lane can then be computed by adding a vector of length $y_{\text{off},i+t}$ perpendicular to the driven path, see Figure 3, i.e.,

$$\tilde{x}_{i,t} = \tilde{x}_{i,t}^{\text{veh}} + \sin(\Psi_{i,t}) y_{\text{off},i+t}, \; i \in I, \tag{13a}$$

$$\tilde{y}_{i,t} = \tilde{y}_{i,t}^{\text{veh}} + \cos(\Psi_{i,t}) y_{\text{off},i+t}, \; i \in I. \tag{13b}$$

In the $(x,y)$-coordinate system, the centre of the lane is just a straight line in the $x$-direction:

$$x_{i,t} = \sum_{\tau=0}^{i} v_{t+\tau} T_s, \; i \in I, \tag{14a}$$

$$y_{i,t} = 0, \; i \in I. \tag{14b}$$

For time $t$, we now have a set of points with known coordinates in both coordinate systems $(x,y)$ and $(\tilde{x},\tilde{y})$, i.e., $(x_{i,t}, y_{i,t})$ corresponds to $(\tilde{x}_{i,t}, \tilde{y}_{i,t})$ for all $i$ in $I$. Note that in the model 2, $\tilde{x}_{i,t}$ is not needed, but it might be needed if a different road model is to be used. It is included here for completeness.

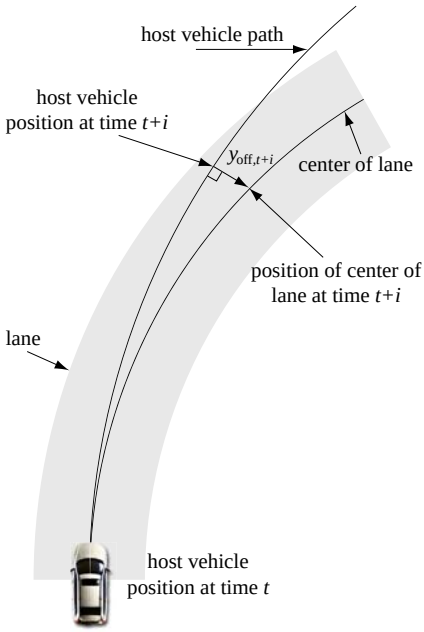


***Figure 3:*** *The path of the host vehicle might be different from the centre of the lane. That is why compensation with* $y_{\text{off,i+t}}$ *is needed.*

## 3.2 Least squares algorithm

The least squares problem for time $t$ can now be formulated by stacking $\eta_{i,t}$ and $\varphi_{i,t}$ from (4) and (5), where $i \in I$, in the two vectors

$$Y_t = \begin{pmatrix} \eta_{-L/2,t} \\ \vdots \\ \eta_{L/2,t} \end{pmatrix} \quad \text{and} \quad \Phi_t = \begin{pmatrix} \varphi_{-L/2,t} \\ \vdots \\ \varphi_{L/2,t} \end{pmatrix}. \tag{15}$$

Using these, the total problem for time $t$ can be written

$$Y_t = \Phi_t \theta_t. \tag{16}$$

The conventional least squares projection can then be used to obtain the $\theta_t$ that gives the minimum square distance to the true trajectory

$$\theta_t = (\Phi_t^T \Phi_t)^{-1} \Phi_t^T Y_t \tag{17}$$

Note that this is done once for each time step, i.e., performing these computations gives the road geometry parameters for one time instant only. An example of where the $c_{0,t}$ component of $\theta_t$ for a five minute test drive has been plotted is shown in Figure 2.

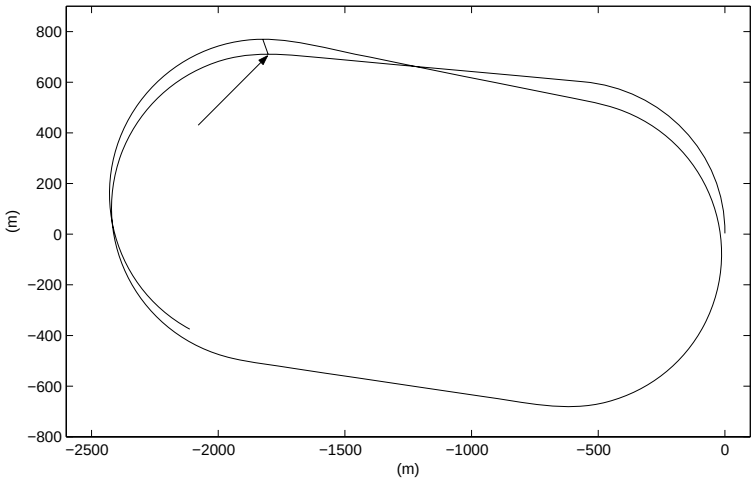


***Figure 4:*** *This is the trajectory based on the yaw rate and velocity information. The arrow indicates where the position error was measured.*

# 4 Accuracy of the proposed method

One of the causes of error in this computation is, of course, the drift that is generated by integrating yaw rate sensor in the dead reckoning process. An error in the yaw rate signal will give an error in the position which in turn will give an error in the road geometry parameters. In this section we try to quantify this error, and in particular the error in the curvature reference signal.

## 4.1 Dead reckoning error growth

In order to quantify the error in the dead reckoning procedure, a test vehicle is driven on a track with known shape. The trajectory, based on yaw-rate and velocity of the host vehicle only, is then plotted, see Figure 4. Since it is known that the vehicle returns to the same position after one lap on the test track, this data can be used to measure the accumulated position error.

During this test drive, the total distance error was 62.8 [m] after a driven distance of 6.26 [km] and a time of 187 [s]. Performance accuracy of the same order is also demonstrated by for example Fjellström and Andersson (2004) and Carlson et al. (2002). In order to analyse how the error grows, a simple curve integration is carried out where it is assumed that there is a constant error in the yaw rate measurement. If $\dot{\Psi}(t)$ is the true yaw rate of the vehicle and $\dot{\Psi}_{\text{err}}$ is a constant error, i.e., $\dot{\Psi}_{\text{meas}}(t) = \dot{\Psi}(t) + \dot{\Psi}_{\text{err}}$ is measured, the following measured absolute yaw angle is obtained:

$$\Psi_{\text{meas}}(t) = \int_0^t (\dot{\Psi}(\tau) + \dot{\Psi}_{\text{err}})d\tau = \int_0^t \dot{\Psi}(\tau)d\tau + \dot{\Psi}_{\text{err}}t \tag{18}$$

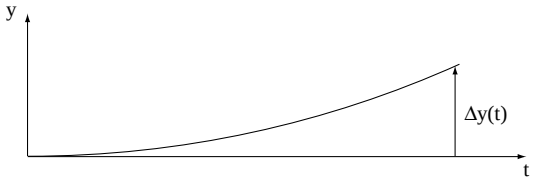


***Figure 5:*** *In the error analysis it is assumed that the error is perpendicular to the travelled path.*

If the error growth perpendicular to the travelled path is analysed, see Figure 5, and assuming constant velocity $v$, the following expression for the position is obtained:

$$y(t) = \int_0^t v \sin(\Psi_{\text{meas}}(\tau))d\tau \approx v \int_0^t (\int_0^\tau \dot{\Psi}(\sigma)d\sigma + \dot{\Psi}_{\text{err}}\tau)d\tau =$$

$$= v \int_0^t (\int_0^\tau \dot{\Psi}(\sigma)d\sigma)d\tau + v\dot{\Psi}_{\text{err}}\frac{t^2}{2}, \tag{19}$$

The error comes from the last term, i.e.,

$$\Delta y = \frac{t^2}{2}\dot{\Psi}_{\text{err}}v \;\Leftrightarrow\; \dot{\Psi}_{\text{err}} = \frac{2\Delta y}{t^2 v}. \tag{20}$$

Thus, the error grows with the square of the time. The velocity when this data was recorded was 33.4 [m/s]. This gives

$$\dot{\Psi}_{\text{err}} = \frac{2 \cdot 62.8 \text{ [m]}}{(187 \text{ [s]})^2 \cdot 33.4 \text{ [m/s]}} = 1.07 \cdot 10^{-4} \text{ [1/s]}. \tag{21}$$

Summarising, the position error will grow as

$$\Delta y(t) = v\frac{t^2}{2}\dot{\Psi}_{\text{err}} \tag{22}$$

or, expressing this in distance, with $s = tv$ or $t = s/v$:

$$\Delta y(s) = v\frac{(s/v)^2}{2}\dot{\Psi}_{\text{err}} = \frac{s^2}{2v}\dot{\Psi}_{\text{err}}. \tag{23}$$

## 4.2 Error in curvature estimate

In order to translate the error in the yaw rate measurement into an error in the curvature estimate it is first noted that when driving in a curve the relationship

$$v = \dot{\Psi}r \tag{24}$$

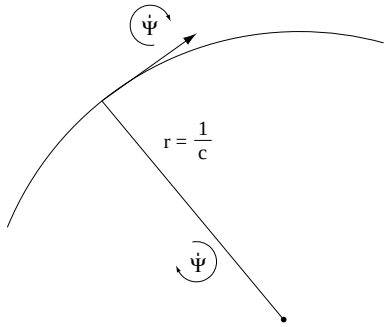


***Figure 6:*** *When driving in a curve, the relation* $v = \dot{\Psi} r$ *hold.*

holds, where $\dot{\Psi}$ is the true yaw rate, $r$ is the momentary radius and $v$ is the velocity. This is illustrated in Figure 6. Using $r = 1/c$ the following expression for the curvature is obtained:

$$v = \frac{\dot{\Psi}}{c} \Leftrightarrow c = \frac{\dot{\Psi}}{v}, \tag{25}$$

which means that when there is an error in the yaw rate measurement, the curvature becomes

$$c^{\star} = \frac{\dot{\Psi} + \dot{\Psi}_{\text{err}}}{v} = \frac{\dot{\Psi}}{v} + \frac{\dot{\Psi}_{\text{err}}}{v} = c + \frac{\dot{\Psi}_{\text{err}}}{v}, \tag{26}$$

i.e., the error in the curvature is

$$\Delta c = c^{\star} - c = \frac{\dot{\Psi}_{\text{err}}}{v}, \tag{27}$$

The main interest of this method is speeds above 50 [km/h] $\approx$ 13.9 [m/s] which implies that the maximum error in the curvature for such driving scenarios is

$$\Delta c = \frac{\dot{\Psi}_{\text{err}}}{v} = \frac{1.07 \cdot 10^{-4} \text{ [1/s]}}{13.9 \text{ [m/s]}} = 7.70 \cdot 10^{-6} \text{ [1/m]}. \tag{28}$$

If this is compared to the magnitude of the curvature signal in Figure 2, which is about $1 \cdot 10^{-3}$ [1/m] it can be found that the relative error is

$$\frac{\Delta c}{c} = \frac{7.7 \cdot 10^{-6} \text{ [1/m]}}{1 \cdot 10^{-3} \text{ [1/m]}} \approx 0.8\%. \tag{29}$$

which indicates that the curvature estimate generated by the proposed method is accurate enough to use as a reference signal in most applications.

# 5 Conclusions

We have discussed a method for obtaining a reference signal for the road geometry parameters. The estimate is a least squares curve fitted to the lane boundary trajectories. It is clear that the error caused by the dead reckoning is insignificant for most applications. The signal can be used as a reference when tuning and verifying filters for estimating road geometry. Of course, there are other sources of error that have been neglected in this analysis. One is the error in the host vehicle lateral position signal, but the algorithm is rather unsensitive to this and it can be shown that the error caused by this is less than or about the same order as the error from the dead reckoning. Another cause of error is the choice of road model. The model presented here is an approximation of a clothoid curve. But even a model which exactly describes a clothoid curve would not always fit perfectly. For example, a road segment of which the first half is a straight line and the other half is a clothoid cannot be parameterised by one clothoid curve. Also, some roads use an immediate transition from a straight segment to a circle segment instead of a clothoid transition.

Despite these facts, we believe that the reconstructed road curvature information from the proposed method has high quality and it has also been very valuable in our research.

# References

Carlson, C. R., Gerdes, J. C., and Powell, J. D. (2002). Practical position and yaw rate estimation with gps and differential wheelspeeds. In *Proceedings of AVEC'02*, Japan.

Dickmanns, E. D. and Zapp, A. (1986). A curvature-based scheme for improving road vehicle guidance by computer vision. In *Proceedings of the SPIE conference on Mobile Robots.*

Eidehall, A. and Gustafsson, F. (2004). Combined road prediction and target tracking in collision avoidance. In *Proceedings of the IEEE Intelligent Vehicles Symposium*, pages 619–624, Parma, Italy.

Fjellström, J. and Andersson, D. (2004). Vehicle positioning with map matching using integration of a dead reckoning system and GPS. Masters Thesis 3457, Department of Electrical Engineering, Linköping University.

Gern, A., Franke, U., and Levi, P. (2000). Advanced lane recognition - fusing vision and radar. In *Proceedings of the IEEE Intelligent Vehicles Symposium*, Dearborn, MI, USA.

Gern, A., Franke, U., and Levi, P. (2001). Robust vehicle tracking fusing radar and vision. In *Proceeding of The International Conference on Multisensor Fusion and Integration for Intelligent Systems*, pages 323–328.

Gustafsson, F. (2000). *Adaptive Filtering and Change Detection.* John Wiley & Sons, Ltd.

Kailath, T., Sayed, A. H., and Hassibi, B. (2000). *Linear estimation.* Prentice Hall.

Vägverket (1994). Vägutformning 94 version s-2. Technical report, Swedish National Road Administration.

Zomotor, Z. and Franke, U. (1997). Sensor fusion for improved vision based lane recognition and object tracking with range-finders. In *Proceedings of the IEEE Conference on Intelligent Transportation Systems.*

**PhD Dissertations**
**Division of Automatic Control**
**Linköpings universitet**

**M. Millnert:** Identification and control of systems subject to abrupt changes. Thesis No. 82, 1982. ISBN 91-7372-542-0.
**A. J. M. van Overbeek:** On-line structure selection for the identification of multivariable systems. Thesis No. 86, 1982. ISBN 91-7372-586-2.
**B. Bengtsson:** On some control problems for queues. Thesis No. 87, 1982. ISBN 91-7372-593-5.
**S. Ljung:** Fast algorithms for integral equations and least squares identification problems. Thesis No. 93, 1983. ISBN 91-7372-641-9.
**H. Jonson:** A Newton method for solving non-linear optimal control problems with general constraints. Thesis No. 104, 1983. ISBN 91-7372-718-0.
**E. Trulsson:** Adaptive control based on explicit criterion minimization. Thesis No. 106, 1983. ISBN 91-7372-728-8.
**K. Nordström:** Uncertainty, robustness and sensitivity reduction in the design of single input control systems. Thesis No. 162, 1987. ISBN 91-7870-170-8.
**B. Wahlberg:** On the identification and approximation of linear systems. Thesis No. 163, 1987. ISBN 91-7870-175-9.
**S. Gunnarsson:** Frequency domain aspects of modeling and control in adaptive systems. Thesis No. 194, 1988. ISBN 91-7870-380-8.
**A. Isaksson:** On system identification in one and two dimensions with signal processing applications. Thesis No. 196, 1988. ISBN 91-7870-383-2.
**M. Viberg:** Subspace fitting concepts in sensor array processing. Thesis No. 217, 1989. ISBN 91-7870-529-0.
**K. Forsman:** Constructive commutative algebra in nonlinear control theory. Thesis No. 261, 1991. ISBN 91-7870-827-3.
**F. Gustafsson:** Estimation of discrete parameters in linear systems. Thesis No. 271, 1992. ISBN 91-7870-876-1.
**P. Nagy:** Tools for knowledge-based signal processing with applications to system identification. Thesis No. 280, 1992. ISBN 91-7870-962-8.
**T. Svensson:** Mathematical tools and software for analysis and design of nonlinear control systems. Thesis No. 285, 1992. ISBN 91-7870-989-X.
**S. Andersson:** On dimension reduction in sensor array signal processing. Thesis No. 290, 1992. ISBN 91-7871-015-4.
**H. Hjalmarsson:** Aspects on incomplete modeling in system identification. Thesis No. 298, 1993. ISBN 91-7871-070-7.
**I. Klein:** Automatic synthesis of sequential control schemes. Thesis No. 305, 1993. ISBN 91-7871-090-1.
**J.-E. Strömberg:** A mode switching modelling philosophy. Thesis No. 353, 1994. ISBN 91-7871-430-3.
**K. Wang Chen:** Transformation and symbolic calculations in filtering and control. Thesis No. 361, 1994. ISBN 91-7871-467-2.
**T. McKelvey:** Identification of state-space models from time and frequency data. Thesis No. 380, 1995. ISBN 91-7871-531-8.
**J. Sjöberg:** Non-linear system identification with neural networks. Thesis No. 381, 1995. ISBN 91-7871-534-2.
**R. Germundsson:** Symbolic systems – theory, computation and applications. Thesis No. 389, 1995. ISBN 91-7871-578-4.
**P. Pucar:** Modeling and segmentation using multiple models. Thesis No. 405, 1995. ISBN 91-7871-627-6.
**H. Fortell:** Algebraic approaches to normal forms and zero dynamics. Thesis No. 407, 1995. ISBN 91-7871-629-2.

**A. Helmersson:** Methods for robust gain scheduling. Thesis No. 406, 1995. ISBN 91-7871-628-4.
**P. Lindskog:** Methods, algorithms and tools for system identification based on prior knowledge. Thesis No. 436, 1996. ISBN 91-7871-424-8.
**J. Gunnarsson:** Symbolic methods and tools for discrete event dynamic systems. Thesis No. 477, 1997. ISBN 91-7871-917-8.
**M. Jirstrand:** Constructive methods for inequality constraints in control. Thesis No. 527, 1998. ISBN 91-7219-187-2.
**U. Forssell:** Closed-loop identification: Methods, theory, and applications. Thesis No. 566, 1999. ISBN 91-7219-432-4.
**A. Stenman:** Model on demand: Algorithms, analysis and applications. Thesis No. 571, 1999. ISBN 91-7219-450-2.
**N. Bergman:** Recursive Bayesian estimation: Navigation and tracking applications. Thesis No. 579, 1999. ISBN 91-7219-473-1.
**K. Edström:** Switched bond graphs: Simulation and analysis. Thesis No. 586, 1999. ISBN 91-7219-493-6.
**M. Larsson:** Behavioral and structural model based approaches to discrete diagnosis. Thesis No. 608, 1999. ISBN 91-7219-615-5.
**F. Gunnarsson:** Power control in cellular radio systems: Analysis, design and estimation. Thesis No. 623, 2000. ISBN 91-7219-689-0.
**V. Einarsson:** Model checking methods for mode switching systems. Thesis No. 652, 2000. ISBN 91-7219-836-2.
**M. Norrlöf:** Iterative learning control: Analysis, design, and experiments. Thesis No. 653, 2000. ISBN 91-7219-837-0.
**F. Tjärnström:** Variance expressions and model reduction in system identification. Thesis No. 730, 2002. ISBN 91-7373-253-2.
**J. Löfberg:** Minimax approaches to robust model predictive control. Thesis No. 812, 2003. ISBN 91-7373-622-8.
**J. Roll:** Local and piecewise affine approaches to system identification. Thesis No. 802, 2003. ISBN 91-7373-608-2.
**J. Elbornsson:** Analysis, estimation and compensation of mismatch effects in A/D converters. Thesis No. 811, 2003. ISBN 91-7373-621-X.
**O. Härkegård:** Backstepping and control allocation with applications to flight control. Thesis No. 820, 2003. ISBN 91-7373-647-3.
**R. Wallin:** Optimization algorithms for system analysis and identification. Thesis No. 919, 2004. ISBN 91-85297-19-4.
**D. Lindgren:** Projection methods for classification and identification. Thesis No. 915, 2005. ISBN 91-85297-06-2.
**R. Karlsson:** Particle Filtering for Positioning and Tracking Applications. Thesis No. 924, 2005. ISBN 91-85297-34-8.
**J. Jansson:** Collision Avoidance Theory with Applications to Automotive Collision Mitigation. Thesis No. 950, 2005. ISBN 91-85299-45-6.
**E. Geijer Lundin:** Uplink Load in CDMA Cellular Radio Systems. Thesis No. 977, 2005. ISBN 91-85457-49-3.
**M. Enqvist:** Linear Models of Nonlinear Systems. Thesis No. 985, 2005. ISBN 91-85457-64-7.
**T. B. Schön:** Estimation of Nonlinear Dynamic Systems — Theory and Applications. Thesis No. 998, 2006. ISBN 91-85497-03-7.
**I. Lind:** Regressor and Structure Selection — Uses of ANOVA in System Identification. Thesis No. 1012, 2006. ISBN 91-85523-98-4.
**J. Gillberg:** Frequency Domain Identification of Continous-Time System Reconstruction and Robustness. Thesis No. 1031, 2006. ISBN 91-85523-34-8.
**M. Gerdin:** Identification and Estimation for Models Described by Differential-Aglebraic Equations. Thesis No. 1046, 2006. ISBN 91-85643-87-4.

**C. Grönwall:** Ground Object Recognition using Laser Radar Data — Geometric Fitting, Performance Analysis, and Applications. Thesis No. 1055, 2006. ISBN 91-85643-53-X.